A STUDY OF CONTINUOUS FOAM FRACTIONATION

Thesis for the Degree of Ph. D.

MICHIGAN STATE UNIVERSITY

KENNETH EDWARD HASTINGS

1967

THESIS

MICHIGAN STATE UNIVERSITY LIBRARIES
3 1293 10814 8267

LIBRARY
Michigan State
University

This is to certify that the

thesis entitled

A STUDY OF

CONTINUOUS FOAM FRACTIONATION

presented by

Kenneth Edward Hastings

has been accepted towards fulfillment
of the requirements for

Ph.D. degree in Chemical Engineering

Major professor

Date August 3, 1967

O-169

JUN 3 1989
M 15614

ABSTRACT

A STUDY OF CONTINUOUS FOAM FRACTIONATION

by Kenneth Edward Hastings

In order to develop a method for predicting the separations achieved in a foam fractionation column, the concept of the height of a transfer unit was applied to the continuous foam fractionation of aqueous sodium lauryl sulfate solution in a column with enriching and stripping sections. The column was first operated as a one-stage separator with no stripping or external refluxing so that equilibrium data could be obtained. In this one-stage separator, liquid in the bottom of the column was gassed to produce a rising foam bed and bottom product liquid. The rising foam was coalesced overhead and pumped to a tank where it was mixed with bottom product. Feed, withdrawn from this tank, entered the column below the foam-liquid interface. At steady state, samples of coalesced foam and bottom product were withdrawn and the concentrations were measured.

The effects of foam drainage, internal reflux, and countercurrent mass transfer were separated by showing that foam drainage and internal reflux were negligible, and hence all incremental separations above one-stage separations were caused by countercurrent mass transfer. Enriching and stripping sections of various heights were examined to find out what variables affect the height of a transfer unit. The height of a transfer unit for either an enriching or a stripping section was found to correlate empirically with the flow number.

$$\text{Flow Number} = \frac{L_D}{L_U}\sqrt{\frac{L_D}{G + L_D + L_U}}$$

Where:

L_D = Downflow liquid flow rate (cm^3/min.)

L_U = Upflow liquid flow rate (cm^3/min.)

G = Gas flow rate (cm^3/min.)

This height of a transfer unit correlation was used to predict top and bottom product concentrations for experimental runs in a column with a 32.4" enriching section and a 31.4" stripping section. The calculated bottom product mole fractions agreed to within $\pm 6\%$ and the calculated top product mole fractions agreed to within $\pm 7.5\%$ of the experimental values for this column.

A STUDY OF
CONTINUOUS FOAM FRACTIONATION

By

Kenneth Edward Hastings

A THESIS

Submitted to
Michigan State University
in partial fulfillment of the requirements
for the degree of

DOCTOR OF PHILOSOPHY

Department of Chemical Engineering

1967

647109
12-20-67

TO

SUSAN

ACKNOWLEDGMENTS

The author would like to express deep appreciation to Dr. Donald K. Anderson, Department of Chemical Engineering, and Dr. James L. Dye, Department of Chemistry, Michigan State University, for their cooperation and guidance in the preparation of this thesis.

Appreciation is also extended to the Division of Engineering Research and the Department of Chemical Engineering, Michigan State University, for financial support. The author also wishes to thank Mr. Andrew W. Seer, glass blower, and Mr. Donald L. Childs, shop supervisor, for helping in the design and construction of equipment.

The patience, understanding, and endurance of the author's wife, Susan, is sincerely appreciated.

TABLE OF CONTENTS

LIST OF ILLUSTRATIONS

Figure | Page

INTRODUCTION

Although many techniques are available for separating homogeneous solutions, only a few of them are economical at low concentrations. One of the most recent techniques is foam fractionation which concentrates surface active agents by foaming them. Foam fractionation utilizes a quantity of feed solution which is gassed to produce a rising foam bed and residual solution. This foam is collected overhead and coalesced to form a solution of higher surfactant concentration than the original feed solution. This fractionation process can be made more efficient by countercurrent mass transfer in the column of foam which produces a multi-staged effect.

Foam is essentially a honeycombed arrangement of gas bubbles separated by liquid lamellae. Some types of foams, for example the head on beer, are uniform and stable; while others, such as sea foam produced in the surf, are composed of a wide range of bubble sizes and are quite unstable. Some foams are rigid and contain very little liquid, while others are fluids with thick liquid walls. The most stable configuration of foam has been theorized (45) and found to be one where all liquid lamellae intersect at angles of 120°. These points of intersection form "Plateau's borders" where liquid films are the thickest. Most of the liquid drains down through the foam by way of Plateau's borders, because of a pressure differential (6) between liquid lamellae and Plateau's borders. This pressure differential is caused by the amount of surface curvature existing at different points along a polyhedron shaped bubble. Pressures in liquid films are the lowest at Plateau's borders where the air-water interface is the most concave

towards the air phase. This effect of curvature causes smaller bubbles to have a higher gas pressure than larger bubbles; therefore foam will always coalesce into larger bubbles.

Gas bubbles are found in many different shapes and sizes. Spherically shaped bubbles (k = 6.0) are formed if large amounts of liquid are entrained in the foam (wet foam). But as liquid lamellae become extremely thin and accordingly the fraction of liquid in the foam decreases, the gas bubbles are distorted to polyhedral shapes (dry foam). Dry foams have been found to consist mainly of dodecahedron shaped bubbles (13) with k = 6.59. Where k is equal to the area constants divided by the volume constants (area constants = area of bubble/D_A^2, volume constants = volume of bubble/D_V^3).

$$\frac{\text{Area of Bubbles}}{\text{Volume of Bubbles}} = k \frac{D_A^2}{D_V^3} \qquad (1)$$

Where:

D_A = Area averaged bubble diameter

D_V = Volume averaged bubble diameter

A study of surface chemistry explains why foam fractionation is economical at low concentrations. Interaction forces between molecules are greater for a liquid than for a gas. Molecules in the liquid which are within a few molecular diameters of the gas-liquid interface are subject to different environmental forces than molecules well within the bulk of the liquid. These environmental surface forces decrease with the addition of a positively adsorbed surface active agent, which concentrates at the interface. Surface active agents (surfactants) may either be positively or

negatively adsorbed at the surface. If they are adsorbed at the interface, then a partial separation can be achieved by removing the surface from the bulk liquid by some means. For instance, a knife edge could be used as a mechanical means for skimming off the surface of a liquid, but this is not practical. The simple process of generating a foam is an excellent way of producing a large amount of surface area and removing this generated surface from the bulk of the liquid in the same operation.

Foam fractionation is different from froth flotation although both involve the gassing of a liquid. Froth flotation is an established procedure in mineral dressing where the surface characteristics of one solid are modified so that the particles will readily attach themselves to air bubbles. Froth flotation involves the gassing of a liquid which contains suspended solids, while foam fractionation involves the gassing of a homogeneous liquid which has surfactant dissolved in it.

A one stage foam fractionation column can be transformed into a multistaged column by the application of any or all of the following factors; external reflux, internal reflux, central feed, and drainage. External reflux is caused by coalesced overhead foam being added back to the top of the column. This results in the upper part of the column acting as an enriching section. Internal reflux is caused by poor foam stability with bubbles coalescing in the column, and this effect reduces the amount of surface area and forces some of the surface active agent back into the bulk of the liquid. The feed stream entering into the middle of a foam bed causes the lower section of the column to act as a stripping section. Downflow in a stripping section is usually composed of either the feed stream

or a mixture of the feed and external reflux. Drainage results from excess liquid being entrained in the foam and draining down through Plateau's borders as the liquid lamellae become thinner. The external reflux and feed flow rates are quite easy to measure experimentally, but the other two factors are rather difficult to take into account.

Stable foams are produced by a combination of uniform bubble diameters and a high elasticity. Uniform bubble diameters decrease the chance of bubble coalescence due to a gas pressure driving force. Elasticity, as defined by Gibbs (17), is important because it determines how well foam will resist coalescence.

$$E = 2A \frac{d\phi}{dA} \qquad (2)$$

Where:

E = Gibbs' elasticity

A = Area of the liquid film

ϕ = Surface tension

Foam persists only as long as liquid lamellae exist. A surfactant that is positively adsorbed at the interface causes the surface tension to be smaller at the interface than in the bulk of the solution. If the surface layer is damaged and the underlying liquid is exposed, then the greater surface tension of the underlying layer pulls the edges of the wound together and thus causes complete healing of the surface. A stable foam should therefore have a large positive elasticity.

Foam stability may also be affected by the application of other less common conditions. High viscosity liquid lamellae resist drainage and hence enhance foam persistence. Liquid films with a large surface area are less stable than those with a small surface area. This causes small bubbles to

have a longer life than large bubbles. Foam stability usually decreases with increasing temperature and this is primarily due to decreased liquid viscosity and increased gas pressure within the bubbles. The pH of a surfactant solution does not affect the stability of foams, except for those produced by colloidal agents. Neither pure liquids nor saturated solutions usually have appreciable foam persistence. Detergents are the exception to this rule and have considerable foam stability at saturation.

The present interest in foam fractionation has increased over the past ten years because of the increased usage of synthetic detergents. Biodegradable as well as non-biodegradable detergents are widely used in large quantities in industry and in the home, and these detergents pollute the country's streams, river, and lakes. In some cases, the nation's water supplies are polluted faster than bacterial action can break down biodegradable detergents. Foam fractionation might serve as an excellent means for removing these surface active contaminates. Foam fractionation is presently used in the sugar industry to remove color contaminates which are surface active. Another possible use for foam fractionation is in the separation of non-surface active ions (44, 46). A detergent sometimes has an affinity for a particular ion and forms a surface active complex with the non—surface active ion. This complex can then be separated from other ions in the bulk solution by foam fractionation.

BACKGROUND WORK

There have been many papers published in the field of foam fractionation, but only a few have contributed significantly to the state of the art. Most researchers have taken an empirical approach in solving foam fractionation problems. This leaves a researcher at a loss when trying to scale-up the already studied system or in looking at a new one. The following review of past work has supplied this author with the necessary basis upon which to build a more theoretical approach.

Lemlich and Lavi (31) studied foam fractionation of dilute aqueous solutions of Aresket-300 (monobutyl diphenyl sodium monosulfonate) in an enriching column. They gathered data on the separations achieved as the external reflux ratio was varied from zero to infinity. Their results have shown that at various gas flow rates and bottom product compositions, increasing the external reflux ratio improves the separation. While they apparently have shown the above, they have not separated the effects of internal reflux and drainage from the effect of external reflux.

Lemlich and Brunner (8) developed a mathematical model for the foam fractionation of aqueous Aresket-300 in an enriching column. Data were gathered on a one theoretical stage foam column and an equilibrium equation was presented

$$C_T = C_B + \frac{S\ G\ T_B}{L_C} \qquad (1)$$

Where

C_T = Top product concentration of Aresket-300 (mg. moles/ml.)

C_B = Bottom product concentration of Aresket-300 (mg. moles/ml.)

S = Bubble surface area per volume of gas (cm^2/ml.)

G = Gas flow rate (ml./min.)

T_B = Surface excess of Aresket-300 based on C_B (mg. moles/cm^2)

L_O = Overhead liquid flow rate (ml./min.)

Their experimental results indicated that surface excess is constant over part of the concentration region. They chose this concentration region for a study of a multi-staged enricher. This enriching column model assumes drainage to occur but neglects internal reflux.

$$\frac{C_T}{C_B} = \frac{(R_{EX} + 1)\ G\ S\ T_B}{L_O\ C_B} + \frac{C_{DB}}{C_B} + \frac{(R_{EX} + 1)L_U(1 - \frac{C_{DB}}{C_B})}{L_O} \qquad (2)$$

Where

R_{EX} = External reflux ratio

C_{DB} = Concentration of downflow stream draining into the liquid pool at the bottom of the column (mg. moles/ml.)

L_U = Upflow liquid flow rate from the bottom pool (ml./min.)

For an infinitely tall enricher with low reflux ratios, C_{DB} is assumed to be equal to C_B which is another way of saying that the driving force at the bottom of the enriching section is zero.

$$\left(\frac{C_T}{C_B}\right)_{max.} = \frac{(R_{EX} + 1)\ G\ S\ T_B}{L_O\ C_B} + 1 \qquad (3)$$

Their experimental results have shown that Equation 3 overestimates the separation achieved for $R_{EX} > 1$, and becomes more accurate as R_{EX} approaches zero.

Walling (49) has developed a method for studying the effect of column height on foam density for a one-stage separator. From his foam density profiles, it is possible to qualitatively predict how much foam drainage is taking place. Walling measured overhead foam densities for aqueous sodium lauryl sulfate as well as four other systems, four different column heights, and various drainage times. The drainage time can be approximated by dividing the volume of the column of foam by the overhead foam rate, and this is exact for the case of negligible drainage. These experimental data were then cross-plotted for different constant foam flow rates to yield a plot of foam density versus column height. Walling found that sodium lauryl sulfate exhibited a foam flow rate region where foam density did not vary with column height, and hence foam drainage was negligible. Not all of the systems that he studied had such a region.

Lemlich and Leonard (32) have developed an equation for predicting the overhead liquid flow rate for a stripping column with negligible foam coalescence. Their model is the solution of a differential momentum balance for interstitial flow in Plateau's borders which are of noncircular cross section. This solution assumes laminar flow and Newtonian surface viscosity, and the velocity profiles had to be integrated numerically. Their model predicts foam density to be constant throughout a column section and this is contrary to a great deal of literature data. Leonard's column was not constructed properly to handle moving foam beds and so stationary foam beds were

studied in order to verify this equation. A great deal more work needs to be done in this area before reliable overhead liquid flow rates can be calculated.

Haas and Johnson (23) calculated heights of a transfer unit, based on the downflow stream, for a stripping section which concentrated the Sr-89 (sodium dodecylbenzenesulfonate)$_2$ complex. Their column had a drainage section directly over the stripping section and a drainage model was developed to predict the amount of liquid drainage entering the top of the stripping section. Many different liquid feed distributors were examined and the simple process of adding liquid through one tube at the column axis was found to be adequate for column diameters equal to or less than two inches. They gathered data on eight different liquid distributors for a six inch column and two different distributors for a 24 inch column. These studies indicated that downflow liquid channeling was the biggest problem in scaling-up column diameters above two inches. Six different types of gas spargers were tested and the importance of producing a uniform foam with small bubble diameters was observed. For the same set of conditions, stripping sections from 10 to 28 cm gave approximately the same height of a transfer unit, but stripping sections from 50 to 85 cm did not even yield the same order of magnitude height of a transfer unit as the shorter columns. These discrepancies were blamed on inaccuracies in measuring more than 8 to 10 transfer units, liquid channeling in columns greater than two inches in diameter, and inaccuracies in estimating the amount of drainage. This paper was the first step in trying to calculate heights of a transfer unit, but the results were too inconsistent to develop a correlation.

THEORY

This section presents the mathematical solutions of proposed models for estimating the separations achieved in a foam fractionation column which is composed of enriching and stripping sections. Unless otherwise referred to, these same models and equations were derived by the author of this thesis by using the standard definitions of surface excess, a one stage separator, number of transfer units, and the height of a transfer unit.

Foam is made up of a large amount of surface area and a small volume of liquid. The concentration of surfactant in the liquid is constant up to a couple of molecular diameters from the air-water interface where it increases to a higher value due to surface excess. Surface excess is the amount of surfactant at the solution surface in excess of what would be present if the bulk concentration were extended to the surface, and is expressed as excess surfactant per unit area of surface. This equilibrium surface excess is described by the Gibbs (17) equation which is given below for a dissociating surfactant.

$$\Gamma = -\frac{C}{prt}\frac{d\phi}{dC} = -\frac{1}{prt}\frac{d\phi}{d\ln C} \qquad (1)$$

The above equation was derived from thermodynamic considerations of a solution in static equilibrium and should only be applied to highly pure surfactant solutions well below the critical micelle concentration.

In this region, the surfactant molecules exist as independent entities. They only feel the effects of environmental water molecules and are not influenced by other surfactant molecules.

Adamson (1) has reviewed research which was performed by Brady on the sodium lauryl sulfate and water system. Brady was able to show that trace amounts of lauryl alcohol will greatly affect the surface tension data for this system. The Gibbs surface excess equation may not be used to predict surface excess in this thesis because the surface tension data taken by this author were similar to those taken by Brady for sodium lauryl sulfate solution contaminated with a trace of lauryl alcohol.

A. Equilibrium Equation

An equilibrium expression relating the concentration of coalesced foam to the concentration in the bulk of the liquid may be derived by studying the mathematics of a one-stage separator. The surfactant which is carried up into the foam column will be treated mathematically as two separate contributions. The first contribution is the surfactant which would have been carried up in the bulk solution if no surface excess were present and the second is surface excess. A material balance may now be written around the column of foam in Figure 1.

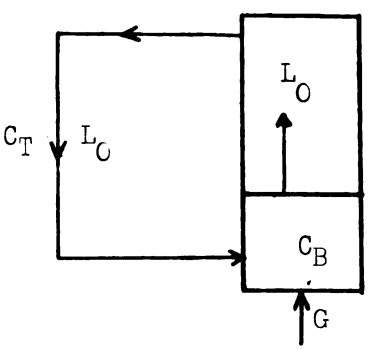

Figure 1 A One-Stage Separator

Input - Output = Accumulation

At steady state conditions, the accumulation term is zero.

$$\begin{bmatrix}\text{Surfactant entering}\\ \text{due to liquid en-}\\ \text{trained in the ris-}\\ \text{ing foam}\end{bmatrix}_I + \begin{bmatrix}\text{Surfactant entering}\\ \text{due to surface ex-}\\ \text{cess at the gas-liquid}\\ \text{interface of the foam}\end{bmatrix}_I - \begin{bmatrix}\text{Surfactant}\\ \text{leaving in}\\ \text{the top}\\ \text{product}\end{bmatrix}_O = 0$$

The first term, $L_C C_B$, takes into account surfactant which is carried along in the bulk solution around the bubbles. The second term accounts for surface excess surfactant which exists as a monomolecular layer at the interface, and is calculated by taking the product of the area to volume ratio of dodecahedron shaped bubbles $k\frac{D_A^2}{D_V^3}$, the gas flow rate G, and the surface excess T_B. The third term, $L_C C_T$, represents the rate of surfactant leaving the overhead foam breaker.

$$L_C C_B + \frac{k\, D_A^2\, G\, T_B}{D_V^3} - L_C C_T = 0 \qquad (2)$$

Equation (2) may be rearranged into the following form

$$C_T = C_B + \frac{k\, D_A^2\, G\, T_B}{D_V^3\, L_O} \qquad (3)$$

Similarly for Y_T, the above equation is divided by $C_{Soln.}$ which is the total gm moles of solute and water per cm^3 of solution.

$$\frac{C_T}{C_{Soln.}} = \frac{C_B}{C_{Soln.}} + \frac{k\, D_A^2\, G\, T_B}{C_{Soln.} D_V^3\, L_O} \qquad (4)$$

Therefore,

$$Y_T = X_B + \frac{k\, D_A^2\, G\, T_B}{C_{Soln.} D_V^3\, L_C} \qquad (5)$$

Let us assume that the surface excess T_B can be expressed as a linear function of the bulk liquid mole fraction.

$$T_B = aX_B + b \tag{6}$$

By substituting Equation (6) into (5)

$$Y_T = X_B + \frac{a\ k\ D_A^2\ G}{C_{Soln.}\ L\ C\ V^3}\ X_B + \frac{b\ k\ D_A^2\ G}{C_{Soln.}\ L\ C\ V^3} \tag{7}$$

The assumptions used in deriving Equation (7) are the following:

1) The liquid below the foam-liquid interface is thoroughly mixed and of concentration X_B.
2) If internal drainage does exist, then the bulk liquid that drains down from the column of foam has the same concentration as bottom product X_B. This assumption implies:
   a) Liquid entrained in the foam has the same concentration as bottom product X_B.
   b) Bubbles do not coalesce to form internal reflux as they rise through the column, since this would decrease the surface area and increase the concentration of bulk liquid in the foam.
3) Bubbles are dodecahedrally shaped with k = 6.59.
4) The gas-liquid interface of a bubble comes to equilibrium with the bulk liquid around it before the bubble leaves the pool of liquid and enters the column of foam.

E. <u>Definition of a Transfer Unit</u>

A foam fractionation column is analogous to a packed distillation or gas absorption column. They all are continuous countercurrent

mass transfer operations and the bubbles in a column of foam serve as rising packing. Experience in distillation and gas absorption theory (48) has shown that the concept of the height of a theoretical plate should only be applied to step-wise operations such as a plate column, and the concept of the height of a transfer unit should only be applied to continuous contact operations such as a packed tower.

A foam fractionation column of cross-sectional area A and height Z is shown in Figure 2. The differential material balance for the volume element AdZ equates the rate of mass transfer to the product of the over-all mass transfer coefficient, concentration driving force, and the area for mass transfer.

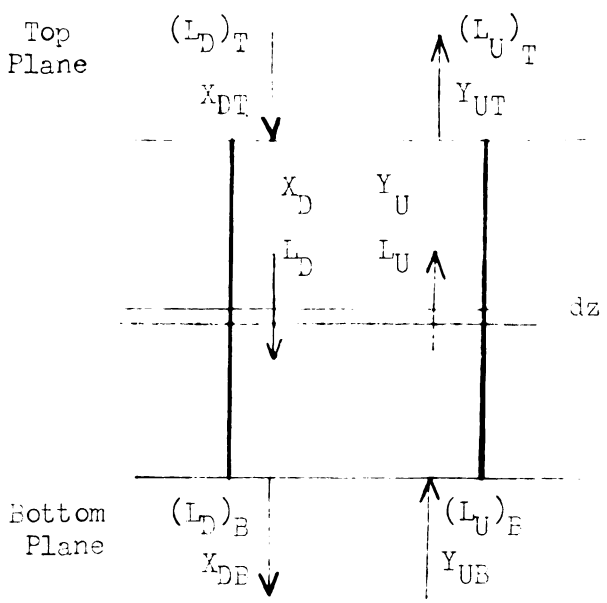

Figure 2 Enriching or Stripping Section

$$d(L_U Y_U C_{Soln.}) = k_m(Y_U^* - Y_U)\, C_{Soln.} a_m A dZ \qquad (8)$$

The upflow rate L_U is approximately constant because the mole fraction of surfactant Y_U is very small and internal foam drainage is assumed to be negligible.

Therefore,

$$C_{Soln.} L_U dY_U = k_m a_m (Y_U^* - Y_U)\, C_{Soln.} A dZ \qquad (9)$$

Rearranging terms and integrating

$$\int_{Y_{UB}}^{Y_{UT}} \frac{dY_U}{(Y_U^* - Y_U)} = \frac{k_m a_m A}{L_U} \int_0^Z dZ = \frac{k_m a_m A Z}{L_U} \qquad (10)$$

Let us define certain groups of variables in the customary way:

$$\text{Number of transfer units} = N = \int_{Y_{UB}}^{Y_{UT}} \frac{dY_U}{(Y_U^* - Y_U)}$$

$$\text{Height of a transfer unit} = H = \frac{L_U}{k_m a_m A}$$

Therefore,

$$Z = HN \qquad (11)$$

C. <u>Number of Transfer Units In An Enriching Section</u>

The enriching section shown below is assumed to have constant upflow and downflow liquid flow rates. The number of transfer units is given by

$$N_E = \int_{Y_{UB}}^{Y_{UT}} \frac{dY_U}{(Y_U^* - Y_U)} \qquad (12)$$

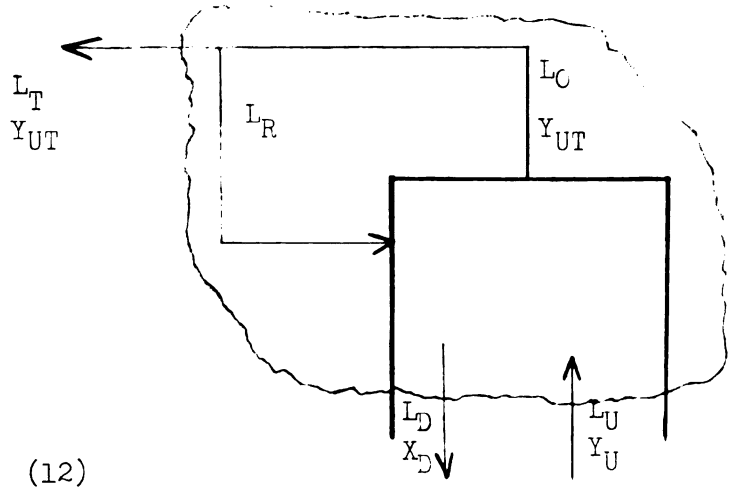

Figure 3
Upper Section of an Enriching Column

Where:

$L_U = L_O$

$L_R = L_D$

Y_{UT} = Experimentally measured top product concentration = X_T

$$Y_{UB} = X_B + \frac{a\ k\ D_A^2\ G}{C_{Soln.} L_U D_V^3}\ X_B + \frac{b\ k\ D_A^2\ G}{C_{Soln.} L_U\ D_V^3}$$

$$Y_U^* = X_D + \frac{a\ k\ D_A^2\ G}{C_{Soln.} L_U D_V^3}\ X_D + \frac{b\ k\ D_A^2\ G}{C_{Soln.} L_U D_V^3} \qquad (13)$$

$Y_{UB} \leqslant Y_U \leqslant Y_{UT}$

$X_{DB} \leqslant X_D \leqslant X_T$

X_B = Experimentally measured bottom product concentration

Material balances are given below for any arbitrary section of foam column at steady state.

Input - Output = Accumulation = 0

The material balance for the total amount of material is

$$L_U C_{Soln.} - L_D C_{Soln.} - L_T C_{Soln.} = 0$$

or

$$L_U = L_D + L_T \qquad (14)$$

and for surfactant

$$L_U Y_U C_{Soln.} - L_D X_D C_{Soln.} - L_T Y_{UT}\ C_{Soln.} = 0$$

or

$$Y_U = \frac{L_D}{L_U} X_D + \frac{L_T}{L_U} Y_{UT} \qquad (15)$$

The above linear equilibrium equation, 13, and linear operating line equation, 15, indicate (48), as derived below, that the logarithmic mean driving force is the correct average driving force to be used

in calculating the number of transfer units.

Rearranging Equation 15

$$X_D = \frac{L_U}{L_D} Y_U - \frac{L_T}{L_D} Y_{UT},$$

and then,

$$Y_U^* = \left(\frac{L_U}{L_D} Y_U - \frac{L_T}{L_D} Y_{UT}\right)\left(\frac{a\ k\ D_A^2\ G}{C_{Soln.} L_U D_V^3} + 1\right) + \frac{b\ k\ D_A^2\ G}{C_{Soln.} L_U D_V^3} \qquad (16)$$

Substituting into Equation 12

$$N_E = \int_{Y_{UB}}^{Y_{UT}} \frac{dY_U}{\left[\left(\frac{L_U}{L_D} Y_U - \frac{L_T}{L_D} Y_{UT}\right)\left(\frac{a\ k\ D_A^2\ G}{C_{Soln.} L_U D_V^3} + 1\right) + \frac{b\ k\ D_A^2\ G}{C_{Soln.} L_U D_V^3} - Y_U\right]} \qquad (17)$$

and integrating by observing that Y_U is the only variable

$$N_E = \frac{Y_{UT} - Y_{UB}}{(Y_{UT}^* - Y_{UT})_E - (Y_{UB}^* - Y_{UB})_E} \ln \frac{(Y_{UT}^* - Y_{UT})_E}{(Y_{UB}^* - Y_{UB})_E} \qquad (18)$$

or

$$N_E = \frac{Y_{UT} - Y_{UB}}{(Y_U^* - Y_U)_{LM}} \qquad (19)$$

D. Height of a Transfer Unit in an Enriching Section

The height of a transfer unit in an enriching section is calculated from experimental data by using the following expression:

$$H_E = \frac{Z_E}{N_E} \qquad (20)$$

E. Number of Transfer Units in a Stripping Section

The general expression for the number of transfer units in a stripping section with constant upflow and downflow liquid flow

rates is similar to that of an enriching section, Equation 12.

$$N_S = \int_{Y_{UB}}^{Y_{UF}} \frac{dY_U}{(Y_U^* - Y_U)} \qquad (21)$$

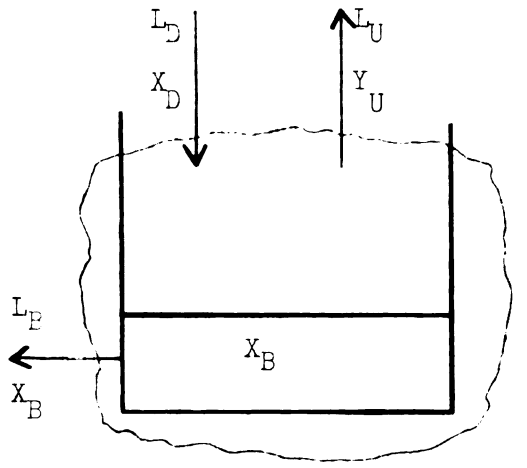

Figure 4
Lower Section of a Stripping Column

Where:

$Y_{UF} = Y_{UT}$

$L_D = L_F$

$L_U = L_C$

Y_{UF} = Experimentally measured top product concentration

$$Y_{UB} = X_B + \frac{a\ k\ D_A^2\ G}{C_{Soln.} L_U D_V^3} X_B + \frac{b\ k\ D_A^2\ G}{C_{Soln.} L_U D_V^3}$$

$$Y_U^* = X_D + \frac{a\ k\ D_A^2\ G}{C_{Soln.} L_U D_V^3} X_D + \frac{b\ k\ D_A^2\ G}{C_{Soln.} L_U D_V^3} \qquad (22)$$

$Y_{UB} \leqslant Y_U \leqslant Y_{UF}$

$X_{DB} \leqslant X_D \leqslant X_{DFB}$

X_B = Experimentally measured bottom product stream

A material balance for water and surfactant around any arbitrary lower section of a stripping section is given by

$$L_D C_{Soln.} - L_U C_{Soln.} - L_B C_{Soln.} = 0$$

or

$$L_D = L_U + L_B$$

and for surfactant

$$L_D X_D C_{Soln.} - L_B X_B C_{Soln.} - L_U Y_U C_{Soln.} = 0$$

$$Y_U = \frac{L_D}{L_U} X_D - \frac{L_B}{L_U} X_B \tag{23}$$

Similarly,

$$X_D = \frac{L_U}{L_D} Y_U + \frac{L_B}{L_D} X_B$$

and substituting into the equilibrium Equation 22

$$Y_U^* = \left(\frac{L_U}{L_D} Y_U + \frac{L_B}{L_D} X_B\right)\left(\frac{a\ k\ D_A^2\ G}{C_{Soln.} L_U D_V^3} + 1\right) + \frac{b\ k\ D_A^2\ G}{C_{Soln.} L_U D_V^3} \tag{24}$$

Substituting Equation 24 into Equation 21

$$N_S = \int_{Y_{UB}}^{Y_{UF}} \frac{dY_U}{\left[\left(\frac{L_U}{L_D} Y_U + \frac{L_B}{L_D} X_B\right)\left(\frac{a\ k\ D_A^2\ G}{C_{Soln.} L_U D_V^3} + 1\right) + \frac{b\ k\ D_A^2\ G}{C_{Soln.} L_U D_V^3} - Y_U\right]} \tag{25}$$

and integrating by observing that Y_U is the only variable

$$N_S = \frac{Y_{UF} - Y_{UB}}{(Y_{UF}^* - Y_{UF})_S - (Y_{UB}^* - Y_{UB})_S} \ln \frac{(Y_{UF}^* - Y_{UF})_S}{(Y_{UB}^* - Y_{UB})_S} \tag{26}$$

or

$$N_S = \frac{Y_{UF} - Y_{UB}}{(Y_U^* - Y_U)_{LM}} \tag{27}$$

F. <u>Height of a Transfer Unit in a Stripping Section</u>

The height of a transfer unit in a stripping section is calculated from experimental data with the help of the following expression:

$$H_S = \frac{Z_S}{N_S} \tag{28}$$

G. Total Rate of Surfactant Exchanged by Mass Transfer in Either an Enriching or Stripping Section

$$N_M = k_m a_m (Y_U^* - Y_U)_{LM} \, C_{Soln.} AZ \tag{29}$$

The above expression for the rate of surfactant mass transfer in a foam fractionation column is the integration of Equation 8 which was derived for a differential section of the column.

H. Test of the Assumption that the Upflow and Downflow Liquid Flow Rates are Constant

Rogers and Olver (41) have pointed out that in order to obtain meaningful results from enriching or stripping sections, the effects of foam drainage and internal reflux must be separated from the effects of the downflow and upflow streams. Internal reflux may be assumed negligible by observing the absence of bubble coalescence. Drainage may only be neglected if the upflow and downflow streams have constant flow rates. Walling (49) developed a method, which was discussed previously (page 8), for cross-plotting experimental data in order to find the effect of column height on overhead foam density at constant foam rates. If the overhead foam density can be shown to be constant for varying column heights at a fixed foam rate, then the upflow liquid flow rate is constant. The downflow liquid flow rate, which is composed of the external reflux stream, feed stream, or both streams, is assumed to be independent of the upflow stream and hence constant.

I. An Infinitely Tall Enriching Section with a Low External Reflux Ratio

An infinitely tall enriching section allows sufficient contact time for the downflow and upflow streams to come to equilibrium in the lower part of the foam column. A low reflux ratio allows sufficient capacity in the upflow stream to reduce the downflow stream concentration from X_{DB} to X_B. A material balance around the entire enriching section for water and surfactant gives

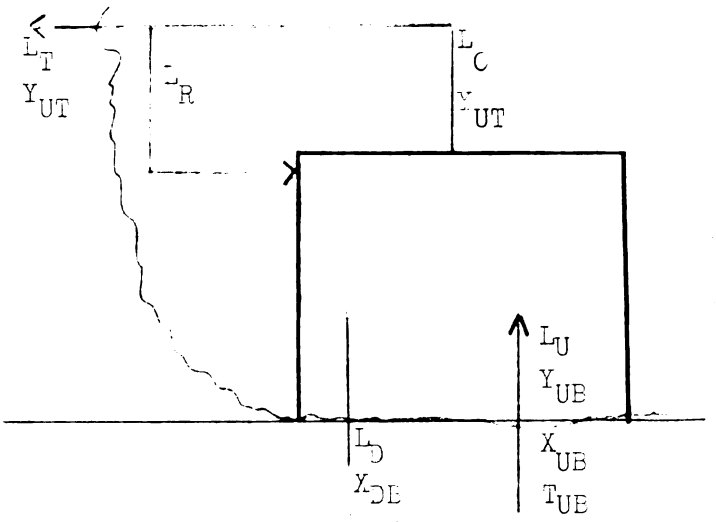

Figure 5
Infinitely Tall Enriching Section

$$L_U C_{Soln.} - L_T C_{Soln.} - L_D C_{Soln.} = 0$$

or

$$L_U = L_T + L_D \tag{30}$$

and a material balance for only surfactant yields

$$L_U Y_{UB} C_{Soln.} - L_D X_{DB}\, C_{Soln.} - L_T Y_{UT} C_{Soln.} = 0$$

Let $X_{DB} = X_B$

then

$$L_U Y_{UB} = L_D X_B + L_T Y_{UT} \tag{31}$$

Subtract the quantity $L_U X_B + L_T X_B$ from both sides of Equation 31

$$L_U Y_{UB} - L_U X_B - L_T X_B = L_D X_B - L_U X_B + L_T Y_{UT} - L_T X_B \tag{32}$$

Rearranging terms and noticing that the first term on the right hand

side of Equation 33 is zero according to Equation 30.

$$L_U(Y_{UB} - X_B) = \cancelto{0}{(L_T + L_D - L_U)}X_B + L_T(Y_{UT} - X_B) \qquad (33)$$

Rearranging terms and eliminating L_U

$$\left(\frac{Y_{UT} - X_B}{Y_{UB} - X_B}\right) = \frac{L_U}{L_T} = \frac{L_T + L_D}{L_T} = 1 + \frac{L_D}{L_T} \qquad (34)$$

Since the downflow rate in the column is constant, therefore $L_R = L_D$ and

$$\left(\frac{Y_{UT} - X_B}{Y_{UB} - X_B}\right) = 1 + \frac{L_R}{L_T} = 1 + R_{EX} \qquad (35)$$

Equation 35 relates the number of stages of separation to the external reflux ratio.

J. <u>Deriving Expressions for the Driving Forces in an Enriching Section</u>

1) <u>Driving force at the top of an enriching section</u> - This driving force is simply described by noticing that Y^*_{UT} is in equilibrium with X_T and that $X_T = Y_{UT}$.

$$(Y^*_{UT} - Y_{UT})_E = X_T + \frac{k\, D_A^2\, G}{C_{Soln.} L_C D_V^3}\, T_T - Y_{UT}$$

$$(Y^*_{UT} - Y_{UT})_E = \frac{k\, D_A^2\, G}{C_{Soln.} L_C D_V^3}\, T_T \qquad (36)$$

Where $L_O = L_U$ and $T_T = aX_T + b$.

2) <u>Driving force at the bottom of an enriching section</u> - This model separates the surfactant in the upflow foam into two contributions which are calculated by assuming $X_{UB} = X_B$ and $T_{UB} = T_B$. The total material balance is the same as before.

$$L_U C_{Soln.} - L_D C_{Soln.} - L_T C_{Soln.} = 0$$

or

$$L_U = L_D + L_T \tag{37}$$

In the material balance for surfactant, surface excess and bulk solution are shown as two terms.

$$L_U X_{UB} C_{Soln.} + \frac{k\, D_A^2\, G\, T_{UB}}{D_V^3} - X_{DB} L_D C_{Soln.} - Y_{UT} L_T C_{Soln.} = 0 \tag{38}$$

Since $X_{UB} = X_B$ and $T_{UB} = T_B$, then

$$X_{DB} L_D = L_U X_B + \frac{k\, D_A^2\, G\, T_B}{C_{Soln.} D_V^3} - Y_{UT} L_T$$

Using Equation 37 to eliminate L_U and solving for X_{DB}

$$X_{DB} = X_B + \frac{L_T}{L_D} X_B + \frac{k\, D_A^2\, G\, T_B}{C_{Soln.} L_D D_V^3} - \frac{L_T}{L_D} Y_{UT}$$

and since $T_B = aX_B + b$

$$X_{DB} = X_B + \frac{L_T}{L_D} X_B + \frac{a\, k\, D_A^2\, G}{C_{Soln.} L_D D_V^3} X_B + \frac{b\, k\, D_A^2\, G}{C_{Soln.} L_D D_V^3} - \frac{L_T}{L_D} Y_{UT} \tag{39}$$

The mathematical expression which describes the driving force at the bottom of an enriching section is given by

$$(Y_{UB}^* - Y_{UB})_E = \left[X_{DB} + \frac{a\, k\, D_A^2\, G}{C_{Soln.} L_C D_V^3} X_{DB} + \frac{b\, k\, D_A^2\, G}{C_{Soln.} L_C D_V^3}\right]$$

$$- \left[X_{UB} + \frac{a\, k\, D_A^2\, G}{C_{Soln.} L_C D_V^3} X_{UB} + \frac{b\, k\, D_A^2\, G}{C_{Soln.} L_C D_V^3}\right] \tag{40}$$

Since $X_{UB} = X_B$

$$(Y_{UB}^* - Y_{UB})_E = \left[X_{DB} + \frac{a\, k\, D_A^2\, G}{C_{Soln.} L_C D_V^3} X_{DB}\right] - \left[X_B + \frac{a\, k\, D_A^2\, G}{C_{Soln.} L_C D_V^3} X_B\right] \tag{41}$$

Eliminating X_{DB} from Equation 41 by combining with Equation 39 yields

$$(Y^*_{UB} - Y_{UB})_E = \left[\frac{k\,D_A^2\,G}{C_{Soln.}L_D D_V^3}\,T_B - \frac{L_T}{L_D}(Y_{UT} - X_B)\right]\left(1 + \frac{a\,k\,D_A^2\,G}{C_{Soln.}L_C D_V^3}\right) \tag{42}$$

For the special case of an enriching section in the state of total external reflux, Equation 36 gives the driving force at the top of the enriching section. Since $L_T = 0$, Equation 42 for the driving force at the bottom of the enriching section reduces to the following expression:

$$(Y^*_{UB} - Y_{UB})_E = \frac{k\,D_A^2\,G}{C_{Soln.}L_D D_V^3}\,T_B\left(1 + \frac{a\,k\,D_A^2\,G}{C_{Soln.}L_C D_V^3}\right) \tag{43}$$

where $L_D = L_C$.

K. <u>A Stripping Section of Finite Height</u>

In a stripping section of finite height, the foam stream Y_{UF} rising past the feed point is not in equilibrium with the feed stream X_F. An excellent empirical approximation to this non-equilibrium foam concentration is to assume that the bulk of the liquid is at concentration X_F and the surface excess is equal to T_B. A material balance around the entire stripping section for water and surfactant results in

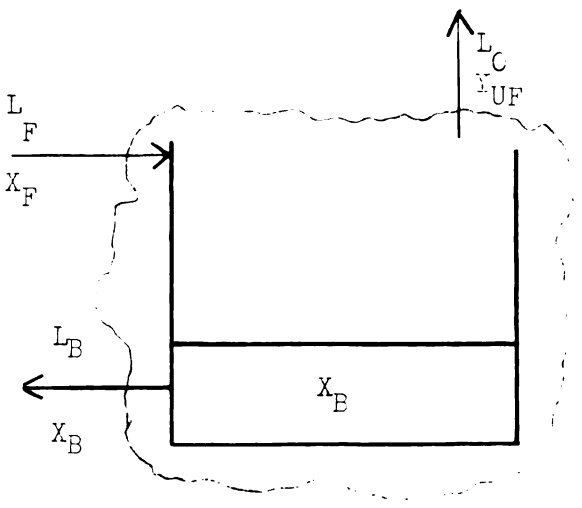

Figure 6
A Stripping Section of Finite Height

$$L_F C_{Soln.} - L_O C_{Soln.} - L_B C_{Soln.} = 0$$

or

$$L_F = L_O + L_B \tag{44}$$

and just for surfactant

$$X_F L_F C_{Soln.} - L_C Y_{UF} C_{Soln.} - L_B X_B C_{Soln.} = 0$$

$$L_B X_B = X_F L_F - L_C Y_{UF} \tag{45}$$

Substituting Equation 44 into Equation 45 and eliminating L_F

$$X_B = X_F \left(\frac{L_O}{L_B} + 1\right) - Y_{UF} \left(\frac{L_C}{L_B}\right) \tag{46}$$

Replacing Y_{UF} with its equilibrium expression where $X_{UF} = X_F$ and $T_{UF} = T_B$

$$X_B = X_F\left(\frac{L_C}{L_F} + 1\right) - \left(X_F + \frac{a\ k\ D_A^2\ G}{C_{Soln.} L_C D_V^3} X_B + \frac{b\ k\ D_A^2\ G}{C_{Soln.} L_C D_V^3}\right) \frac{L_C}{L_B}$$

or

$$X_B = X_F - \left(\frac{a\ k\ D_A^2\ G}{C_{Soln.} L_C D_V^3} X_B + \frac{b\ k\ D_A^2\ G}{C_{Soln.} L_C D_V^3}\right) \frac{L_C}{L_B} \tag{47}$$

The total number of stages in this stripping section is the total separation $(Y_{UF} - X_B)$ divided by the one stage separation $(Y_{UB} - X_B)$

$$\frac{Y_{UF} - X_B}{Y_{UB} - X_B} = \frac{X_F + \frac{a\ k\ D_A^2\ G}{C_{Soln.} L_C D_V^3} X_B + \frac{b\ k\ D_A^2\ G}{C_{Soln.} L_C D_V^3} - X_B}{X_B + \frac{a\ k\ D_A^2\ G}{C_{Soln.} L_C D_V^3} X_B + \frac{b\ k\ D_A^2\ G}{C_{Soln.} L_C D_V^3} - X_B}$$

or

$$\frac{Y_{UF} - X_B}{Y_{UB} - X_B} = \frac{X_F + \frac{a\ k\ D_A^2\ G}{C_{Soln.} L_C D_V^3} X_B + \frac{b\ k\ D_A^2 G}{C_{Soln.} L_C D_V^3} - X_B}{\frac{a\ k\ D_A^2\ G}{C_{Soln.} L_C D_V^3} X_B + \frac{b\ k\ D_A^2\ G}{C_{Soln.} L_C D_V^3}} \tag{48}$$

Substituting X_B from Equation 47 into the fourth term in the numerator of Equation 48 yields

$$\frac{Y_{UF} - X_B}{Y_{UB} - X_B} = \frac{X_F + \frac{aK D_A^2 G}{C_{soln.} L_o D_V^3} X_B + \frac{bK D_A^2 G}{C_{soln.} L_o D_V^3} - X_F + \left(\frac{aK D_A^2 G}{C_{soln.} L_o D_V^3} X_B + \frac{bK D_A^2 G}{C_{soln.} L_o D_V^3}\right)\frac{L_o}{L_B}}{\frac{aK D_A^2 G}{C_{soln.} L_o D_V^3} X_B + \frac{bK D_A^2 G}{C_{soln.} L_o D_V^3}}$$

and this reduces upon simplification to

$$\frac{Y_{UF} - X_B}{Y_{UB} - X_B} = 1 + \frac{L_C}{L_B} \qquad (49)$$

Equation 49 for a finite stripping section is identical in form to Equation 35 for an enriching section since the ratio L_O/L_B is analogous to the external reflux ratio $R_{EX} = L_R/L_T$.

L. <u>Expressions for the Driving Forces in a Stripping Section</u>

1) <u>Driving force at the top of a stripping section</u> — This expression is similar to Equation 36 and is derived by noticing that Y^*_{UF} is in equilibrium with X_F.

$$(Y^*_{UF} - Y_{UF})_S = X_F + \frac{k D_A^2 G}{C_{Soln.} L_O D_V^3} T_F - Y_{UF} \qquad (50)$$

where $T_F = aX_F + b$

2) <u>Driving force at the bottom of a stripping section</u> - This driving force is derived by observing that the foam which leaves the pool of liquid is in equilibrium with

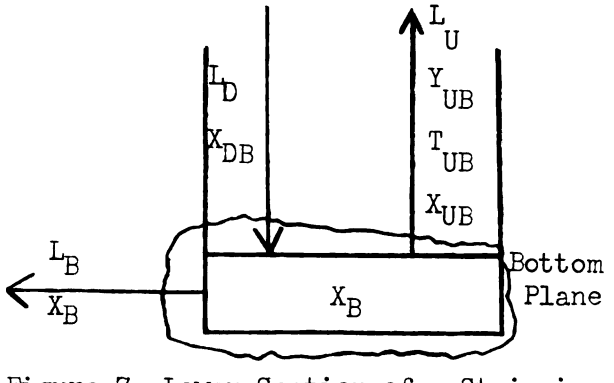

Figure 7 Lower Section of a Stripping Column

it. Thus in calculating the concentration of the foam as it leaves the liquid pool, $X_{UB} = X_B$ and $T_{UB} = T_B$.

The material balance around the liquid pool for water and surfactant yields

$$L_D C_{Soln.} - L_U C_{Soln.} - L_B C_{Soln.} = 0$$

or

$$L_D = L_U + L_B \tag{51}$$

and just for surfactant

$$X_{DB} L_D C_{Soln.} - X_B L_B C_{Soln.} - X_{UB} L_U C_{Soln.} - \frac{k\, D_A^2\, G\, T_{UB}}{D_V^3} = 0$$

Rearranging terms and replacing X_{UB} by X_B and T_{UB} by T_B

$$X_{DB} L_D = (L_B + L_U) X_B + \frac{k\, D_A^2\, G\, T_B}{C_{Soln.}\, D_V^3}$$

Since $L_D = L_B + L_U$ and $T_B = aX_B + b$, then

$$X_{DB} = X_B + \frac{a\, k\, D_A^2\, G}{C_{Soln.}\, L_D D_V^3} X_B + \frac{b\, k\, D_A^2\, G}{C_{Soln.}\, L_D D_V^3} \tag{52}$$

The expression for the driving force at the bottom of a stripping section is written by observing that Y^*_{UB} is in equilibrium with X_{DB}

$$(Y^*_{UB} - Y_{UB})_S = \left[X_{DB} + \frac{a\, k\, D_A^2\, G}{C_{Soln.}\, L_O D_V^3} X_{DB} + \frac{b\, k\, D_A^2\, G}{C_{Soln.}\, L_O D_V^3}\right] - \left[X_{UB} + \frac{a\, k\, D_A^2\, G}{C_{Soln.}\, L_O D_V^3} X_{UB} + \frac{b\, k\, D_A^2\, G}{C_{Soln.}\, L_O D_V^3}\right] \tag{53}$$

Substituting Equation 52 into Equation 53 to eliminate X_{DB} and replacing X_{UB} by X_B results in

$$(Y^*_{UB} - Y_{UB})_S = \frac{k\, D_A^2\, G\, T_B}{C_{Soln.} L_D D_V^3}\left(1 + \frac{a\, k\, D_A^2\, G}{C_{Soln.} L_O D_V^3}\right) \tag{54}$$

At the state of total overhead, the expressions for the driving forces in a stripping section are identical to Equations 50 and 54. The only difference being that since $L_B = 0$, then the upflow rate L_O is equal to the downflow rate L_D.

M. <u>A Foam Column with Enriching and Stripping Sections</u>

Most of the equations derived previously may be applied to the combined foam fractionation column. The only exceptions are that the bottom of the enriching section now rests upon the top of the stripping section instead of a pool of liquid of concentration X_B, and the downflow entering the stripping section is a mixture of extracted reflux and feed instead of just feed.

Equations 12 and 18 may not be used to calculate the number of transfer units in the enriching section because the limits of integration are wrong for the combined column. The correct expressions are:

$$N_E = \int_{Y_{UF}}^{Y_{UT}} \frac{dY_U}{(Y^*_U - Y_U)} \tag{55}$$

and therefore

$$N_E = \frac{Y_{UT} - Y_{UF}}{(Y^*_{UT} - Y_{UT})_E - (Y^*_{UF} - Y_{UF})_E} \ln \frac{(Y^*_{UT} - Y_{UT})_E}{(Y^*_{UF} - Y_{UF})_E} \tag{56}$$

The driving force at the top of the enriching section is given by Equation 36. Equation 42 may not be used to calculate the driving force at the bottom of the enriching section in a combined column of foam because Y_{UF} is the concentration of foam rising into this section instead of Y_{UB}.

Figure 8 displays the new symbols necessary in order to derive this driving force. The material balance for water and surfactant around the entire enriching section is given by

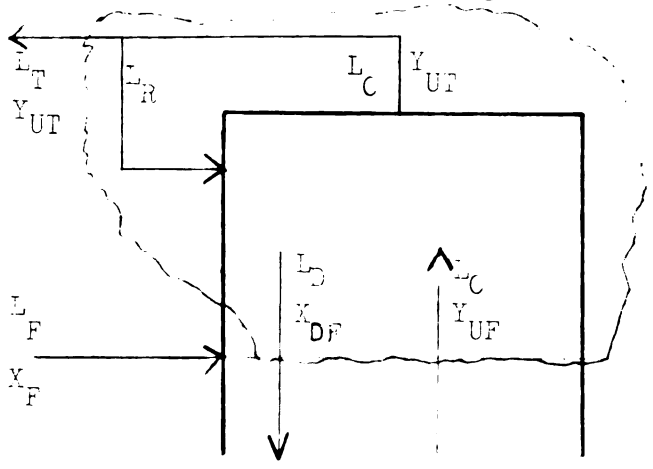

Figure 8
Enriching Section in a Combined Column

$$L_C C_{Soln.} - L_D C_{Soln.} - L_T C_{Soln.} = 0$$

or

$$L_C = L_D + L_T \tag{57}$$

and only for surfactant

$$L_C Y_{UF} C_{Soln.} - L_D X_{DF} C_{Soln.} - L_T Y_{UT} C_{Soln.} = 0$$

or

$$L_D X_{DF} = L_C Y_{UF} - L_T Y_{UT} \tag{58}$$

Eliminating L_C from Equation 58 with the help of Equation 57

$$X_{DF} = \left(\frac{L_T}{L_D} + 1\right) Y_{UF} - Y_{UT}\left(\frac{L_T}{L_D}\right)$$

Since $L_D = L_R$ in an enriching section

$$X_{DF} = \left(\frac{L_T}{L_R} + 1\right) Y_{UF} - Y_{UT}\left(\frac{L_T}{L_R}\right) \tag{59}$$

The expression for the driving force at the bottom of an enriching section in a combined column may be written by observing that Y^*_{UF} is in equilibrium with X_{DF}.

$$(Y^*_{UF} - Y_{UF})_E = \left(X_{DF} + \frac{k\, D_A^2\, G}{C_{Soln.} L_C D^3 V}\, T_{DF}\right) - Y_{UF} \tag{60}$$

Where

Y_{UF} = Experimentally unknown foam concentration at the feed point

$T_{DF} = aX_{DF} + b$

Substituting Equation 59 into Equation 60 to eliminate X_{DF} and T_{DF}

$$(Y^*_{UF} - Y_{UF})_E = \left(\frac{L_T}{L_R}\right)(Y_{UF} - Y_{UT}) + \frac{a\, k\, D_A^2\, G}{C_{Soln.} L_C D^3 V}$$

$$\left[\left(\frac{L_T}{L_R} + 1\right) Y_{UF} - \left(\frac{L_T}{L_R}\right) Y_{UT}\right] + \frac{b\, k\, D_A^2\, G}{C_{Soln.} L_C D^3 V} \tag{61}$$

In the stripping section, Equation 26 may be used to calculate the number of transfer units and Equation 54 describes the driving force at the bottom of the stripping section with $L_D = L_R + L_F$. Equation 50 may not be used to calculate the driving force at the top of this section because the downflow liquid stream enters the top of the stripping section at concentration X_{DFB} instead of concentration X_F or X_{DF}.

The material balance for water and surfactant in the downflow

stream at the feed point is given by

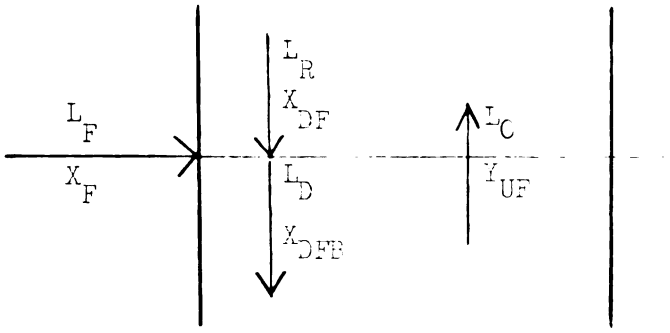

Figure 9 Feed Point in a Combined Column

$$L_R C_{Soln.} + L_F C_{Soln.} - L_D C_{Soln.} = 0$$

or

$$L_D = L_R + L_F \tag{62}$$

and just for surfactant

$$L_R X_{DF} C_{Soln.} + L_F X_F C_{Soln.} - L_D X_{DFB} C_{Soln.} = 0$$

or

$$L_D X_{DFB} = L_R X_{DF} + L_F X_F \tag{63}$$

Eliminating L_D from Equation 63

$$X_{DFB} = \frac{L_R X_{DF} + L_F X_F}{L_R + L_F} \tag{64}$$

The expression for the driving force at the top of the stripping section in a combined column is written by noticing that Y^*_{UF} is in equilibrium with X_{DFB}.

$$(Y^*_{UF} - Y_{UF})_S = X_{DFB} + \frac{k\, D_A^2\, G}{C_{Soln.} L_O \epsilon_V^3}\, T_{DFB} - Y_{UF} \tag{65}$$

Where

Y_{UF} = Experimentally unknown foam concentration at the feed point

$$T_{DFB} = aX_{DFB} + b$$

Combining Equations 64 and 65 in order to eliminate X_{DFB} and T_{DFB}

$$(Y^{*}_{UF} - Y_{UF})_S = \left(\frac{L_R X_{DF} + L_F X_F}{L_R + L_F}\right)\left(1 + \frac{a\ k\ D_A^2\ G}{C_{Soln.}\ L_C D_3 V}\right) + \frac{b\ k\ D_A^2\ G}{C_{Soln.}\ L_C D_3 V} - Y_{UF} \tag{66}$$

L. Summary

The equations given above, unless otherwise referred to, were derived by the author in an effort to present a mathematical model for a continuous foam fractionator. Some of the above equations were used to calculate driving forces for mass transfer in a column of foam. The logarithmic mean driving force was calculated from these driving forces and it was divided into the foam column separation in order to calculate the number of transfer units. The height of a transfer unit was found by dividing the number of transfer units into the height of an enriching or a stripping section. This height of a transfer unit is a measure of how efficient a countercurrent mass transfer section is in utilizing the available driving force under a given set of conditions. A correlation for these experimental heights of a transfer unit versus some group variables would give a means of predicting separations. The following sections of this thesis are presented in order to show the experimental justification of this model.

EXPERIMENTAL METHODS

Standard solutions of sodium lauryl sulfate or potassium chloride were prepared by weighing out the salt on a Sartorius Selecta balance and adding it to a measured volume of distilled water.

Surface tensions of the air-water interface were determined at various concentrations of sodium lauryl sulfate by the use of a Cenco-DuNouy Tensiometer with a four centimeter platinum ring. The experimental surface tension of water distilled in metal was found to be 70.7 dynes/cm and this compared favorably to the literature value for highly distilled water of 71.9 dynes/cm.

A platinum electrode cell in conjunction with a conductivity bridge (Industrial Instruments Inc., model RC-18) was used to measure the bottom product, feed, and top product conductances. Figure 10 is the calibration curve of specific conductance as a function of sodium lauryl sulfate concentration. Specific conductance is defined as the product of conductance and the cell constant. A correlation for specific conductance was necessary in order to calculate the concentrations of product streams from the foam fractionator. Special care was taken in measuring conductance readings. The cell was always filled with distilled water when it was stored. The cell constant was determined at regular intervals with a standard potassium chloride solution (0.0200 molar aqueous KCl, specific conductance = 0.002768 ohm^{-1} cm^{-1}) in order to correct for slight changes. Unknown

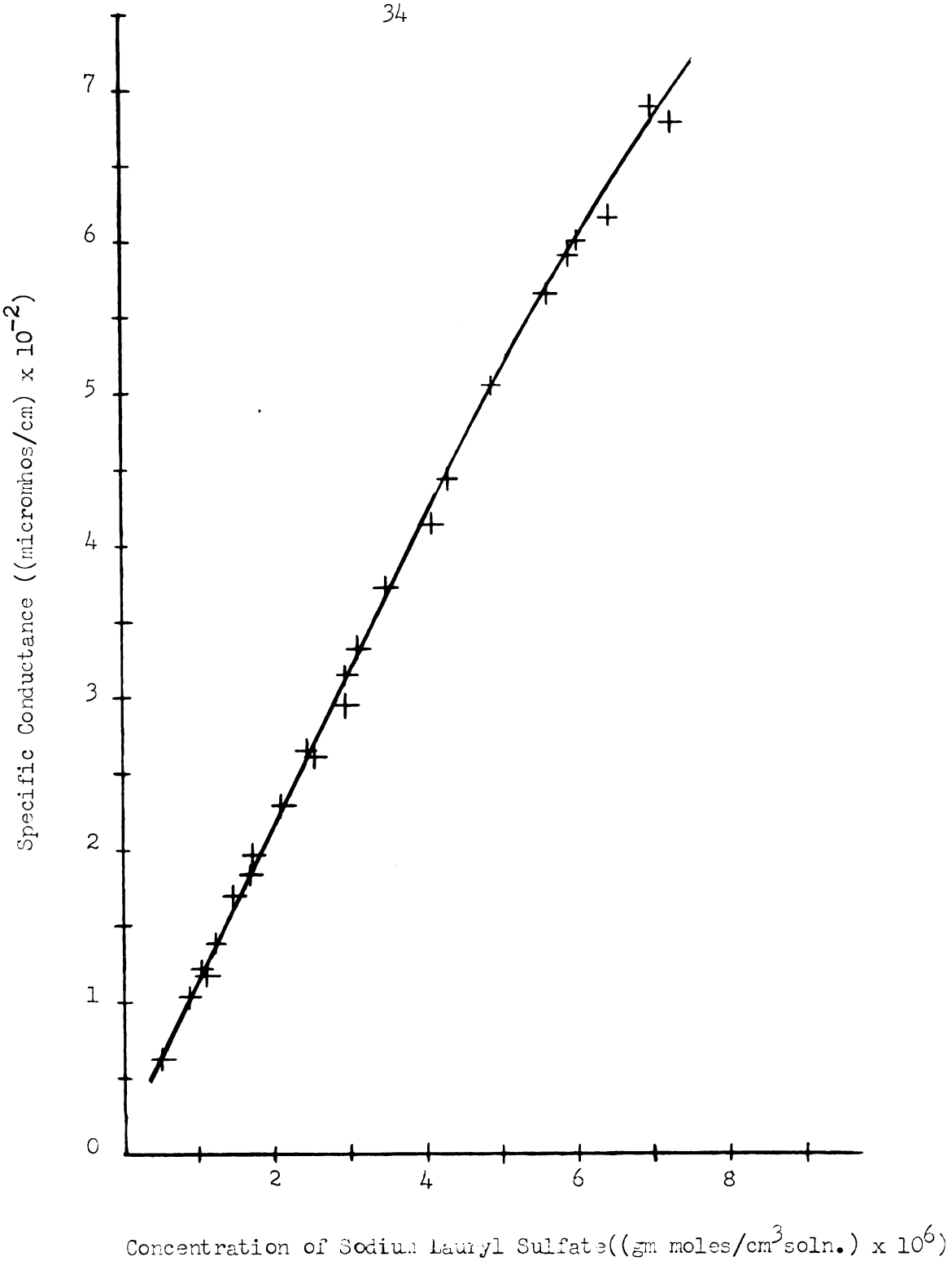

Figure 10 Calibration Curve for the Conductivity Cells.

solutions were used to rinse the cell as many as six times before a reading was taken. This method was repeated until successive readings remained constant.

Gas flow rates were measured with a wet test meter and electric timer. The wet test meter was checked by positive displacement and found to be accurate to within 2-3%. The relative humidity of the air used to generate foam was assumed to be 100% because the relative humidity was 98% at one hundred times the normal gas flow rate. Liquid flow rates were measured with a graduated cylinder and timer, as well as with Brook's precision rotameters (R-2-15A and R-2-15B). Feed and reflux solution were pumped into different parts of the column by diaphragm pumps and flow rates were adjusted with Hoke precision metering valves. Each liquid distributor was made up of a single glass tube discharging liquid along the vertical axis of the column. Liquid levels were controlled by gravity and Hoke precision metering valves. Gas bubbles were produced by forcing air through four sintered glass spargers and the foam was coalesced by centrifugal force in a stainless steel screen basket.

A Nikon F Reflex Camera was used to take pictures of a one square centimeter section of wall bubbles, and the negatives were enlarged to three and one-half by four and one-half inch pictures. These pictures were then enlarged on a Kodagraph Microprint Reader. The overall magnification of the process was 200 times. In order to determine the area averaged (D_A) and volume averaged (D_V) bubble diameters, the bubble diameters of a randomly selected zone of bubbles were measured.

The combined column experimental equipment and accessories were set up as shown in Figure 11. This foam fractionation column was studied as a one stage separator, an enriching section, a stripping section, and a combined column. Prescribed amounts of sodium lauryl sulfate and distilled water were added to the feed tank. Air which was humidified with water was bubbled into the column for 2 to 14 hours while column variables were adjusted and time was allowed to reach steady state. Repetitive samples were taken from each stream until successive readings remained constant. Then all of the other important variables such as gas flow rate, bubble diameters, and liquid flow rates were measured.

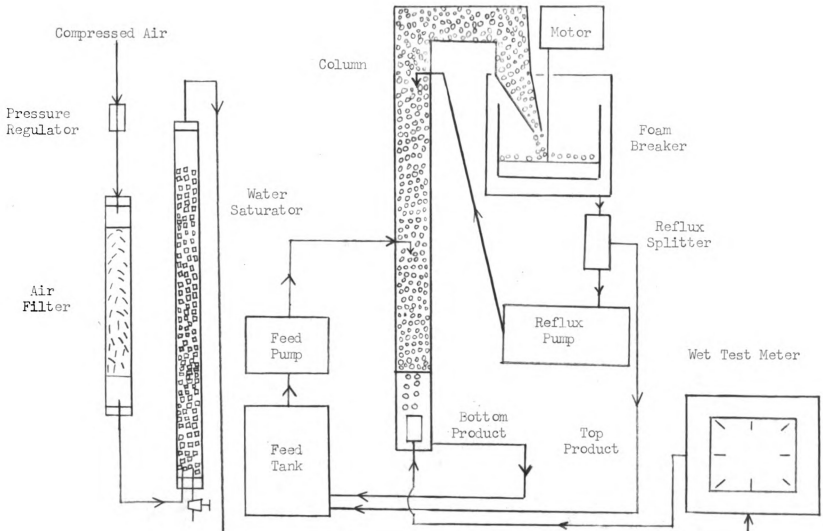

Figure 11 Diagram of the Foam Fractionation Apparatus.

EXPERIMENTAL RESULTS

The development of the equilibrium equation which was used to predict multi-staged separations in this thesis can be traced by examining the first four figures in this section.

As previously explained in the Theory section, surface excess could not be predicted from the Gibbs equation and the surface tension data for aqueous sodium lauryl sulfate solutions as shown in Figure 12, because the surface excess was never zero or negative in the model region as the Gibbs equation would indicate. Experimental data from a one-stage separator have shown that positive surface excess does exist up to a concentration of 10^{-5} gm moles $NaC_{12}H_{25}SO_4/cm^3$ solution.

The diameters of bubbles formed at a sparger are a function of system geometry, bubble formation pressure, and the surface tension of surfactant solution. Since all three of these do not vary over the model region, the area and volume averaged bubble diameters are constant as shown in Figure 13.

In this same model region, the surface excess for a one-stage separator was found to be a linear function of the bottom product mole fraction. A least squares fit to the data is shown in Figure 14. This surface excess equation was then substituted into the equilibrium expression and an equation which relates foam concentration to bulk liquid concentration was derived. Figure 15 is a comparison

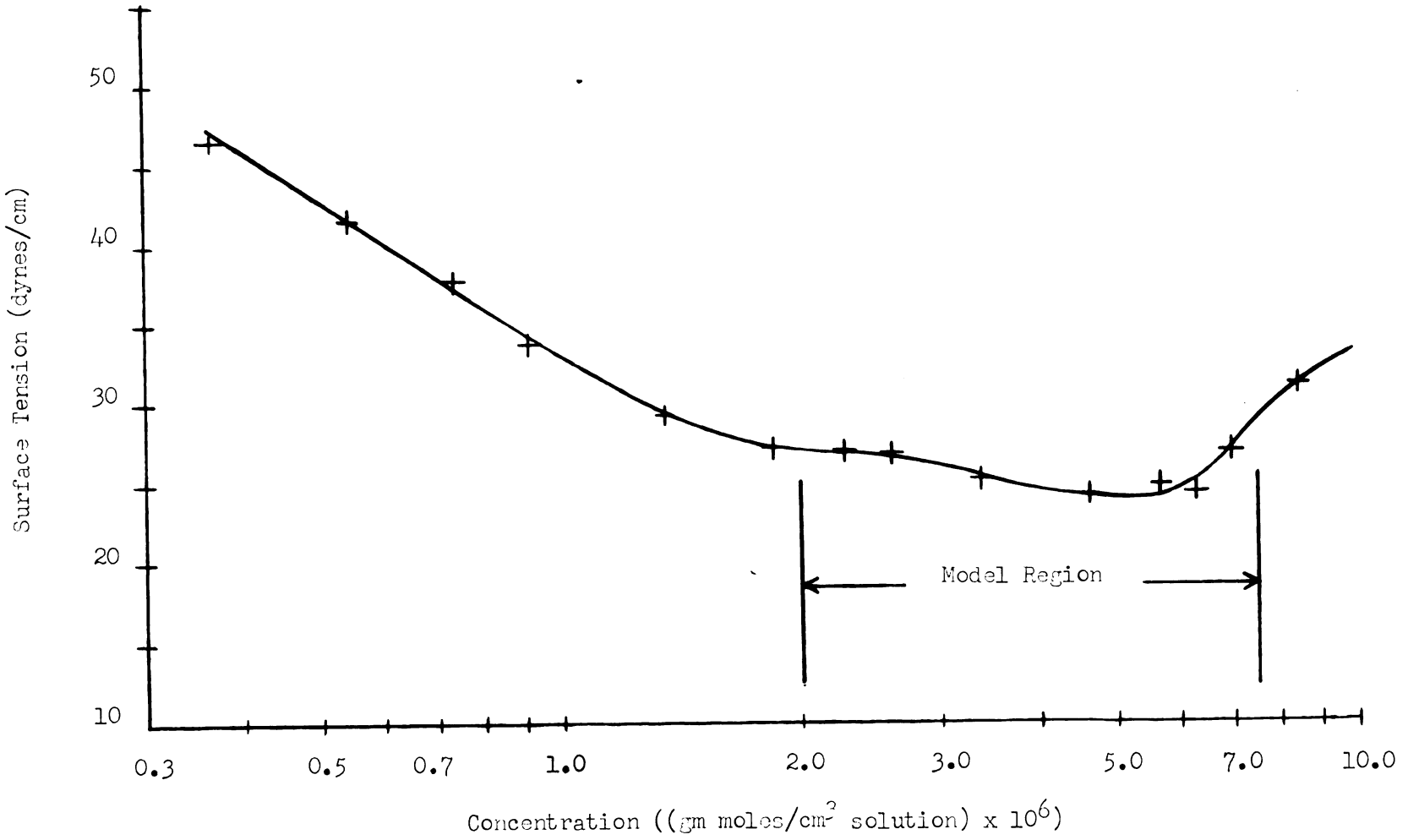

Figure 12 Surface Tension as a Function of Sodium Lauryl Sulfate Concentration.

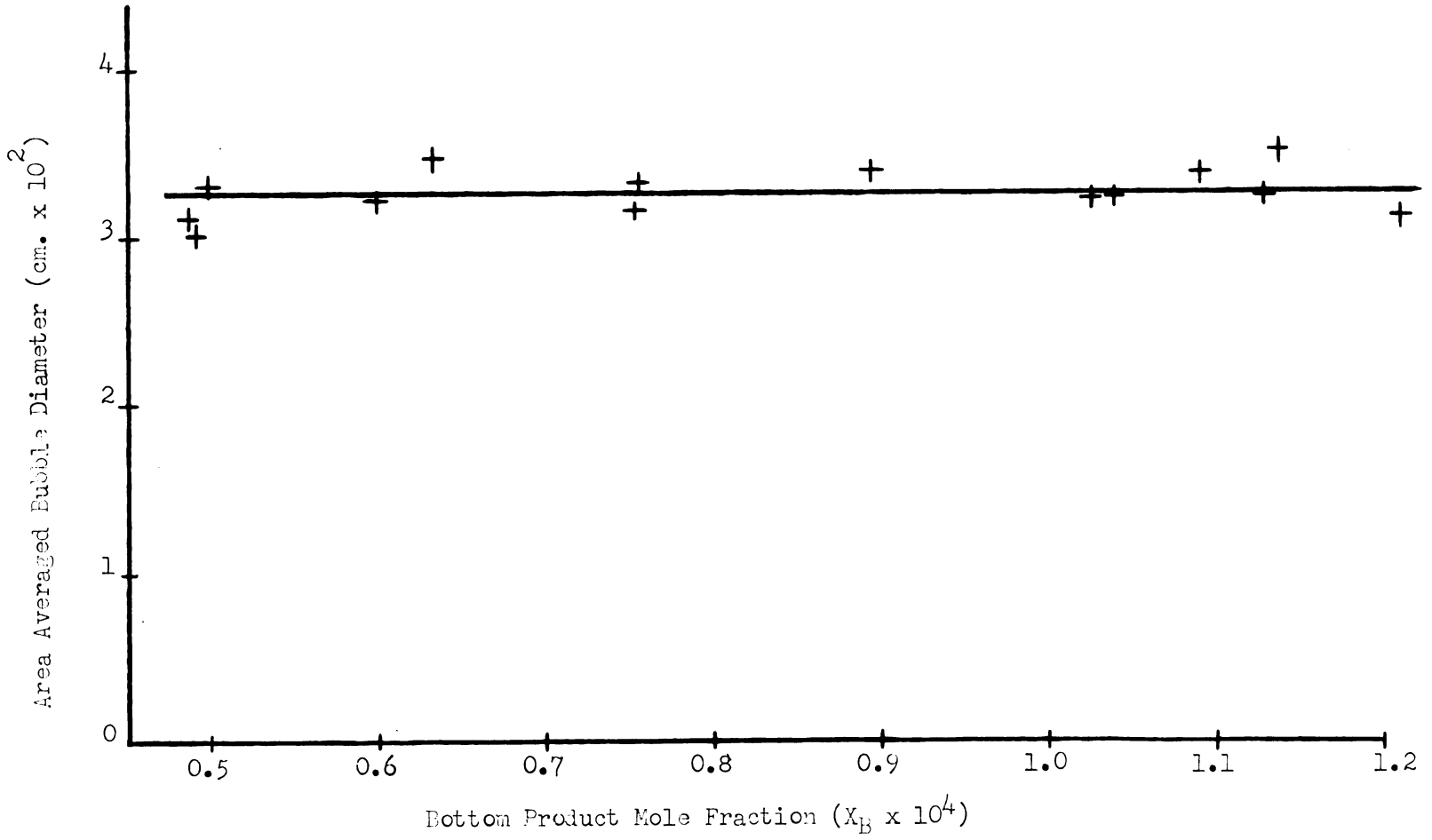

Figure 13 Area Averaged Bubble Diameter as a Function of Bottom Product Mole Fraction.

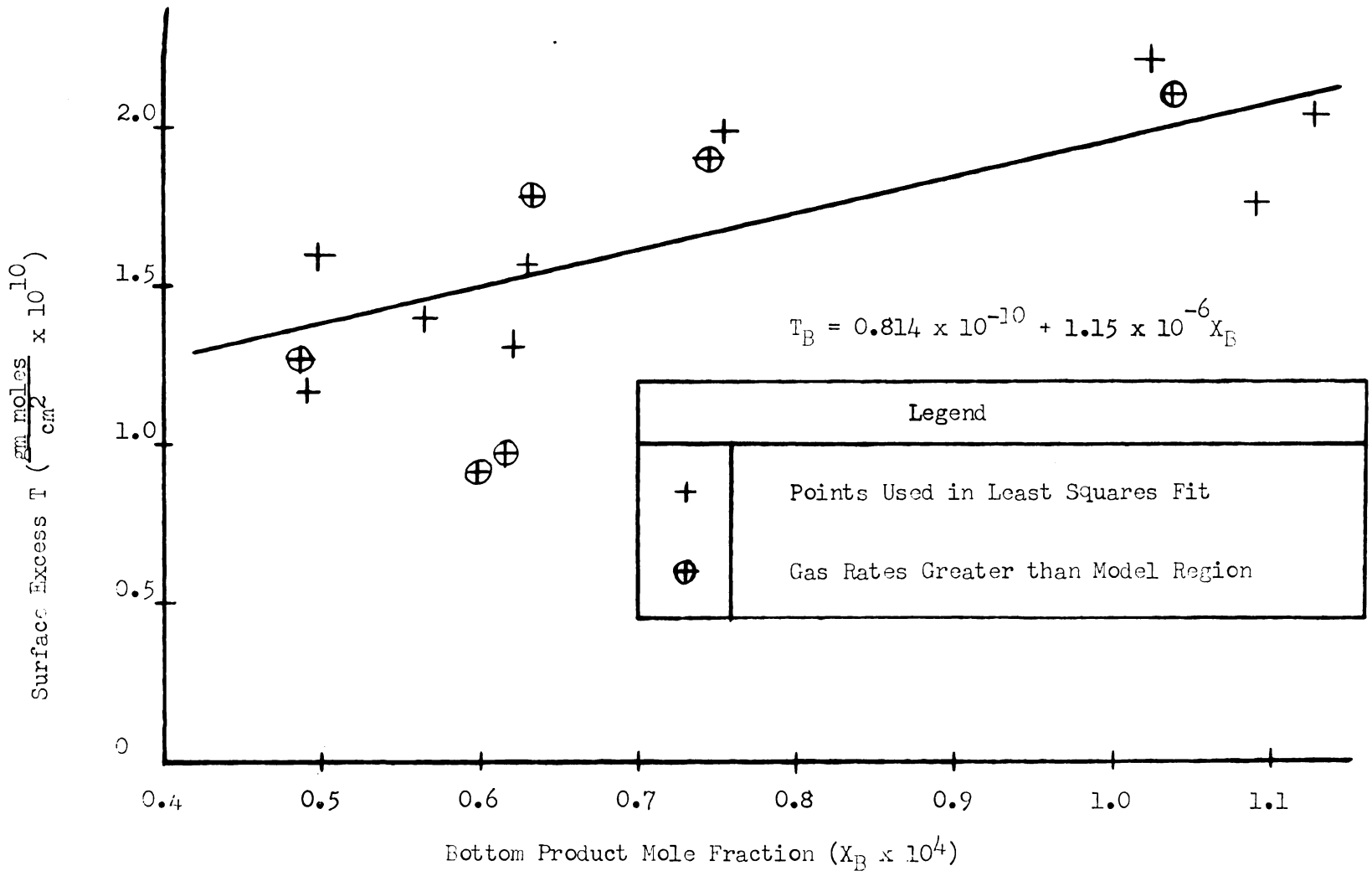

Figure 14 Surface Excess as a Linear Function of Bottom Product Concentration.

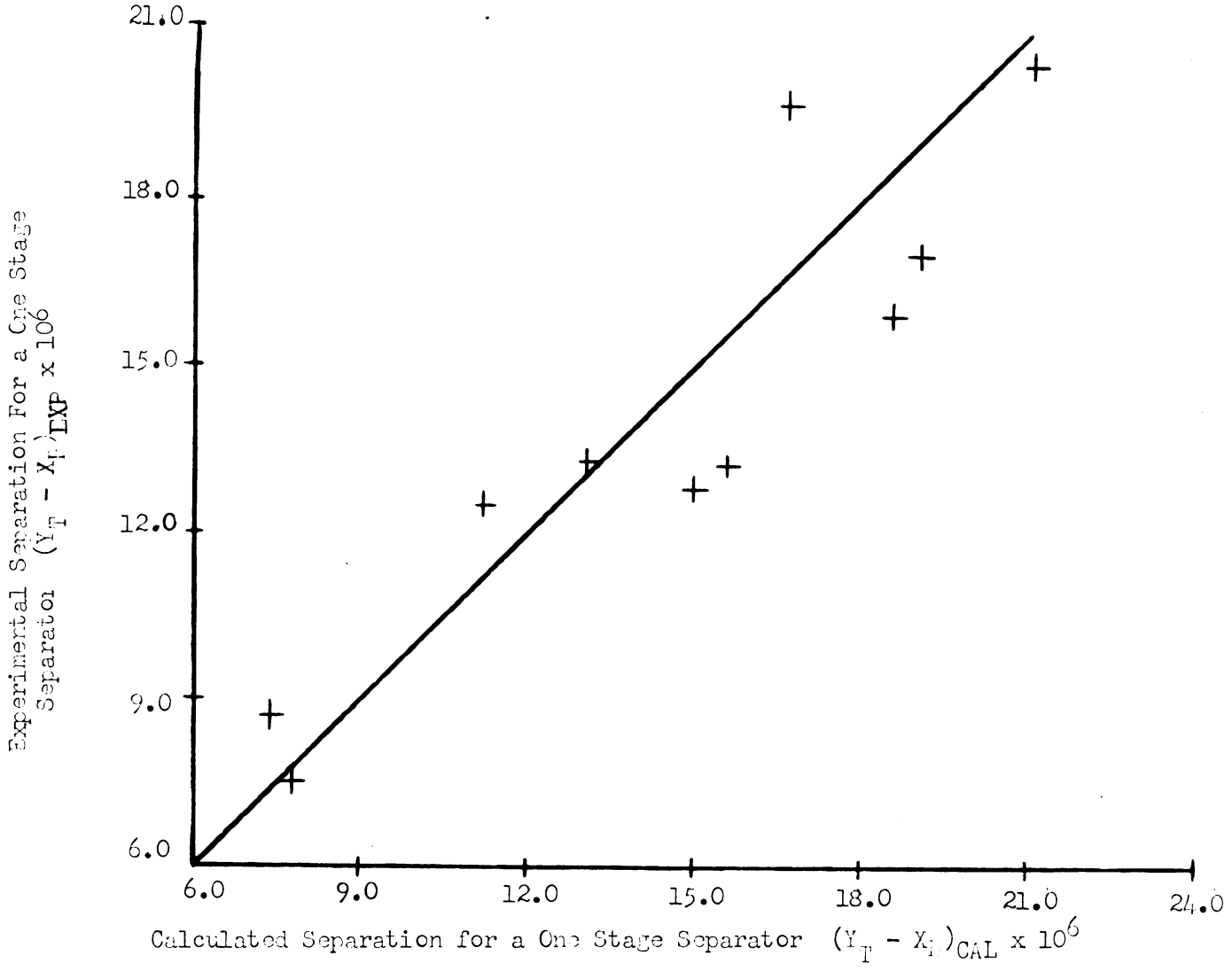

Figure 15 Test of the Equilibrium Relationship on a One Stage Separator.

between calculated separations from this equilibrium expression and experimental separations for a one-stage separator. They are in agreement within $\pm$ 15%.

In the next group of figures (16-19), evidence is given which supports the assumption of constant foam density in the column of foam of this thesis. Experimental foam densities were plotted in Figures 16 and 17 according to the method of Walling (49). The bubble residence time which is used in these illustrations is just another expression for Walling's foam drainage time. Figures 18 and 19 are cross-plots of the two previous figures at various constant foam rates. Both of these figures indicate that overhead foam density is not affected appreciably by changes in column height, and hence foam drainage may be neglected in a one-stage foam fractionator. This result was then carried over to enriching and stripping sections by assuming the upflow and downflow streams to be independent of one another.

A comparison of experimental data with a model for an infinitely tall enriching section is shown in Figure 20. Since the experimental data points follow the theoretical curve so closely, the driving force can be assumed to be nearly zero at the bottom and finite at the top of an enriching section taller than 42.5 inches. The sharp increase in the slope of this curve displays the merit of using reflux to increase the separation over that obtained with a single stage. As the top product rate approaches zero, i. e. - at total reflux, the experimental data indicate an increase in the deviation from this model.

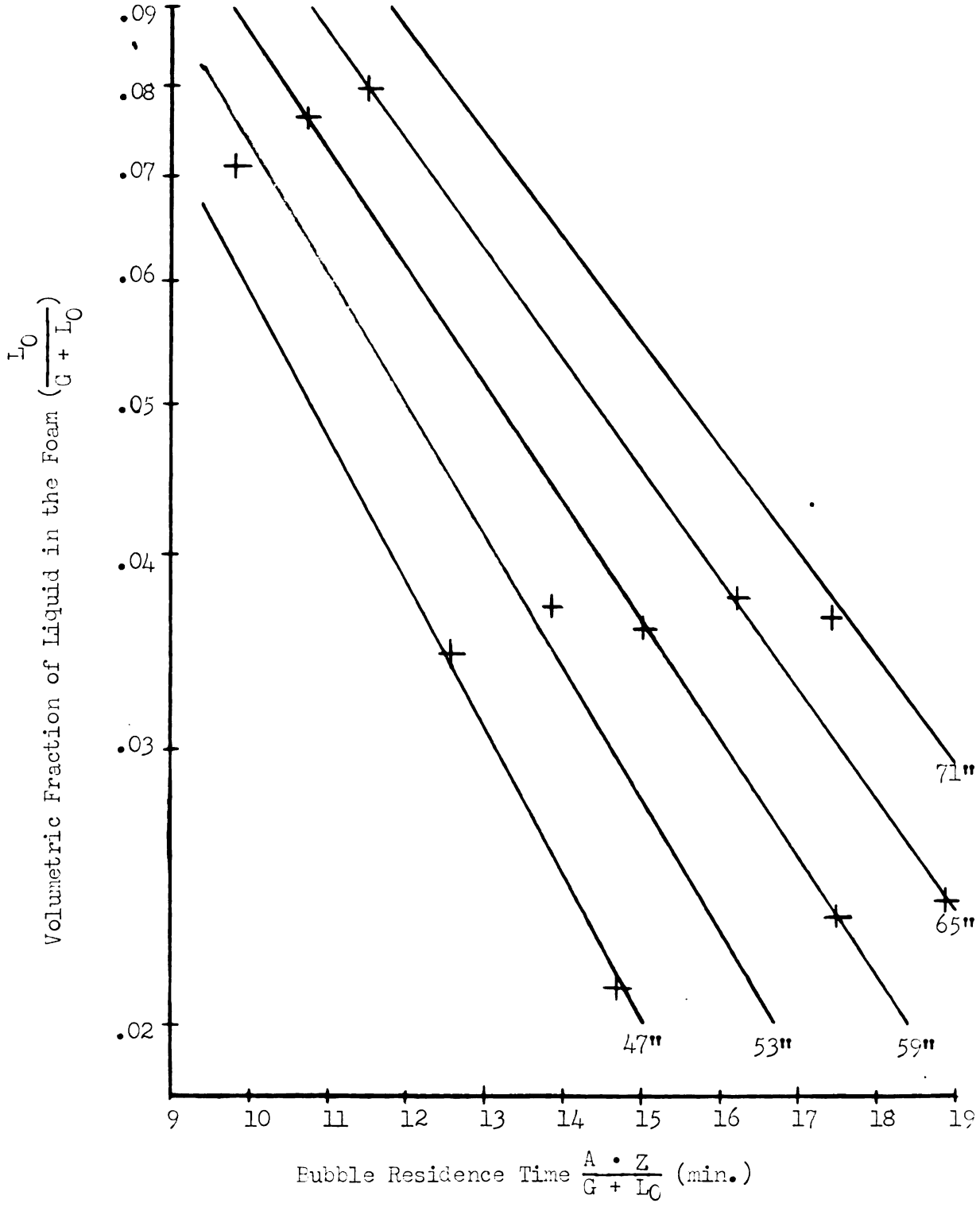

Figure 16 The Effect of Bubble Residence Time on the Fraction of Liquid in the Foam for Different Column Heights (41", 47", 53", 59", 65", 71") with a Bottom Product Concentration of 4.6×10^{-6} gm moles/cm^3 soln.

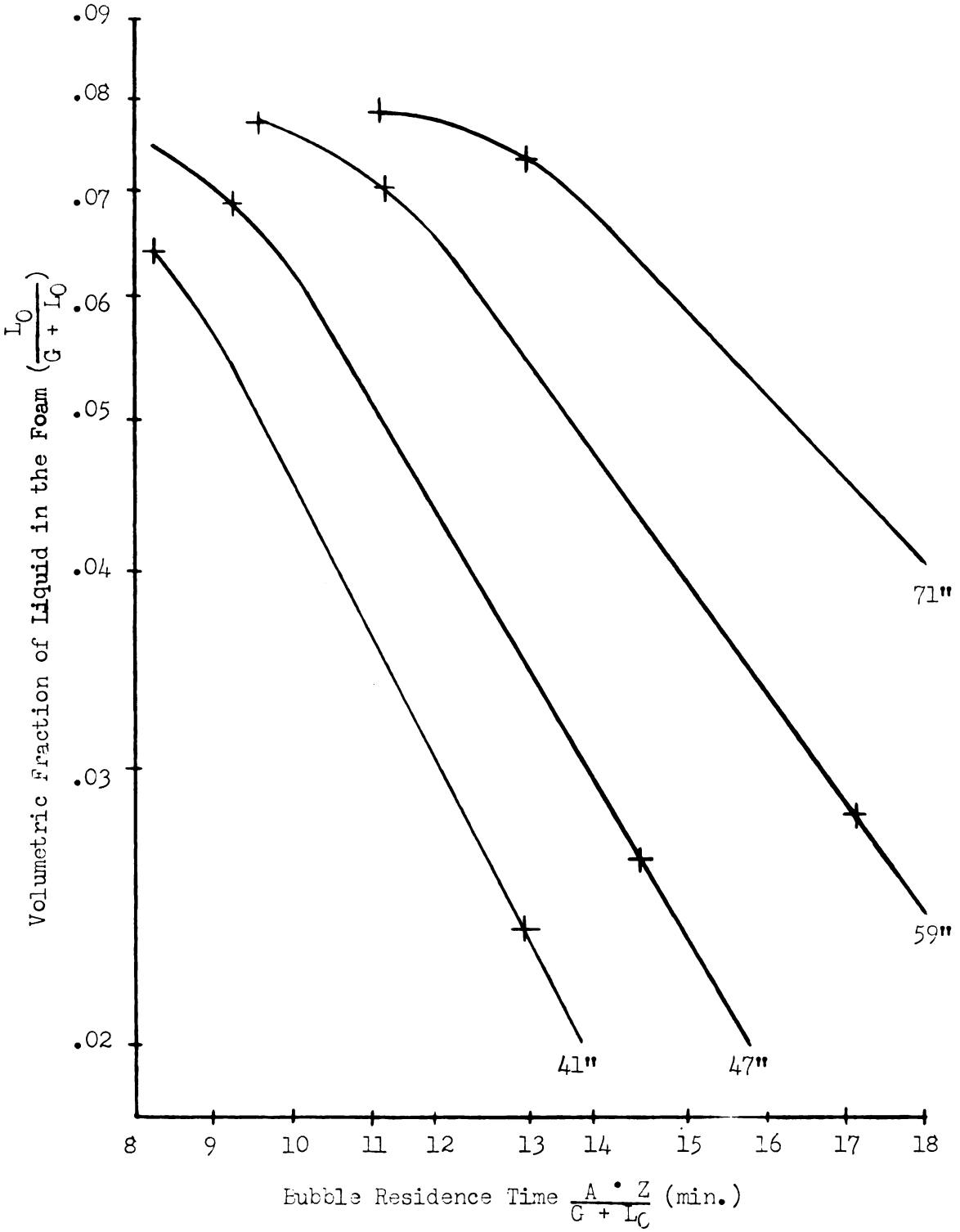

Figure 17 The Effect of Bubble Residence Time on the Fraction of Liquid in the Foam for Different Column Heights (41", 47", 59", 71") with a Bottom Product Concentration of 2.7×10^{-6} gm moles/cm^3 soln.

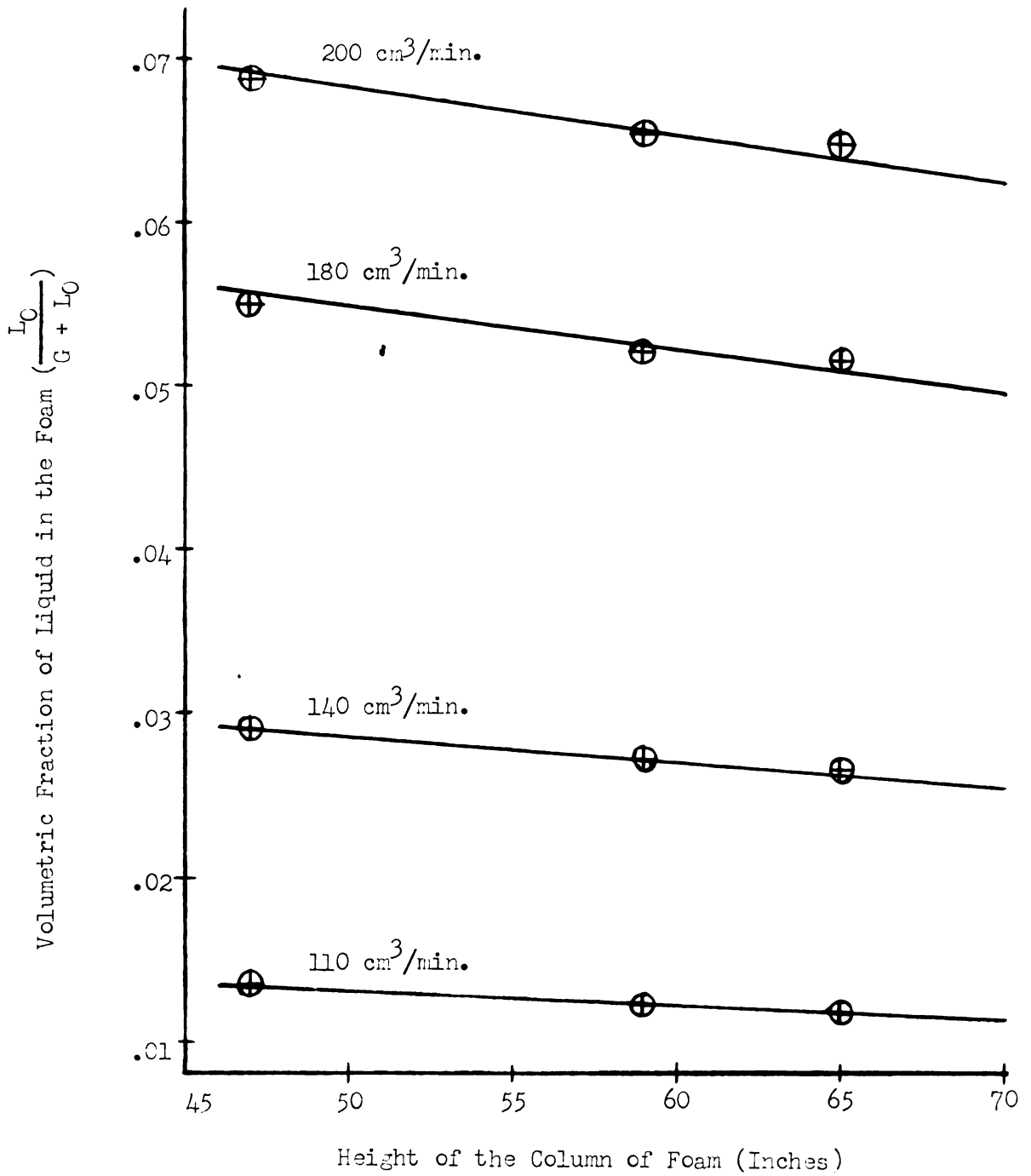

Figure 18 The Effect of the Height of the Column of Foam on the Fraction of Liquid in the Foam at Different Foam Rates (200, 180, 140, 110 cm^3/min.) with a Bottom Product Concentration of 4.6×10^{-6} gm moles/cm^3 soln.

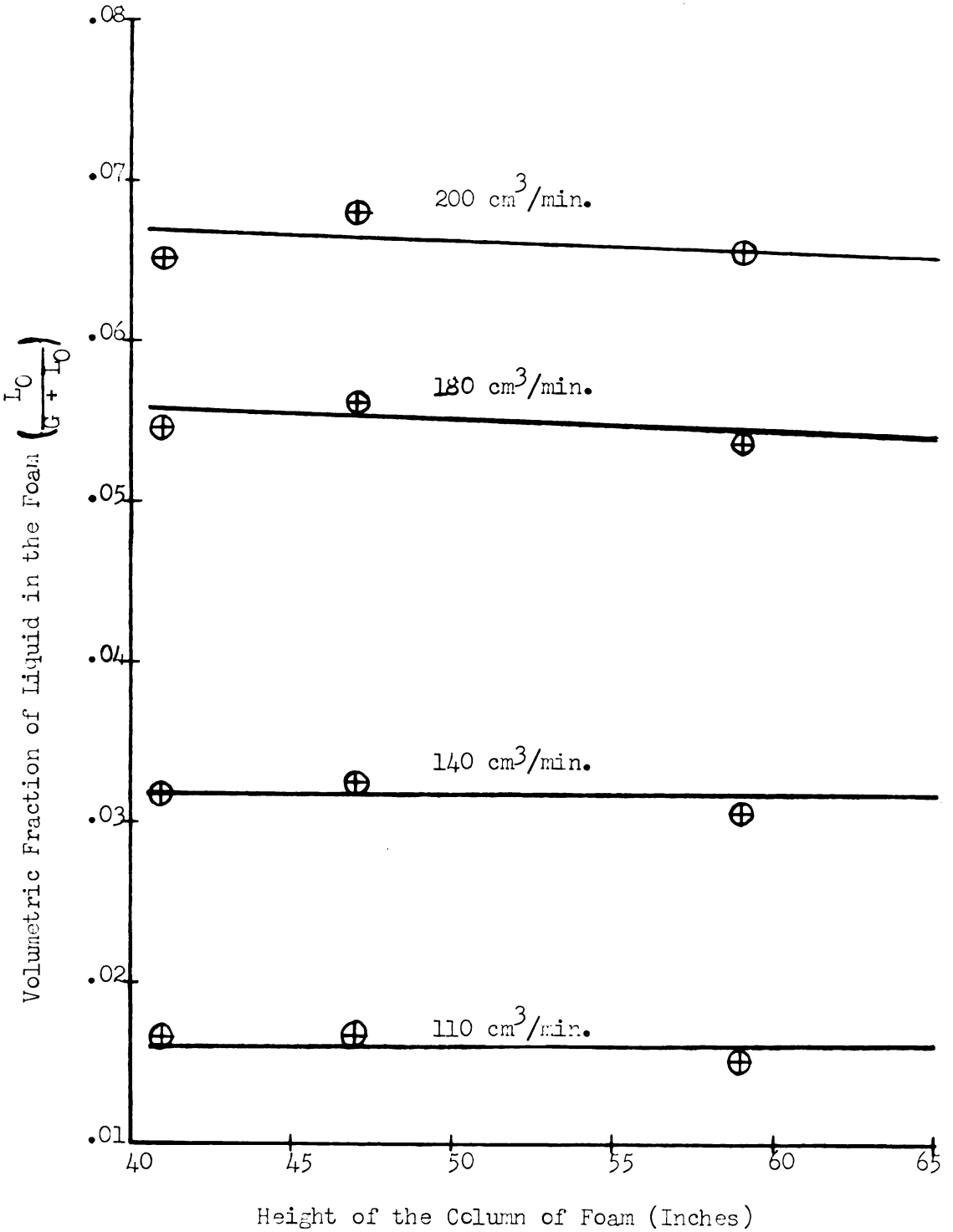

Figure 19 The Effect of the Height of the Column of Foam on the Fraction of Liquid in the Foam at Different Foam Rates (200, 180, 140, 110 cm^3/min.) with a Bottom Product Concentration of 2.7×10^{-6} gm moles/cm^3 soln.

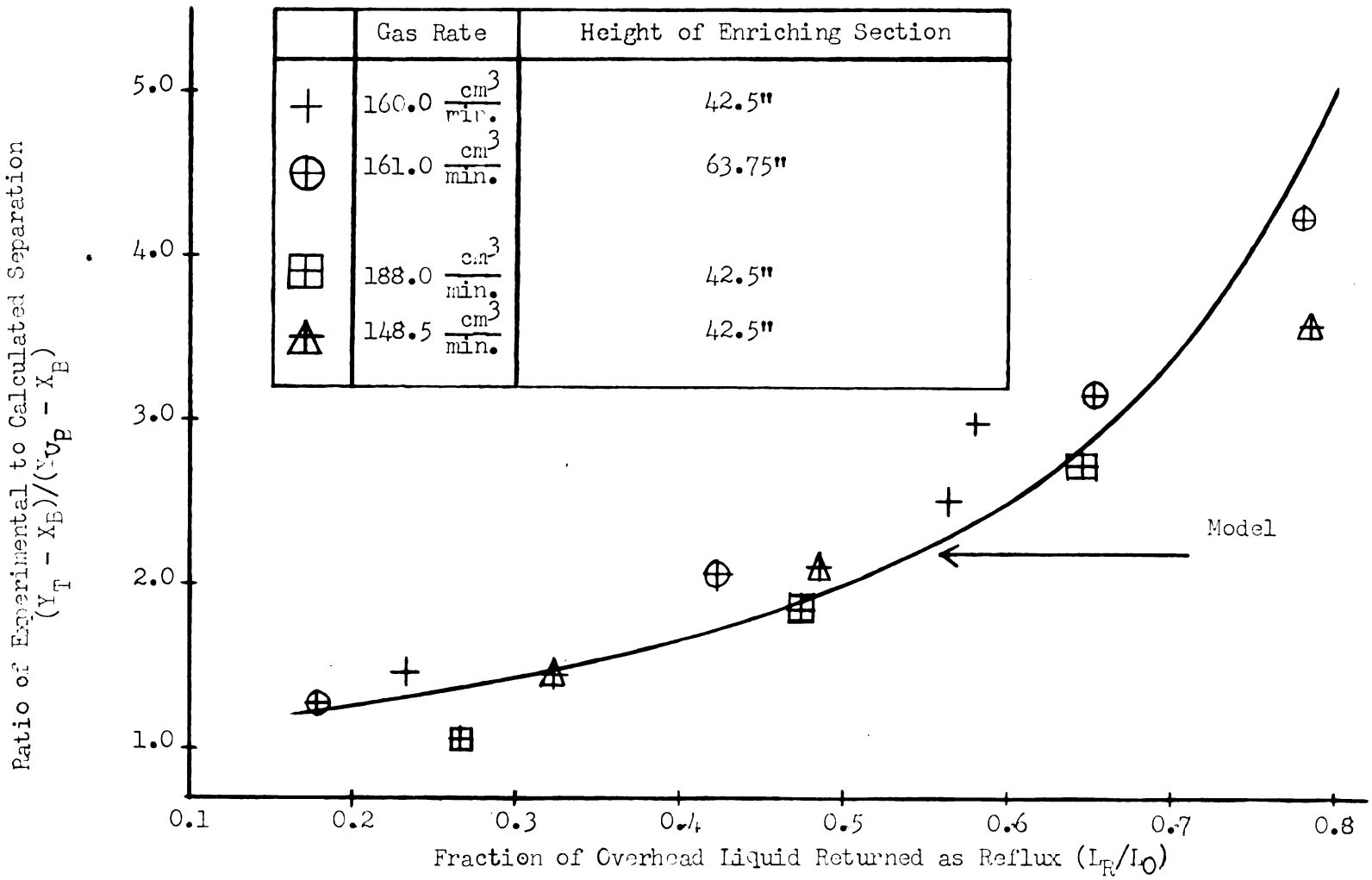

Figure 20 Comparison of Experimental Data with the Model for an Infinitely Tall Enriching Section.

A correlation for the height of a transfer unit in an enriching section as a function of the downflow to upflow ratio is shown in Figure 21. Consistent results were obtained at various gas flow rates and heights of an enriching section in comparison to those of Haas (24) for a stripping section.

The driving forces for mass transfer in a stripping section were found to be very finite at both ends of the column. The curve shown in Figure 22 was calculated assuming that the bulk liquid around the bubbles comes to equilibrium with the feed stream at the feed point, and surface excess, T_B, remains unchanged from its value when it entered the bottom of the column of foam. All other concentrations and driving forces are treated similarly to those derived in the section on theory.

The height of a transfer unit in a stripping section did not correlate with the upflow to downflow ratio as it did for data from a rectifying column. However, the height of a transfer unit divided by the feed liquid flow rate does correlate with the upflow to downflow ratio for short stripping columns, as shown in Figure 23. For taller columns, the data did not correlate very well and this is in agreement with Haas (24), who found data for taller stripping sections to be more inconsistent than for shorter sections.

Figure 24 is an attempt to correlate height of a transfer unit data for both enriching and stripping columns on one figure. The flow number was discovered by a trial and error process, and the intermingling of data points on the V shaped curve is a good indication that there may be some theoretical significance to this plot.

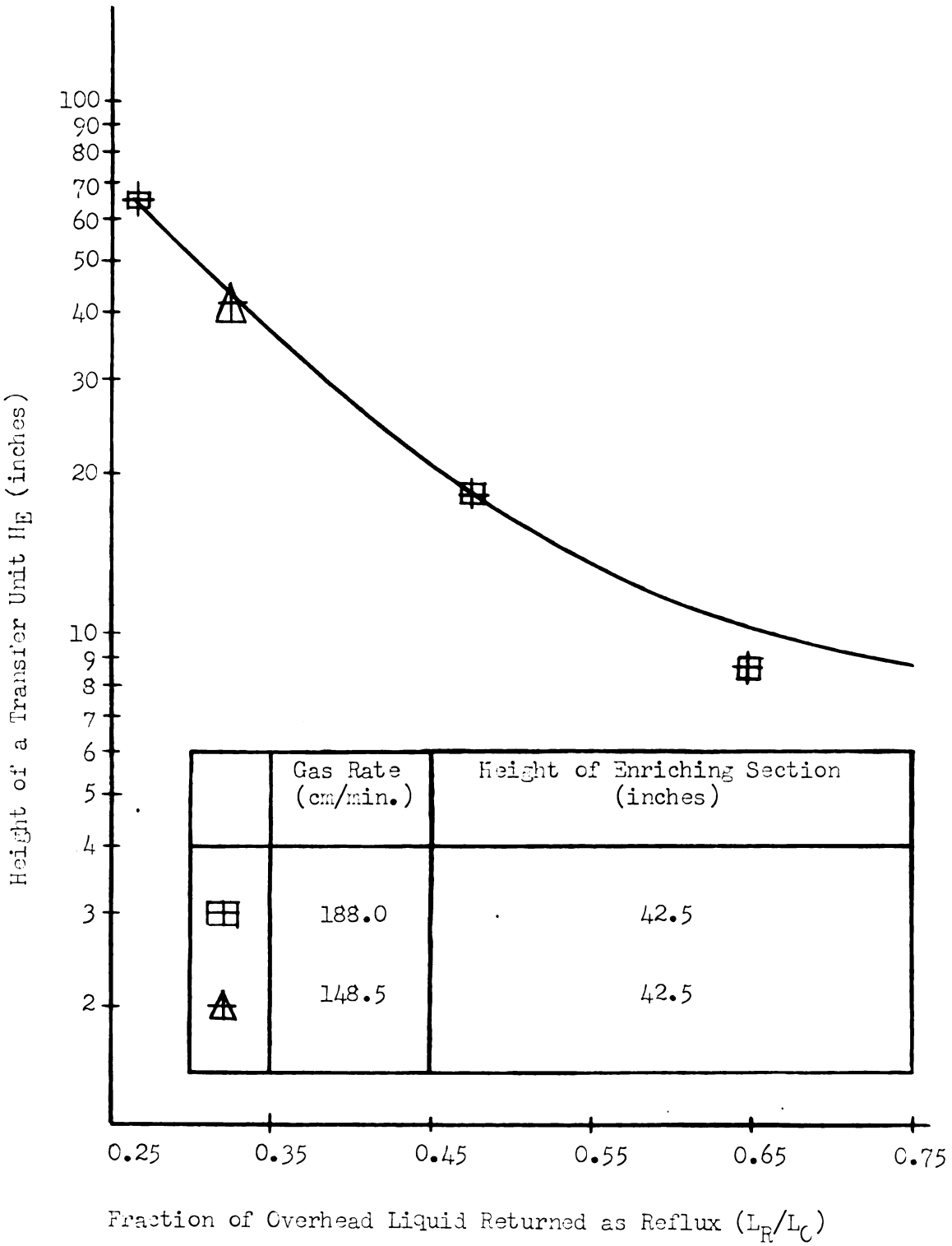

Figure 21 The Height of a Transfer Unit in an Enriching Section Versus the Downflow to Upflow Ratio.

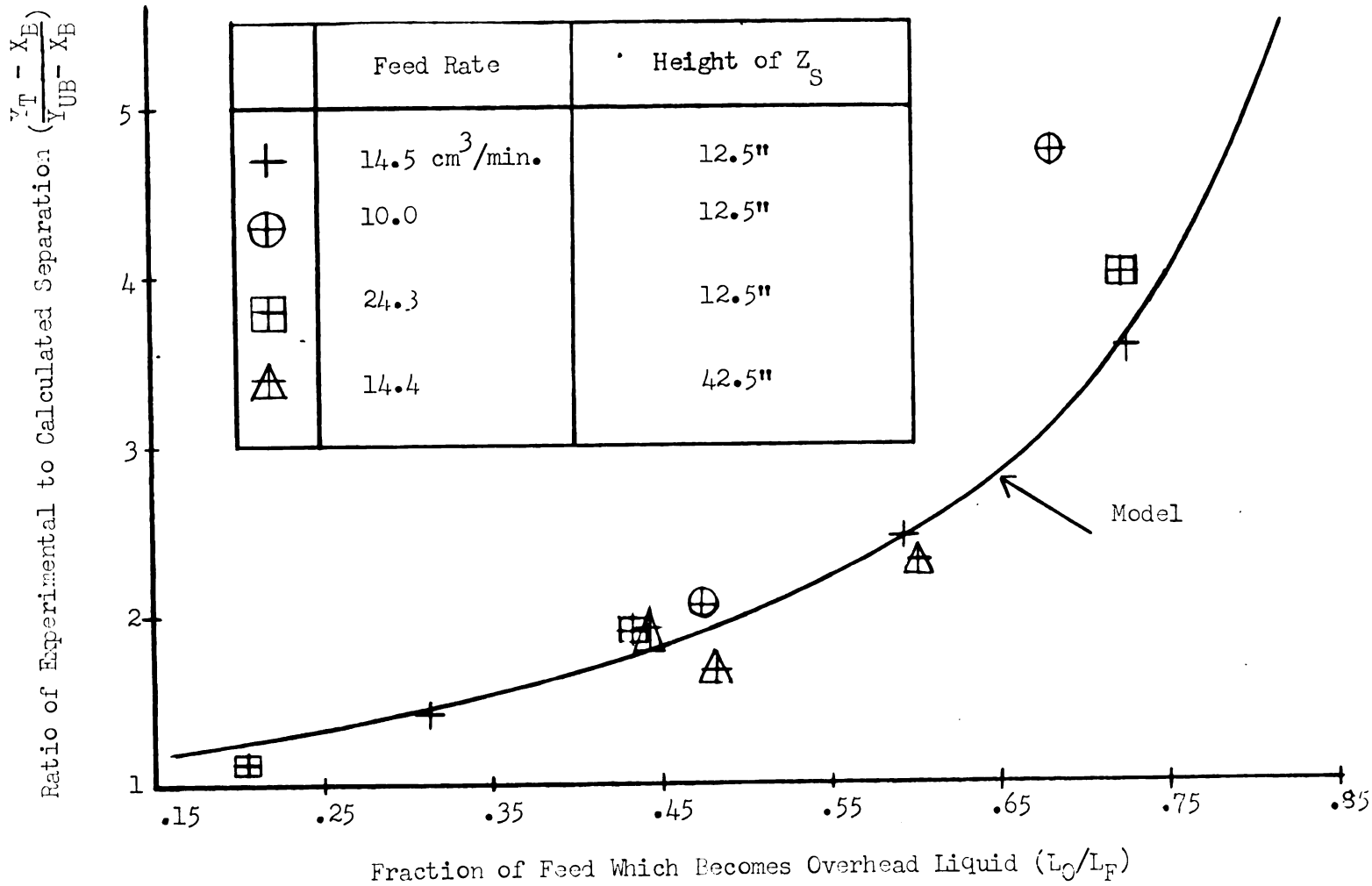

Figure 22 Comparison of Experimental Data with a Model in a Stripping Section.

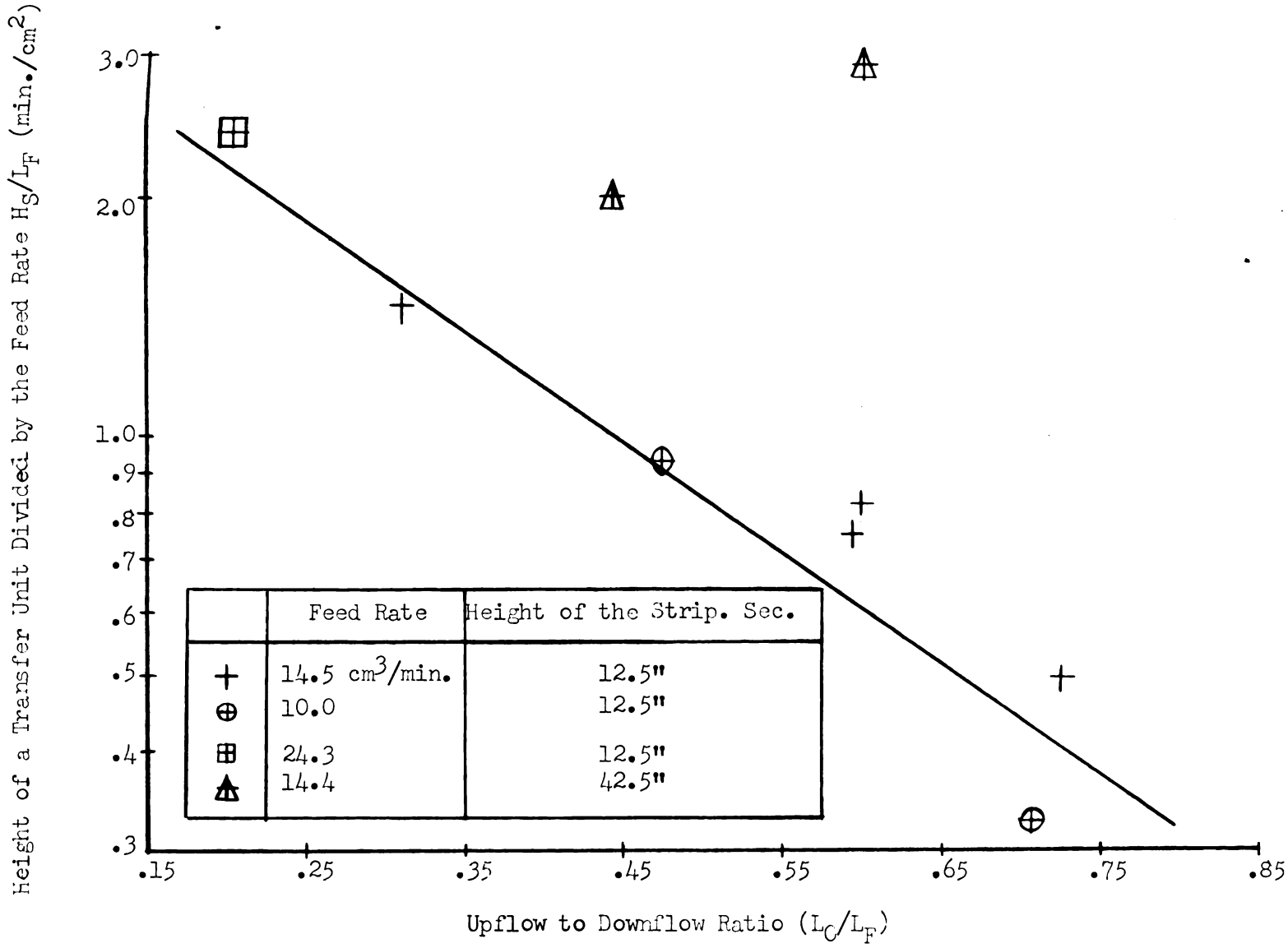

Figure 23 Height of a Transfer Unit in a Stripping Section Correlated with the Upflow to Downflow Ratio.

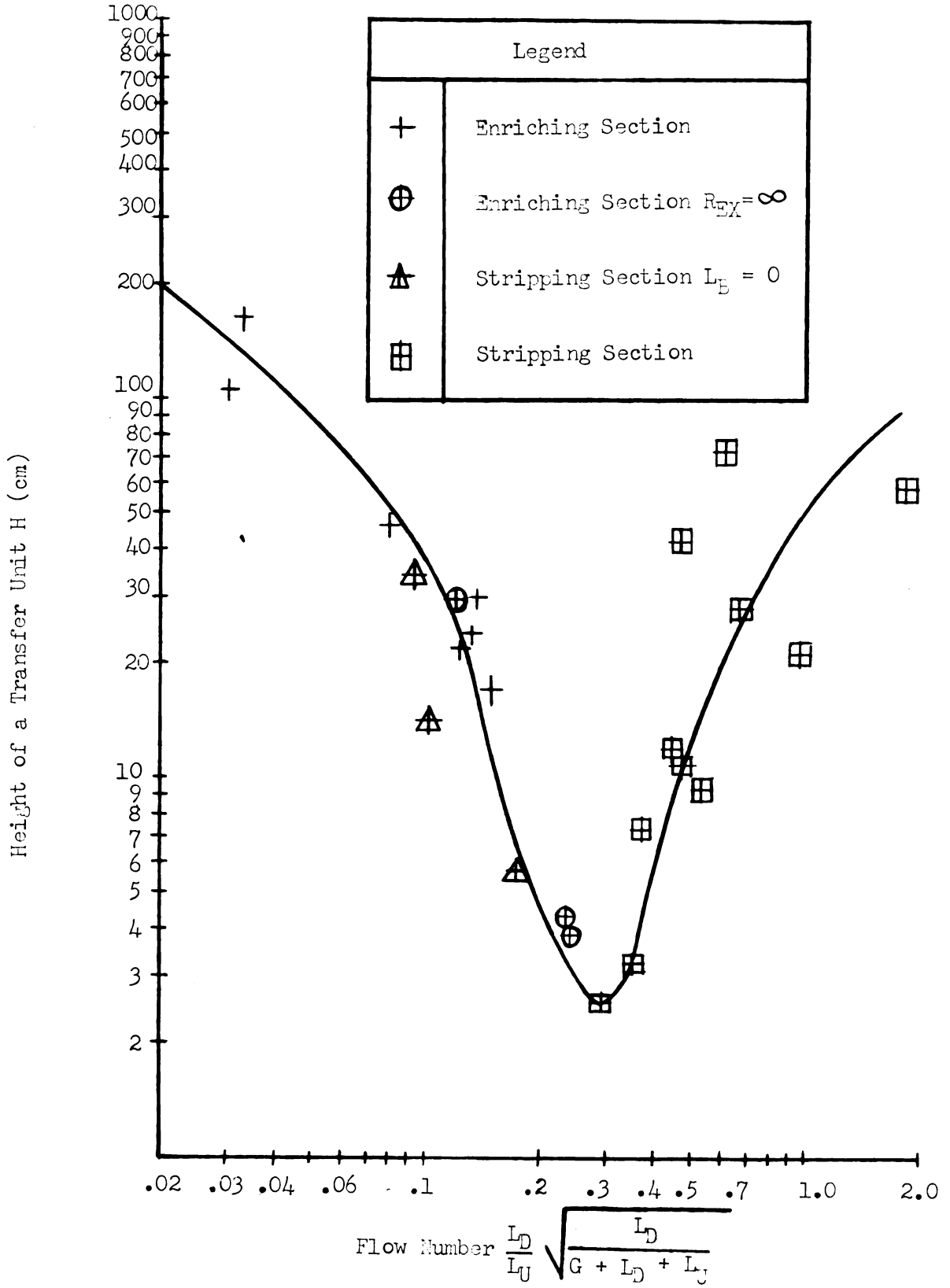

Figure 24 Height of a Transfer Unit Correlation.

An attempt was made to correlate the overhead liquid flow rate to the gas flow rate and other variables. No accurate correlation could be found and so the overhead liquid flow rate was assumed to be another independent variable. Figures 25 and 26 are presented here to indicate some of the difficulties encountered and to give a basis for sizing any future reflux pumps. A very approximate correlation between overhead foam density and gas flow rate was discovered for a one-stage separator as shown by Figure 25. Figure 26 is the approximate correlation for overhead foam density as a function of the foam density number. This last figure utilizes data from an enriching section, a stripping section, and a combined column.

A graphical solution was developed for calculating top and bottom product concentrations in a continuous foam fractionation column with enriching and stripping sections. The solution was found from the over-all material balance, and the top and bottom product concentrations for a set of assumed foam concentrations at the feed point. These assumed concentrations were used to calculate driving forces in the column which in turn permitted the calculation of a set of possible top and bottom product concentrations for run 44A. Figure 27 is the graphical solution to this set of equations. The CDC Digital (3600) Computer was used to make the calculations for a set of runs (Table 30) and the results are given in Table 31. This Digital Computer was also used to calculate the slope and intercept of the over-all material balance for the combined column. A summary of equations, which were derived in the section on theory and used in the computer program, is given below.

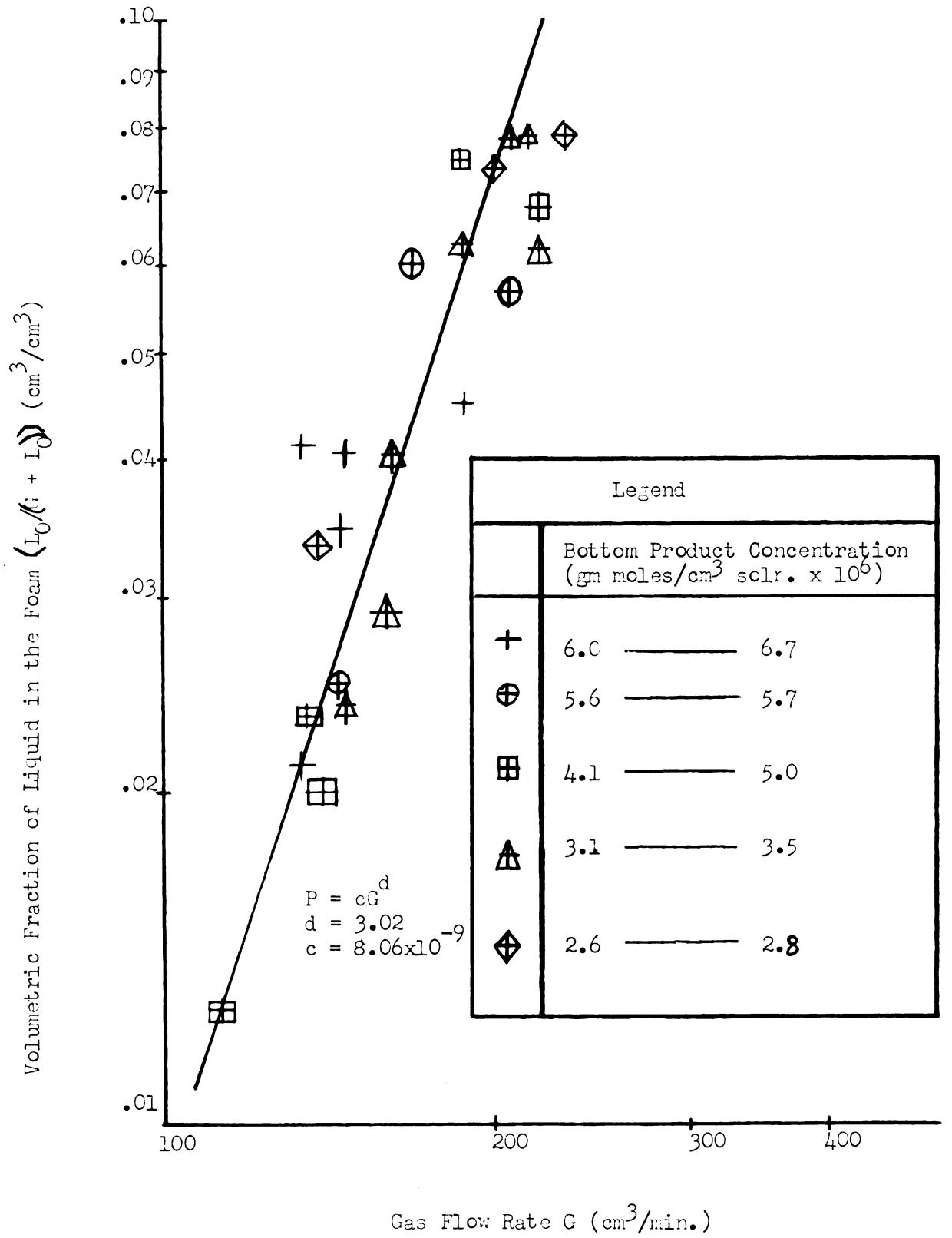

Figure 25 A Correlation Between the Amount of Liquid in the Foam and the Gas Flow Rate for a 71" One Stage Separator.

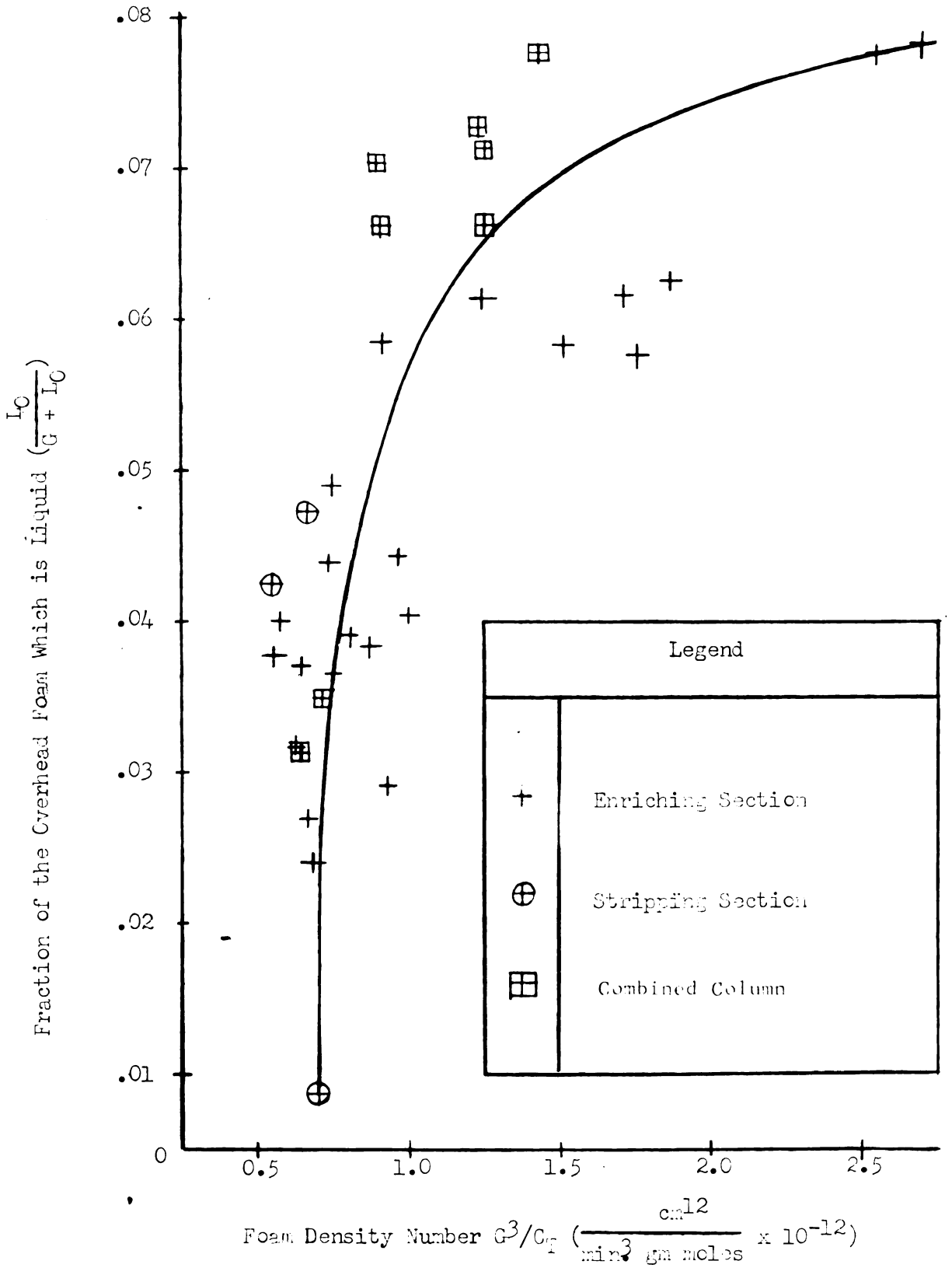

Figure 26 A Correlation for the Overhead Liquid Flow Rate in a Multi-Staged Separator.

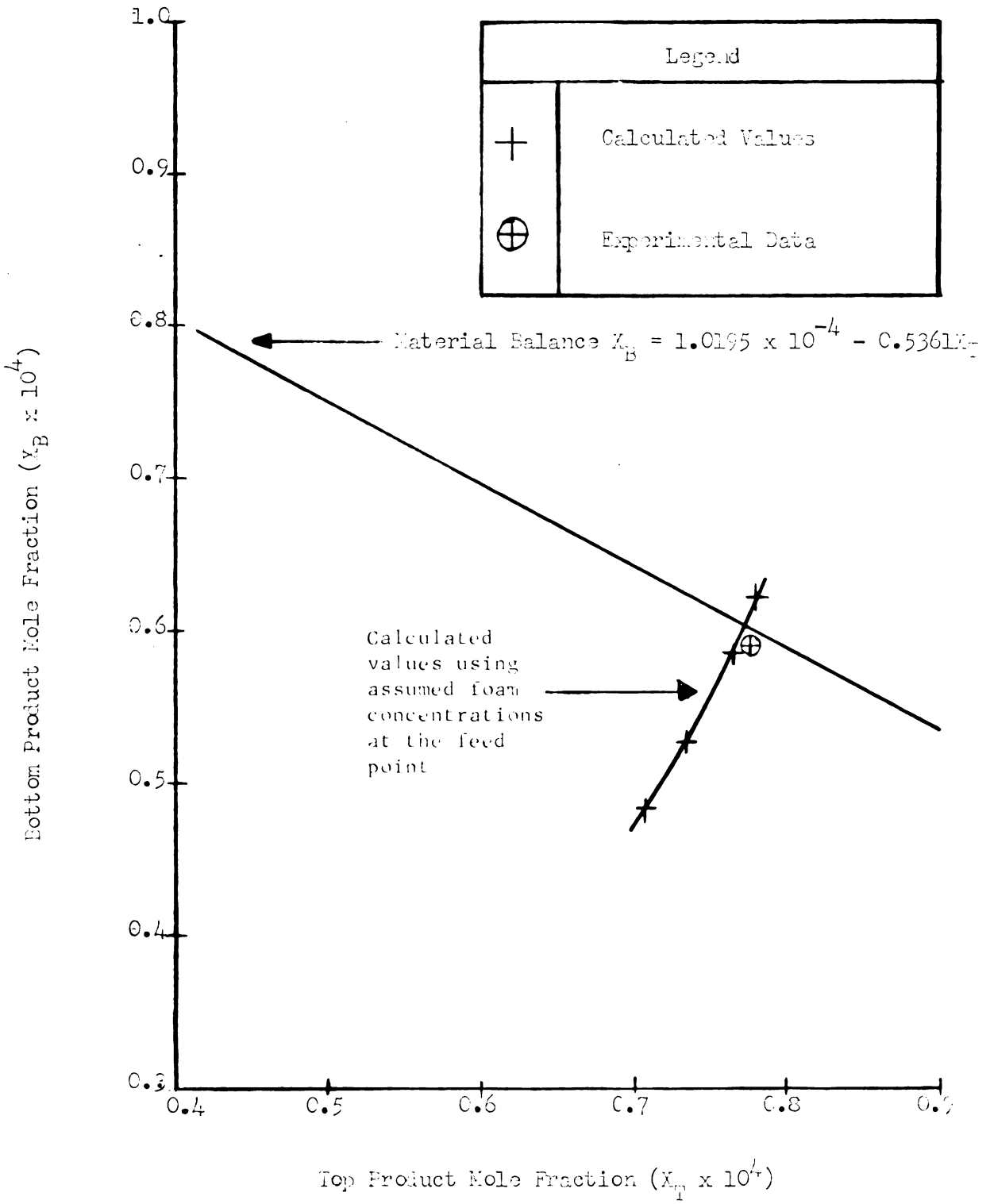

Figure 27 Graphical Solution of Run 44A.

The top product, L_T, and reflux liquid, L_R, flow rates were calculated from the definition of external reflux and a material balance.

$$R_{EX} = \frac{L_R}{L_T} \tag{1}$$

$$L_O = L_R + L_T \tag{2}$$

The bottom product liquid flow rate, L_B, was calculated from the over-all material balance.

$$L_F = L_T + L_B \tag{3}$$

The slope L_T/L_B and intercept $X_F(\frac{L_T}{L_B} + 1)$ of the over-all material balance for surfactant were calculated from known quantities

$$X_B = X_F(\frac{L_T}{L_B} + 1) - X_T(\frac{L_T}{L_B}) \tag{4}$$

The solution to the above equation is known to exist for one combination of X_B and X_T. The correct combination was determined by using the following procedure. The flow numbers for the enriching and stripping sections were calculated and their corresponding heights of a transfer unit were read from Figure 24. The number of transfer units was calculated for each section because the height of each section was known.

$$N_E = \frac{Z_E}{H_E} = \frac{Y_{UT} - Y_{UF}}{(Y^*_{UT} - Y_{UT})_E - (Y^*_{UF} - Y_{UF})_E} \ln \frac{(Y^*_{UT} - Y_{UT})_E}{(Y^*_{UF} - Y_{UF})_E} \tag{5}$$

$$N_S = \frac{Z_S}{H_S} = \frac{Y_{UF} - Y_{UB}}{(Y^*_{UF} - Y_{UF})_S - (Y^*_{UB} - Y_{UB})_S} \ln \frac{(Y^*_{UF} - Y_{UF})_S}{(Y^*_{UB} - Y_{UE})_S} \tag{6}$$

The concentration of the foam at the feed point Y_{UF} was assumed along with the following set of driving forces for mass transfer:

$$(Y^*_{UB} - Y_{UB})_S = \frac{k\, D_A^2\, G\, T_B}{C_{Soln.}(L_R + L_F)D_V^3}\left(1 + \frac{a\, k\, D_A^2\, G}{C_{Soln.} L_C D_V^3}\right) \qquad (7)$$

$$(Y^*_{UF} - Y_{UF})_S = X_{DFB} + \frac{k\, D_A^2\, G\, T_{DFB}}{C_{Soln.} L_C D_V^3} - Y_{UF} \qquad (8)$$

Where

$$X_{DFB} = \frac{L_F X_F + L_R X_{DF}}{L_F + L_R}$$

and

$$T_{DFB} = aX_{DFB} + b$$

$$(Y^*_{UF} - Y_{UF})_E = X_{DF} + \frac{k\, D_A^2\, G\, T_{DF}}{C_{Soln.} L_C D_V^3} - Y_{UF} \qquad (9)$$

Also,

$$X_{DF} = \left(\frac{L_T}{L_R} + 1\right)Y_{UF} - Y_{UT}\left(\frac{L_T}{L_R}\right)$$

$$(Y^*_{UT} - Y_{UT})_E = \frac{k\, D_A^2\, G}{C_{Soln.} L_C D_V^3}\, T_T \qquad (10)$$

These driving forces were calculated by assuming bottom and top product concentrations and comparing trial numbers of transfer units to those calculated from the height of a transfer unit correlation. The circled experimental data point, shown in Figure 27, indicates how accurate this technique is. In Figure 28, the calculated bottom product mole fractions were in agreement to within $\pm$ 6% and the calculated

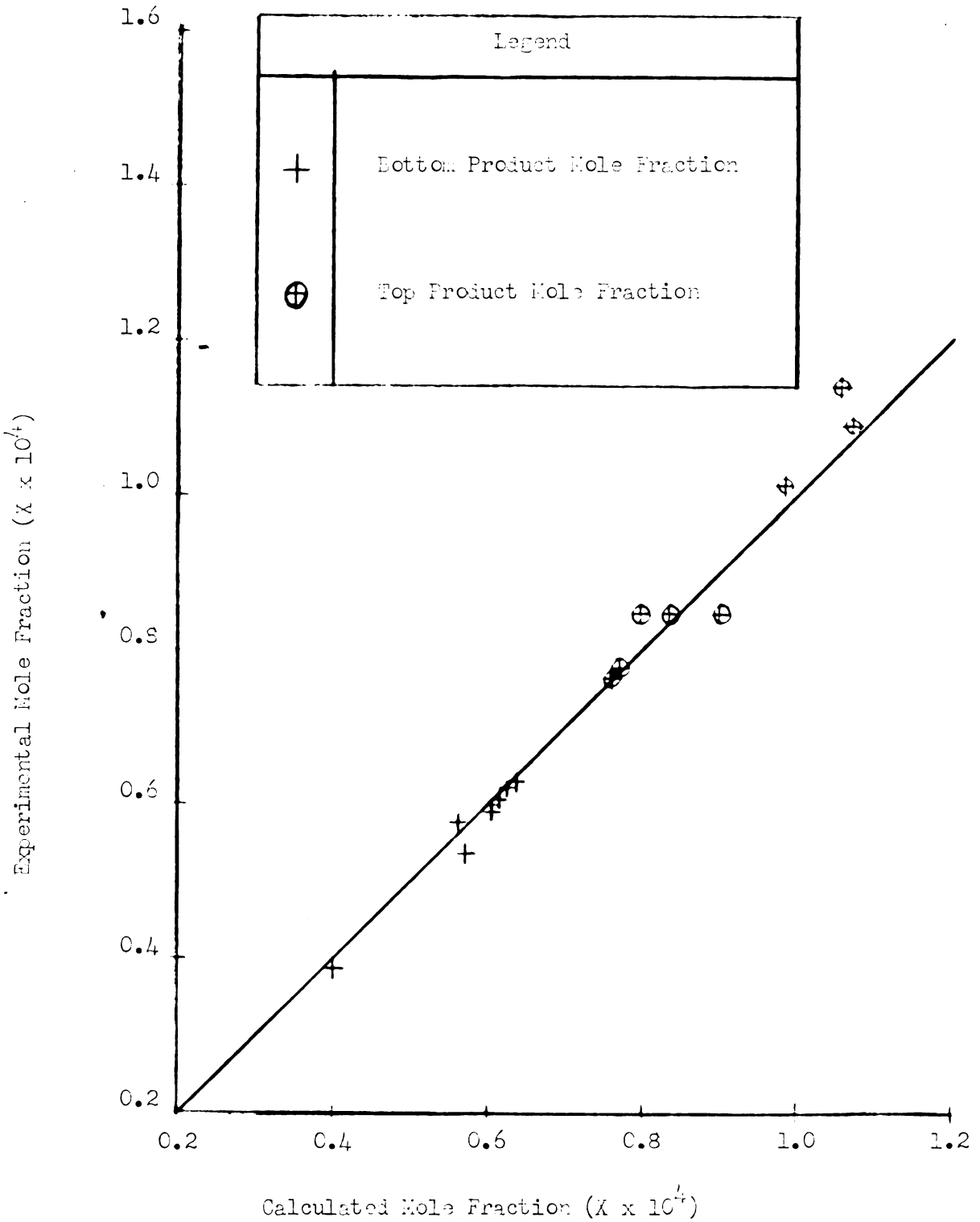

Figure 28 Test of the Combined Column Model.

top product mole fractions were in agreement to within $\pm$ 7.5% of the experimental values. Most of the calculated mole fractions were well within these limits.

DISCUSSION OF ERRORS

The final test of the height of a transfer unit model, which was shown in Figure 28, was a pleasant surprise considering the amount of scatter in the equilibrium relationship. Many error contributors, such as drainage and internal reflux, were partially cancelled out by the use of the height of a transfer unit correlation, Figure 24. This correlation was determined by experimental data and then it was used to predict experimental data, and hence much of the inherent error was voided.

Internal reflux apparently had a negligible effect, since column operating conditions were adjusted so as to produce a uniform foam throughout the column and liquid distributors in the foam did not appear to coalesce the foam rising around them. If appreciable internal reflux had taken place, then it would have been accompanied by drainage because of the decreased amount of surface film area. The overall effect of this internal refluxing and its associated drainage would have been to increase the separations in the enriching and stripping sections. If this effect had taken place, it would have been less prevalent in the combined column than in the individual studies because of the thicker liquid films in the foam and shorter column sections in the combined column.

Experimental evidence indicates that drainage was the least negligible error encountered. Drainage can take place in the absence

of internal reflux by the thinning of foam liquid films without changing their surface area. The upflow liquid flow rate could have varied by as much as 20% due to foam drainage as shown in Figures 18 and 19. This effect would have been more pronounced in the individual studies than in the combined column, and hence the calculated separations should be on the average smaller than the experimental ones for a combined column. This last effect was observed in Figure 28; the experimental top product concentrations were mostly higher and the bottom product concentrations mostly lower than the corresponding calculated ones.

FUTURE WORK

Other two component surfactant systems should be studied in order to find out how the theory developed in this thesis applies to them. A general height of a transfer unit correlation might then be derivable which would predict the height of a transfer unit from the flow number and surfactant properties.

A high purity two component surfactant system should be foam fractionated in order to determine the concentration regions where the Gibbs equation can be used to calculate surface excess from surface tension data. This would permit the calculation of equilibrium data from surface tension data.

A three component surfactant system should be examined to see whether the height of a transfer unit or the height equivalent to a theoretical plate is the best concept to apply to the foam fractionation of multi-component systems. The height of a transfer unit concept best approximates the continuous countercurrent mass transfer in a foam fractionation column but the mathematics may become unwieldy. In that case, the height equivalent to a theoretical plate would be the only usable concept even though the height of a transfer unit is more theoretically correct.

CONCLUSIONS

The height of a transfer unit model was found to be an accurate method for predicting separations in a foam fractionation column with enriching and stripping sections. The surface tension data gathered in this thesis were that of sodium lauryl sulfate contaminated with lauryl alcohol and therefore, the Gibbs equation could not be used to calculate surface excess.

An empirical equilibrium equation was developed which was based on the following experimental observations. Area and volume averaged bubble diameters were constant over the model concentration region. Surface excess was a linear function of the bulk liquid concentration and accordingly the equilibrium equation became a linear function between bulk liquid and foam concentrations.

The height of a transfer unit in an enriching or a stripping section for all downflow to upflow ratios correlated empirically with the flow number

$$F_N = \frac{L_D}{L_U} \sqrt{\frac{L_D}{G + L_U + L_D}}$$

This correlation was successfully used to predict top and bottom product concentrations in a column with center feed and reflux. Foam drainage caused experimental combined column separations to be slightly larger than those calculated from the height of a transfer unit model which used individual studies of enriching and stripping sections.

APPENDIX

TABLE [illegible]

SPECIFIC CONDUCTANCE OF SODIUM LAURYL SULFATE IN DISTILLED WATER FOR THE TEMPERATURE REGION FROM 76.0 TO 84.0° F.

Concentration of Sodium Lauryl Sulfate in Distilled Water C $\frac{\text{gm moles}}{\text{cm}^3\text{ soln.}} \times 10^{[illegible]}$	Concentration of Sodium Lauryl Sulfate in Distilled Water X Mole Fraction of Sodium Lauryl Sulfate in Solution	Type of Cell	Cell Constant (cm^{-1})	Conductance (micromhos)	Specific Conductance (micromhos/cm)
[illegible].98	0.0000126	Conductivity cell constructed by M. S. U. glass blower	0.384	1,792.0	[illegible]
5.89	0.0000196		0.384	1,519.0	591.[illegible]
4.89	0.0000855		0.384	1,119.0	566.0
[illegible].49	0.0000650		0.384	969.0	372.0
2.94	0.0000[illegible]1		0.384	820.0	319.0
2.44	0.0000441		0.384	691.0	2[illegible].0
2.10	0.0000379		0.384	597.0	222.0
1.74	0.0000[illegible]4		0.384	511.0	197.0
1.47	0.0000265		0.384	442.0	[illegible]9.7
1.22	0.0000220		0.384	362.0	[illegible]9.[illegible]
1.05	0.0000190		0.384	[illegible].0	[illegible]
0.[illegible]74	0.0000[illegible]8		0.384	267.0	[illegible]
0.61[illegible]	0.0000926		0.384	164.0	[illegible].0
0.46[illegible]	0.0000787		0.384	143.0	[illegible].9
0.256	0.0000462		0.384	89.5	[illegible].[illegible]
0.000	0.0000000		0.384	10.[illegible]	[illegible].9

TABLE -- Continued

Concentration of Sodium Lauryl Sulfate in Distilled Water		Type of Cell	Cell Constant	Conductance	Specific Conductance
C	X				
$\frac{\text{gm moles}}{\text{cm}^3\text{soln.}} \times 10^4$	Mole fraction of Sodium Lauryl Sulfate in Solution		(cm^{-1})	(micromhos)	(micromhos/cm)
17.9	0.000341	Dip type	0.0952	15,900.0	[illegible]
12.1	0.000291	Conductivity	0.0952	12,570.0	[illegible]
11.2	0.000202	Cell (Cell #1)	0.0952	9,756.0	928.8
7.25	0.000151		0.0952	7,157.[illegible]	[illegible]
5.[illegible]2	0.000101		0.0952	5,942.0	[illegible]
2.97	0.0000536		0.0952	3,111.4	29[illegible].2
17.6	0.000118	Flow through	0.00991	130,500.0	1,29[illegible].0
15.7	0.000247	type Conductivity	0.00991	109,300.0	1,0[illegible].0
9.77	0.000176	Cell (Cell #2	0.00991	85,810.0	[illegible]
7.90	0.000143		0.00991	75,529.0	7[illegible]
6.01	0.000108		0.00991	60,490.0	599.[illegible]
4.51	0.0000778		0.00991	44,8[illegible].0	44[illegible]
3.13	0.0000565		0.00991	35,467.0	[illegible]
1.40	0.0000307		0.00991	1[illegible],570.0	1[illegible].0
15.7	0.000283	Flow through	0.009[illegible]	120,3[illegible]7.0	1,[illegible].0
10.5	0.000190	type Conductivity	0.009[illegible]	94,251.0	935.[illegible]
6.43	0.000116	Cell (Cell #3	0.009[illegible]	64,185.0	[illegible]
4.07	0.0000735		0.009[illegible]	45,040.0	41[illegible]
2.56	0.0000462		0.009[illegible]	27,174.0	2[illegible].0
1.05	0.0000195		0.009[illegible]	12,200.0	[illegible].2

TABLE II

SURFACE TENSIONS OF SODIUM LAURYL SULFATE [illegible] WATER
IN THE TEMPERATURE RANGE OF FROM 70.[illegible] TO 75.[illegible] °C.

Concentration of Sodium Lauryl Sulfate in Distilled Water		Scale Reading	Correction Factor	Surface Tension
C	X	S	[illegible]	γ
$\frac{\text{gm moles}}{\text{cm}^3\text{ soln.}} \times 10^{9}$	Mole Fraction of Sodium Lauryl Sulfate in Solution	(dynes/cm)		(dynes/cm)
46.9	0.000846	37.0	0.9215	[illegible].2
14.92	0.000269	37.4	0.9242	34.[illegible]
10.[illegible]1	0.000190	36.0	0.9210	[illegible]
8.49	0.000153	33.8	0.9[illegible]0	[illegible]
6.96	0.000126	29.[illegible]	0.9056	2[illegible]
6.27	0.000113	27.0	0.8991	24.[illegible]
5.67	0.000102	27.6	0.9005	24.8
4.70	0.000080	26.9	0.8988	24.2
3.98	0.000070	28.0	0.9016	2[illegible].2
2.10	0.000049	29.[illegible]	0.9056	2[illegible]
2.27	0.000040	29.[illegible]	0.90[illegible]1	27.0
1.842	0.000033	30.0	0.90[illegible]7	27.2
1.[illegible]2	0.000024	32.0	0.9215	29.2
0.908	0.000014	36.[illegible]	0.9225	[illegible]
0.7[illegible]5	0.000013	40.[illegible]	0.9[illegible]14	[illegible]
0.[illegible]41	0.000009	44.[illegible]	0.9[illegible]95	4[illegible]
0.[illegible]	0.000006	49.0	0.9491	46.[illegible]
0.294	0.000005	5[illegible].[illegible]	0.9[illegible]75	[illegible]
0.21[illegible]	0.000003	[illegible]	0.9[illegible]25	[illegible]

TABLE [illegible] -- Continued

Concentration of Sodium Lauryl Sulfate in Distilled Water		Scale Reading	Correction Factor	Surface Tension
C	X	S	Fc	γ
$\left(\frac{\text{gm mole}}{\text{cm}^3\text{ soln.}} \times 10^{6}\right)$	Mole Fraction of Sodium Lauryl Sulfate in Solution	(dynes/cm)		(dynes/cm)
0.1452	0.00000262	59.1	0.9687	[illegible]
0.1[illegible]	0.00000212	60.[illegible]	0.9712	[illegible]
0.0666	0.00000156	62.1	0.9744	60.5
0.0000	0.00000000	71.4	0.9907	70.7
0.0000	0.00000000	70.9	0.9895	70.2

TABLE [illegible]

EXPERIMENTAL DATA FOR A ONE STAGE SEPARATOR WHICH CONCENTRATES SODIUM LAURYL SULFATE IN WATER

Run	Height of Column of Foam	Gas Flow Rate	Overhead Liquid Flow Rate	Bottom Product Concentration	Top Product Concentration	Area Average Bubble Diameter	Volume Average Bubble Diameter
	Z	G^b	F_O	C_B	C_T	D_A	D_V
	(in.)	$\left(\frac{cm^3}{min.}\right)$	$\left(\frac{cm^3}{min.}\right)$	$\left(\frac{gm\ mol\ [illegible]}{cm^3\ soln.} \times 10^6\right)$	$\left(\frac{gm\ mol\ [illegible]}{cm^3\ soln.} \times 10^6\right)$	(cm)	(cm)
1	71	188.8	8.9	6.043	6.751	0.0[illegible]	[illegible]
2A	71	206.3	12.4	5.756	6.4[illegible]	0.0[illegible]24	[illegible]
2B[a]	47	188.6	9.7	5.827	6.469	0.0327	[illegible]
2C[a]	59	197.7	11.7[illegible]	5.878	6.592	0.0[illegible]27	[illegible]
3	71	219.1	14.4[illegible]	5.505	4.011	0.0347	[illegible]
3A[a]	71	219.1	15.45	4.1[illegible]4	4.000	0.0327	0.0329
4A	71	156.8	15.[illegible]	4.15[illegible]	4.066	0.0312	[illegible]
4B	71	147.0	6.2	6.906	7.293	0.0312	[illegible]
5A	71	139.4	2.95	4.95[illegible]	[illegible]	[illegible]	[illegible]
6A	[illegible]	1[illegible]8.4	10.75	5.086	[illegible]	0.0324	[illegible]
[illegible][a]	59	102.4	9.[illegible]	5.[illegible]	[illegible]	[illegible]	[illegible]
7A[a]	71	1[illegible]9.9	2.93	6.001	7.29[illegible]	[illegible]	[illegible]
8A	71	1[illegible].9	5.75	6.101	7.[illegible]	[illegible]	[illegible]
9A[a]	71	1[illegible].4	1.25	4.979	[illegible]	[illegible]	[illegible]
10A[a]	47	122.2	1.25	2.289	4.[illegible]9	[illegible]	[illegible]
11A	71	1[illegible]	1.45	4.1[illegible]	5.7[illegible]	[illegible]	[illegible]
12A[a]	71	144.0	1.70	5.659	7.[illegible]	[illegible]	[illegible]
13A	71	144.[illegible]	5.20	6.251	7.[illegible]	[illegible]	[illegible]

TABLE [illegible] -- Continued

Run	Height of Column of Foam	Gas Flow Rate	Overhead Liquid Flow Rate	Bottom Product Concentration	Top Product Concentration	Area Averaged Bubble Diameter	Volume Averaged Bubble Diameter
	Z	q^b	L_0	C_B	C_T	D_A	D_V
	(in.)	$\left(\frac{cm^3}{min.}\right)$	$\left(\frac{cm^3}{min.}\right)$	$\left(\frac{cm\ mole}{cm^3\ soln.} \times 10^6\right)$	$\left(\frac{cm\ mole}{cm^3\ soln.} \times 10^6\right)$	(cm)	(cm)
13B[a]	59	140.1	9.95	6.409	7.569	0.0327	0.0329
14A[a]	47	152.0	5.85	5.705	7.245	0.0327	0.0329
14B[a]	47	176.0	12.55	5.790	6.409	0.0327	0.0329
15A[a]	59	172.5	11.70	4.421	5.105	0.0327	0.0329
19A	71	199.5	15.76	2.762	3.149	0.0310	0.0332
20A	71	222.2	19.76	2.697	3.001	0.0311	0.0314
21A[a]	71	148.0	4.77	2.720	3.451	0.0301	0.0305
22A[a]	71	159.2	4.77	3.446	4.329	0.0327	0.0329
23B[a]	71	161.7	6.80	3.492	4.224	0.0327	0.0329
27A[a]	71	224.5	18.22	3.418	3.760	0.0327	0.0329
28A[a]	71	177.7	12.55	3.430	3.943	0.0327	0.0329
30A[a]	71	147.0	3.62	3.634	4.079	0.0327	0.0329
31A[a]	71	204.1	17.57	3.522	3.524	0.0325	0.0324
34A[a]	71	145.3	2.36	8.496	9.911	0.0327	0.0329
34B[a]	71	199.8	8.38	11.789	11.408	0.0327	0.0329

[a] Bubble diameters taken from Fig. 17 and Table 4.
[b] Gas Pressure of one atmosphere and temperatures from 75.7 to 77.8°C.

TABLE IV

AVERAGE BUBBLE DIAMETERS FOR THE FOAM PRODUCED IN A ONE STAGE SEPARATOR FILLED WITH SODIUM LAURYL SULFATE SOLUTION

Run Number	Number of Bubbles in Sample	Largest Bubble in Sample (cm.)	Smallest Bubble in Sample (cm.)	Area Averaged Bubble Diameter D_A (cm.)	Volume Averaged Bubble Diameter D_V (cm.)
1	50	0.0454	0.0266	0.0338	0.0341
2A	50	0.0398	0.0241	0.0324	0.0326
[illegible]	50	0.0404	0.0276	0.0347	0.0349
4A	50	0.0450	[illegible]	0.0332	[illegible]
4B	50	0.0495	0.0270	0.0352	0.0354
5A	50	0.0459	0.0273	0.0340	[illegible]
6A	25	0.0426	0.0274	0.0324	0.0326
8A	50	0.0400	0.0256	0.0312	0.0314
11A	50	0.0410	0.0252	0.0317	0.0320
13A	50	0.0405	0.0252	0.0325	0.0327
19A	50	0.0417	0.0273	0.0330	0.0332
20A	50	0.0328	0.0242	0.0311	[illegible]
21A	50	0.0362	0.0235	0.0301	[illegible]
22A	50	0.0412	0.0251	0.0323	0.0324

$\overline{D_A}$ = 0.0327

$\overline{D_V}$ = 0.0329

TABLE V

CALCULATED VARIABLES NEEDED IN THE CALCULATION OF THE SURFACE EXCESS (T) FOR A 7½ INCH COLUMN OF FOAM IN A ONE STAGE SEPARATOR

Run Number	Top Product Mole Fraction	Bottom Product Mole Fraction	Separation	Group of Variables in Equilibrium Relationship	Surface Excess
	Y_T	X_B	$(Y_T - X_B)$	$\left(\frac{k\ D_A^2\ G}{C_{Soln.}\ D_B}\right)^a$	T
	$(Y_T \times 10^4)$	$(X_B \times 10^4)$	$(Sep. \times 10^4)$	$\left(\frac{cm^2}{gm\ mole} \times 10^{-4}\right)$	$\left(\frac{gm\ moles}{cm^2} \times 10^{10}\right)$
1	1.219	1.091	0.128	7.27	1.76
2A	1.165	1.039	0.126	6.00	2.10
3	0.724	0.633	0.091	5.12	1.78
3A	0.840	0.746	0.094	4.94	1.93
4A	0.842	0.755	0.087	4.55	1.99
4B	1.335	1.138	0.197	7.88	2.50
5A[b]	1.183	0.895	0.288	16.47	1.[illegible]
6A	1.151	1.026	0.125	5.45	2.21
7A[b]	1.317	1.084	0.233	10.50	1.41
8A	1.380	1.210	0.170	8.47	1.96
9A[b]	1.205	0.899	0.306	14.88	2.07
11A[b]	1.574	0.753	0.821	28.46	2.48
12A[b]	1.278	1.025	0.253	13.91	1.82
13A	1.332	1.128	0.204	10.51	2.14
19A	0.568	0.499	0.069	4.35	1.59
20A	0.542	0.487	0.055	4.31	1.37

TABLE V --Continued

Exp. Number	Top Product Mole Fraction	Bottom Product Mole Fraction	Separation	Group of Variables in Equilibrium Relationship	Surface Excess
	Y_T	X_B	$(Y_T - X_B)$	$\left(\frac{k\, D_A^2\, C}{C_{Soln.}\, L_0\, D_V^2}\right)$ [a]	Γ
	$(Y_T \times 10^4)$	$(X_B \times 10^4)$	$(Sep. \times 10^4)$	$\left(\frac{cm^2}{gm\ mole} \times 10^{-4}\right)$	$\left(\frac{gm\ moles}{cm^2} \times 10^{10}\right)$
21A	0.623	0.391	0.132	11.33	1.17
22A	0.781	0.622	0.159	12.14	1.11
25B	0.763	0.630	0.133	5.49	1.57
27A	0.557	0.517	0.040	4.21	0.95
28A	0.640	0.565	0.075	5.35	1.40
30A[b]	0.845	0.620	0.225	24.51	1.58
33A[c]	0.634	0.598	0.036	4.32	0.83
34A[c]	1.789	1.534	0.255	22.0	1.16
34B[c]	2.059	2.127	-0.068	8.13	-0.84

[a] Let k = 6.59, and $C_{Soln.}$ = 0.05539 gm moles/cm^3 soln.

[b] Separation is greater than Ph. D. model region.

[c] Bottom product concentration is greater than Ph. D. model region.

TABLE VI

TEST OF THE EQUILIBRIUM RELATIONSHIP FOR A ONE STAGE SEPARATOR

Run	Bottom Product Mole Fraction	Calculated Surface Excess	Group of Variables in Equilibrium Relationship	Calculated Separation	Experimental Separation
	X_B	T^a	$\left(\frac{k\, D_A^2\, C}{C_{soln.}\, 10^{-4}\, D_B^2}\right)^b$	$(Y_T - X_B)_{CAL}$	$(Y_T - X_B)_{EXP}$
	$(X_B \times 10^4)$	$(\frac{gm\ moles}{cm^2} \times 10^{10})$	$(\frac{cm^2}{gm\ mole} \times 10^{-4})$	$(Sep. \times 10^4)$	$(Sep. \times 10^4)$
1	1.091	2.07	7.27	0.150	0.125
4A	0.755	1.48	4.38	0.074	0.087
4B	1.138	2.12	7.88	0.167	0.197
6A	1.026	1.99	5.65	0.112	0.120
8A	1.210	2.20	8.47	0.191	0.178
15A	1.128	2.11	10.01	0.211	0.204
19A	0.499	1.39	4.33	0.060	0.069
21A	0.491	1.38	11.33	0.150	0.172
22A	0.422	1.53	12.14	0.186	0.199
25B	0.730	1.54	8.49	0.131	0.113
25A	0.[illegible]	1.46	5.35	0.078	0.075

[a] $T = 0.814 \times 10^{-10} + 1.19 \times 10^{-9}\, X_b$

[b] $k = 0.59$, and $C_{soln.} = 0.05559$ (gm moles/cm³ soln.)

TABLE VII

TEST THE CONSISTENCY OF FOAM DENSITY ALONG THE COLUMN OF FOAM

Run	Bottom Product Concentration C_B $\left(\frac{gm\ moles}{cm^3 soln.} \times 10^{[illegible]}\right)$	Height of the Column of Foam Z (inches)	Volume of the Column of Foam $A \cdot Z$ (cm^3)	Gas Flow Rate G $\left(\frac{cm^3}{min.}\right)$	Overhead Liquid Flow Rate L_0 $\left(\frac{cm^3}{min.}\right)$	Foam Rate $L_0 + G$ $\left(\frac{cm^3}{min.}\right)$	Volumetric Fraction of Liquid in the Foam $\frac{L_0}{G + L_0}$	Bubble Residence Time $\frac{A \cdot Z}{G + L_0}$ (min.)
16A	4.552	59	2,326.0	199.4	16.5	215.9	0.0764	10.7
16B	4.601	53	2,089.0	197.6	15.1	212.7	0.0710	9.82
16C	4.632	47	1,853.0	193.5	15.5	209.0	0.0[illegible]	8.85
16D	4.656	41	1,616.0	189.8	14.2	204.0	0.0696	7.92
16E	4.681	65	2,562.0	205.2	17.8	223.0	0.0798	11.49
17A	4.552	71	2,799.0	154.8	5.87	160.7	0.0365	17.42
17B	4.556	65	2,562.0	152.0	5.94	157.9	0.0376	16.23
17C	4.566	59	2,326.0	149.2	5.55	154.8	0.0359	15.03
17D	4.576	53	2,089.0	145.5	5.59	150.9	0.0370	13.84
17E	4.646	47	1,853.0	142.5	5.10	147.6	0.0346	12.55
18A	4.517	71	2,799.0	135.5	3.46	138.5	0.0250	20.21
18B	4.437	65	2,562.0	132.4	3.27	135.7	0.0241	18.88
18C	4.440	59	2,326.0	130.0	3.12	133.1	[illegible]	17.48
18D	4.517	47	1,853.0	125.[illegible]	2.[illegible]6	128.5	0.0211	14.[illegible]

TABLE VII -- Continued

Run	Bottom Product Concentration	Height of the Column of Foam	Volume of the Column of Foam	Gas Flow Rate	Overhead Liquid Flow Rate	Foam Rate	Volumetric Fraction of Liquid in the Foam	Bubble Residence Time
	C_B	Z	$A \cdot Z$	G	L_0	$L_0 + G$	$\frac{L_0}{G + L_0}$	$\frac{A \cdot Z}{G + L_0}$
	$\left(\frac{gm\ moles}{cm^3\ soln.} \times 10^{[illegible]}\right)$	(inches)	(cm^3)	$\left(\frac{cm^3}{min.}\right)$	$\left(\frac{cm^3}{min.}\right)$	$\left(\frac{cm^3}{min.}\right)$		(min.)
19A	2.762	71	2,799.0	199.8	15.76	215.6	0.0731	12.97
19B	2.764	59	2,326.0	19[illegible].4	14.[illegible]	208.0	0.0702	11.18
19C	2.764	47	1,85[illegible].0	18[illegible].0	13.78	200.6	0.0686	9.2[illegible]
19D	2.784	41	1,616.0	18[illegible].8	12.56	196.4	0.0640	8.[illegible]
20A	2.679	71	2,799.0	232.2	19.76	252.0	0.0764	11.11
20B	2.[illegible]61	59	2,326.0	224.0	18.71	242.7	0.0771	9.[illegible]
20C	2.714	47	1,853.0	215.1	17.64	232.7	0.0758	7.96
20D	2.714	41	1,616.0	210.3	16.56	226.7	0.0729	[illegible]
21A	2.720	71	2,799.0	138.0	4.77	142.8	0.0334	[illegible]
21B	2.7[illegible]7	59	2,326.0	132.0	[illegible].91	135.9	0.0351	[illegible]
21C	2.744	47	1,853.0	125.5	3.39	128.9	0.0263	14.3[illegible]
21D	2.784	41	1,616.0	122.0	2.96	125.0	0.0211	12.9[illegible]

TABLE [illegible]

CROSS-PLOT DATA FROM FIGURE [illegible], IN ORDER TO OBTAIN THE EFFECT OF THE HEIGHT OF THE COLUMN OF FOAM (Z) ON THE FRACTION OF LIQUID IN THE FOAM

Height of the Column of Foam	Volume of the Column of Foam	Foam Rate	Bubble Residence Time	Volumetric Fraction of Liquid in the Foam
Z	$A \cdot Z$	$L_0 + G$	$\frac{A \cdot Z}{G + L_0}$	$\frac{L_0}{G + L_0}$
(inches)	(cm^3)	(cm^3/min.)	(min.)	
47	1,855.0	110.0	16.85	[illegible]
59	2,326.0	110.0	21.15	[illegible]
65	2,562.0	110.0	23.29	[illegible]
71	2,799.0	110.0	25.45	[illegible]
47	1,855.0	140.0	13.24	[illegible]
59	2,326.0	140.0	16.61	0.0271
65	2,562.0	140.0	18.30	[illegible]
71	2,799.0	140.0	19.99	0.0254
47	1,855.0	170.0	10.91	[illegible]
59	2,326.0	170.0	13.68	[illegible]
65	2,562.0	170.0	14.93	[illegible]
71	2,799.0	170.0	16.46	[illegible]
47	1,855.0	200.0	9.26	[illegible]
59	2,326.0	200.0	11.63	0.0324
65	2,562.0	200.0	12.81	[illegible]
71	2,799.0	200.0	14.00	[illegible]

TABLE IX

CROSS-PLOT DATA FROM FIGURE 17, IN ORDER TO OBTAIN THE AFFECT OF THE HEIGHT OF THE COLUMN OF FOAM (Z) ON THE FRACTION OF LIQUID IN THE FOAM

Height of the Column of Foam	Volume of the Column of Foam	Foam Rate	Bubble Residence Time	Volumetric Fraction of Liquid in the Foam
Z	$A \cdot Z$	$L_0 + G$	$\frac{A \cdot Z}{G + L_0}$	$\frac{L_0}{G + L_0}$
(inches)	(cm^3)	(cm^3/min.)	(min.)	
71	2,799.0	110.0	25.45	[illegible]
59	2,326.0	110.0	21.15	[illegible]
47	1,853.0	110.0	16.85	[illegible]
41	1,616.0	110.0	14.69	[illegible]
71	2,799.0	140.0	19.99	[illegible]
59	2,326.0	140.0	[illegible]	[illegible]
47	1,853.0	140.0	13.24	[illegible]
41	1,616.0	140.0	11.54	[illegible]
71	2,799.0	160.0	17.49	[illegible]
59	2,326.0	140.0	12.92	[illegible]
47	1,853.0	140.0	10.29	[illegible]
41	1,616.0	160.0	7.95	[illegible]
71	2,799.0	200.0	14.00	[illegible]
59	2,326.0	200.0	11.63	[illegible]
47	1,853.0	200.0	9.26	[illegible]
41	1,616.0	200.0	8.08	[illegible]

TABLE X

EXPERIMENTAL DATA FOR ENRICHING EFFECT ON
IN A 7½ INCH COLUMN OF FOAM

Run	Gas Flow Rate G^b (cm³/min.)	Bottom Product Concentration C_B ($\frac{\text{gm moles}}{\text{cm}^3\text{soln.}} \times 10^6$)	Top Product Concentration C_T ($\frac{\text{gm moles}}{\text{cm}^3\text{soln.}} \times 10^6$)	Height of Enriching Section Z_E (inches)	Overhead Liquid Flow Rate L_O (cm³/min.)	Top Product Liquid Flow Rate L_T (cm³/min.)	Reflux Liquid Flow Rate L_R (cm³/min.)
22A	159.2	3.446	4.325	42.5	4.77	4.77	0.00
22B[a]	160.6	2.896	7.951	42.5	5.08	0.250	4.83
23A	160.3	3.571	4.098	42.5	6.19	4.90	1.49
23B	161.5	3.574	5.008	42.5	6.14	2.68	3.46
24A	158.4	3.417	5.375	42.5	7.38	3.09	4.29
24B	159.5	3.350	7.238	42.5	6.27	0.913	5.30
25A	160.8	3.380	4.307	63.75	7.46	6.13	1.33
25B	161.7	3.492	4.224	63.75	6.80	6.80	0.00
25C	160.0	3.435	5.294	63.75	8.25	2.56	5.69
26A	158.4	3.390	4.914	63.75	6.44	3.71	2.73
26B	162.0	3.103	6.394	63.75	6.22	1.37	4.85
27A	214.5	3.418	3.040	42.5	15.22	15.22	0.00
28A	187.7	3.130	3.543	42.5	12.93	12.93	0.00
28B	187.3	3.215	3.723	42.5	11.90	8.45	3.45
29A	188.1	3.057	3.6[illegible]	42.5	12.30	6.49	5.81
29B	184.0	3.059	4.[illegible]	42.5	11.61	4.10	7.51
30A	247.0	3.434	4.079	42.5	3.72	3.62	0.09
30B	249.5	3.410	4.954	42.5	4.13	2.79	1.34

TABLE X -- Continued

Run	Gas Flow Rate	Bottom Product Concentration	Top Product Concentration	Height of Enriching Section	Overhead Liquid Flow Rate	Top Product Liquid Flow Rate	Reflux Liquid Flow Rate
	G^b	C_B	C_T	Z_E	L_O	L_T	L_R
	(cm³/min.)	$\left(\frac{\text{gm moles}}{\text{cm}^3\text{-soln.}} \times 10^6\right)$	$\left(\frac{\text{gm moles}}{\text{cm}^3\text{-soln.}} \times 10^6\right)$	(inches)	(cm³/min.)	(cm³/min.)	(cm³/min.)
31A	149.2	5.367	5.292	42.5	4.88	2.51	2.37
32A	147.4	5.080	5.519	42.5	6.14	1.32	4.82
33A	208.1	5.313	5.324	42.5	17.57	17.57	0.00

[a] Run not at steady state.

[b] Has pressure of one atmosphere and temperatures from 75.0 to 79.0° F.

TABLE X

EXPERIMENTAL SEPARATIONS FOR ENRICHING SECTION X
A 72 INCH COLUMN OF FOAM

Run	Bottom Product Mole Fraction	Top Product Mole Fraction	Experimental Separation	Area Averaged Bubble Diameter	Volume Averaged Bubble Diameter
	X_B ($X_B \times 10^4$)	Y_T ($Y_T \times 10^4$)	$(Y_T - X_B)_{EXP.}$ (Sep. $\times 10^4$)	D_A (cm)	D_V (cm)
22A	0.622	0.781	0.159	0.0327	0.0329
22B[a]	0.523	1.435	0.912	0.0327	0.0329
23A	0.645	0.848	0.203	0.0327	0.0329
23B	0.645	1.012	0.367	0.0327	0.0329
24A	0.617	0.970	0.353	0.0327	0.0329
24B	0.583	1.306	0.723	0.0327	0.0329
25A	0.628	0.778	0.150	0.0327	0.0329
25B	0.[illegible]0	0.765	0.133	0.0327	0.0329
25C	0.620	0.956	0.336	0.0327	0.0329
26A	0.612	0.887	0.275	0.0327	0.0329
26B	0.596	1.190	0.594	0.0327	0.0329
27A	0.6272	0.6672	0.0401	0.0327	0.0329
28A	0.5651	0.6396	0.0745	0.0327	0.0329
28B	0.5634	0.[illegible]721	0.0917	0.0327	0.0329
29A	0.552	0.698	0.146	0.0327	0.0329
29B	0.558	0.788	0.230	0.0327	0.0329
30A	0.620	0.845	0.225	0.0327	0.0329
30B	0.616	0.900	0.284	0.0327	0.0329
31A	0.608	0.955	0.347	0.0327	0.0329
32A[b]	0.556	1.004	0.448	0.0353	[illegible]
33A[b]	0.598	0.6344	0.0365	0.0325	[illegible]

[a] Run not at steady state.
[b] Bubble diameters are experimental and are not taken from Table 4 or Figure 1[illegible].

TABLE XI

RATIO OF EXPERIMENTAL MULTI-STAGED SEPARATION TO THE CALCULATED SEPARATION FOR A ONE STAGE ENRICHING SECTION

Run	Group of variables in Equilibrium Relationship	Calculated Surface Excess Based on X_B	Calculated One Stage Separation	Ratio of Experimental to Calculated Separation	Fraction of Overhead Liquid Returned as Reflux
	$\left(\frac{k D_A^2}{C_{Sol.} \cdot 10^{20}}\right)$	Γ_B	$(X_B - X_{B\,CA})$	$\frac{(X_B - X_{B\,EXP})}{(X_B - X_{B\,CA})}$	$\frac{L_R}{O}$
	$\left(\frac{cm^2}{gm\ moles} \times 10^{-4}\right)$	$\left(\frac{gm\ moles}{cm^2} \times 10^{10}\right)$	$(Sep. \times 10^4)$		
22A	11.95	1.529	0.182	0.77	[illegible]
22B	11.29	1.415	0.160	0.70	0.951
24A	8.96	1.556	0.139	1.46	[illegible]
24B	9.40	1.556	0.146	2.51	[illegible]
24A	7.77	[illegible]	0.118	2.99	[illegible]
24B	9.09	1.464	0.155	5.56	[illegible]
25A	7.70	1.535	0.115	1.27	[illegible]
25B	8.50	1.548	0.134	1.02	[illegible]
25C	6.95	1.527	0.106	[illegible]	[illegible]
26A	8.79	1.518	0.133	2.07	[illegible]
26B	9.52	1.499	0.140	[illegible]	[illegible]
27A	4.21	1.524	0.0642	0.[illegible]2	[illegible]
28A	5.55	1.464	0.0785	0.95	[illegible]
28B	5.82	1.491	0.0862	1.06	[illegible]
29A	5.44	1.449	0.0788	1.85	[illegible]
29B	5.78	1.456	[illegible]	2.75	[illegible]
[illegible]A	14.51	1.527	0.222	1.01	[illegible]
[illegible]	12.95	1.522	0.197	1.44	[illegible]

TABLE XII -- Continued

Run	Group of Variables in Equilibrium Relationship	Calculated Surface Excess Based on X_p	Calculated One Stage Separation	Ratio of Experimental to Calculated Separation	Fraction of Overhead Liquid Returned as Reflux
	$\left(\frac{k\,D_A^2}{C_{Soln.}\,10^{-3}}\right)$	T_p	$(X_T - X_p)_{CAL}$	$\frac{(X_T - X_p)_{EXP}}{(X_T - X_p)_{CAL}}$	$\frac{L_p}{L_0}$
	$\left(\frac{cm^2}{gm\ moles} \times 10^{-4}\right)$	$\left(\frac{gm\ moles}{cm^2} \times 10^{-6}\right)$	$(Sep. \times 10^4$		
31A	10.92	1.513	0.165	2.10	0.46[illegible]
32A	8.58	1.453	0.125	3.08	0.38[illegible]
33A	4.23	1.502	0.0655	0.57	0.[illegible]

[a] Run not at steady state.

TABLE XIII

DRIVING FORCES AT THE ENDS OF AN ENRICHING SECTION

Run.	Driving Force at the Top of the Column $(Y_U^* - Y_U)_T$ (Dr. x 10^4)	Driving Force at the Bottom of the Column $(Y_U^* - Y_U)_B$ (Dr. x 10^4)
23A	0.160	-0.077
23B	0.186	-0.027
24A	0.190	-0.060
24B	[illegible]	+0.030
25A	0.132	-0.027
25C	0.133	-0.017
26A	0.101	-0.065
26B	0.203	+0.012
28B	0.0924	+0.070
29A	0.0880	+0.002
29B	0.0994	+0.004
30B	0.209	+0.016
31A	0.209	-0.030
32A	0.139	+0.040

TABLE XIV

HEIGHT OF A TRANSFER UNIT IN AN ENRICHING SECTION

Run	Logarithmic Mean Driving Force	Separation Caused by Reflux	Number of Transfer Units	Height of Enriching Section in the Column of Foam	Height of a Transfer Unit	Fraction of Overhead Liquid Returned as Reflux
	$\frac{D_T - D_B}{\ln \frac{D_T}{D_B}}$	$(Y_{OT} - Y_{OB})$	N_E	Z_E	H_E	$\frac{L_R}{L_O}$
	$(D_{LM} \times 10^4)$	$(Sep. \times 10^4)$		(inches)	(inches)	
23A	.....	0.064	....	42.5	.....	0.233
23B	.....	0.221	....	[illegible]	.....	[illegible]
24A	.....	0.235	....	[illegible]	.....	[illegible]
24B	0.0928	0.986	[illegible]	[illegible]	[illegible].70	[illegible]
25A	.....	0.032	....	63.75	.....	[illegible]
25C	.....	0.230	....	63.75	.....	[illegible]
2[illegible]A	.....	0.142	....	63.75	.....	[illegible]
2[illegible]	0.0[illegible]75	0.454	[illegible]	63.75	9.47	[illegible]
28B	0.0859	0.055	[illegible]	42.5	64.8	[illegible]
29A	0.0259	0.047	2.32	42.5	18.3	[illegible]
29B	0.0297	0.146	4.92	42.5	[illegible].4	[illegible]
[illegible]	0.0853	0.087	1.02	42.5	41.7	[illegible]
[illegible]A	.....	0.182	....	42.5	.....	[illegible]
[illegible]A	0.0899	0.325	[illegible]	42.5	11.8	[illegible]

TABLE XV

EXPERIMENTAL DATA FOR STRIPPING SECTION IN A [illegible] INCH COLUMN OF FOAM

Run	Gas Flow Rate	Bottom Product Concentration	Feed Concentration	Top Product Concentration	Height of Stripping Section	Bottom Product Liquid Flow Rate	Overhead Liquid Flow Rate	Feed Liquid Flow Rate
	G^a	C_B	C_F	C_T	Z_S	L_B	L_O	L_F
	$(cm^3/min.)$	$(\frac{gm\ moles}{cm^3 soln.} \times 10^6)$	$(\frac{gm\ moles}{cm^3 soln.} \times 10^6)$	$(\frac{gm\ moles}{cm^3 soln.} \times 10^6)$	(in.)	$(cm^3/min.)$	$(cm^3/min.)$	$(cm^3/min.)$
38C	179.3	4.647	5.903	6.417	12.5	5.82	8.72	14.54
39A	181.5	4.335	5.977	6.427	12.5	4.03	10.70	14.73
40A	162.2	5.003	6.181	6.705	12.5	5.86	8.59	14.45
40B	143.8	5.462	6.167	7.219	12.5	9.96	4.49	14.45
40C	143.3	4.962	6.171	7.228	12.5	5.31	4.78	10.09
41A	152.5	3.350	5.730	6.519	12.5	3.15	6.77	9.92
41B	163.7	2.612	5.889	6.565	12.5	1.92	8.12	10.04
42A	194.1	4.990	5.940	6.589	12.5	6.80	17.77	24.57
42B	172.0	5.472	5.963	6.686	12.5	13.77	10.43	24.10
42C	143.1	5.441	5.991	6.913	12.5	19.15	4.95	24.10
43A	140.8	5.439	6.232	7.080	42.5	7.94	6.32	14.26
43B	145.3	5.435	6.241	6.788	42.5	7.46	6.96	14.42
43C	154.1	[illegible]	6.302	6.839	42.5	5.73	8.68	14.41

[a] Gas Pressure of one atmosphere and temperatures from 75.0 to 79.0° F.

TABLE XVI

RATIO OF EXPERIMENTAL MULTISTAGE SEPARATION TO THE CALCULATED SEPARATION FOR A ONE STAGE STRIPPING SECTION

Run	Bottom Product Mole Fraction	Feed Mole Fraction	Top Product Mole Fraction	Experimental Column Separation	Calculated One Stage Separation	Ratio of Experimental to Calculated Separation	Fraction of Feed Flow Rate Which Becomes Overhead Liquid
	X_B	X_F	X_T	$(X_T - X_B)$	$(X_{TE} - X_B)$	$\left(\frac{X_T - X_B}{X_{TE} - X_B}\right)$	$\frac{L_O}{F}$
	$(X_B \times 10^4)$	$(X_F \times 10^4)$	$(X_T \times 10^4)$	$(\text{Sep.} \times 10^4)$	$(\text{Sep.} \times 10^4)$		
38C	0.8590	1.076	1.178	0.319	0.131	2.44	0.400
39A	0.7862	1.079	1.158	0.372	0.104	3.58	0.[illegible]
40A	0.9031	1.116	1.210	0.307	0.125	2.4[illegible]	0.394
40B	0.8859	1.113	1.305	0.417	0.223	1.42	0.[illegible]1
40C	0.8958	1.114	1.305	0.409	0.195	2.07	0.474
41A	0.6048	1.055	1.177	0.572	0.121	4.73	0.[illegible]52
41B	0.4716	1.063	1.185	0.713	0.0977	7.30	0.509
42A	0.9001	1.072	1.189	0.289	0.0722	4.00	0.723
42B	0.9877	1.076	1.207	0.219	0.115	1.90	0.4[illegible]
42C	1.015	1.081	1.248	0.230	0.205	1.12	0.205
43A	0.9818	1.125	1.278	0.296	0.155	1.91	0.44[illegible]
43B	0.9810	1.127	1.225	0.244	0.145	1.[illegible]	0.45[illegible]
43C	0.9934	1.148	1.254	0.281	0.121	2.32	0.[illegible]02

TABLE XIII

CALCULATION OF THE LOGARITHMIC MEAN DRIVING FORCE
IN A STRIPPING SECTION

Run	Driving Force at the Top of the Column $(Y_A - Y_B)_T$ (Dr. x 10^4)	Driving Force at the Bottom of the Column $(Y_A - Y_B)_B$ (Dr. x 10^4)	Logarithmic Mean Driving Force $(Y_A - Y_B)_{LM}$ (Dr. x 10^4)
38C	+0.058	0.0850	0.0706
39A	+0.046	0.0809	0.0628
40A	+0.047	0.0801	0.0621
40B	+0.050	0.0784	0.0631
40C	+0.033	0.1091	0.0622
41A	+0.019	0.0906	0.0458
41B	+0.025	0.0855	0.0491
42A	-0.037	0.0545	.....
42B	-0.010	0.0551	.....
42C	+0.045	0.0471	0.0460
[illegible]	+0.015	0.0748	[illegible]
[illegible]	[illegible]	[illegible]	[illegible]
[illegible]	[illegible]	[illegible]	[illegible]

TABLE XVIII

CALCULATION OF THE HEIGHT OF A TRANSFER UNIT IN A STRIPPING SECTION

Run	Separation Caused by Feed Stream	Number of Transfer Units	Height of the Stripping Section	Height of a Transfer Unit	Height of a Transfer Unit Divided By the Feed Rate	Fraction of Feed Flow Rate Which Becomes Overhead Liquid
	$(Y_T - Y_{T'})$	N_S	Z_S	H_S	$\frac{H_S}{L_F}$	$\frac{L_O}{L_F}$
	(Sep. x 10^4)		(inches)	(inches)	(min./cm^2)	
38C	0.188	2.66	12.5	4.70	0.821	0.000
39A	0.268	4.34	12.5	2.88	0.497	0.726
40A	0.182	2.93	12.5	4.27	0.751	0.594
40B	0.094	1.49	12.5	8.39	1.47	0.511
40C	0.211	3.39	12.5	3.69	0.929	0.474
41A	0.452	9.45	12.5	1.27	0.326	0.062
41B	0.015	12.5	12.5	1.00	0.253	0.409
42A	0.217	....	12.5	....	.....	0.725
42B	0.104	....	12.5	....	.....	0.433
42C	0.025	0.543	12.5	23.0	2.42	0.209
43A	0.141	3.79	42.5	11.2	2.00	0.445
43B	0.099	1.48	42.5	28.7	5.06	0.495
43C	0.140	2.56	42.5	16.6	2.93	0.002

TABLE XIX

EXPERIMENTAL DATA FOR AN ENRICHING SECTION IN THE STATE OF TOTAL REFLUX

Run	Gas Flow Rate	Bottom Product Concentration	Top Product Concentration	Height of Enriching Section	Overhead Liquid Flow Rate	Area Averaged Bubble Diameter	Volume Averaged Bubble Diameter
	G^a	C_B	C_T	Z_E	L_O	D_A	D_V
	(cm³/min.)	$\left(\frac{\text{gm moles}}{\text{cm}^3\text{ soln.}} \times 10^6\right)$	$\left(\frac{\text{gm moles}}{\text{cm}^3\text{ soln.}} \times 10^6\right)$	(inches)	(cm³/min.)	(cm)	(cm)
32B	196.2	0.45	11.47	42.5	2.86	0.0327	0.0329
35A[b]	193.9	2.948	7.979	12.5	12.04	0.0327	0.0329
35B[b]	215.0	2.776	8.011	12.5	14.06	0.0327	0.0329

[a] Gas pressure of one atmosphere and temperatures from 75.0 to 79.0° F.

[b] Bubble diameters taken from Table 4 and Figure 12.

TABLE XX

NUMBERS NEEDED IN THE CALCULATION OF DRIVING FORCES
IN AN ENRICHING SECTION IN THE STATE OF TOTAL REFLUX

Run	Bottom Product Mole Fraction	Top Product Mole Fraction	Surface Excess Based on X_B	Surface Excess Based on X_T	Variable Group Based on L_D
	X_B	X_T	T_B	T_T	$\frac{k \; L_A^2 \; L}{C_{Soln.} \; L_D^3 \; V}$
	$(X_B \times 10^4)$	$(X_T \times 10^4)$	$(\frac{gm\ moles}{cm^2} \times 10^{10})$	$(\frac{gm\ moles}{cm^2} \times 10^{10})$	$(\frac{cm^2}{gm\ moles} \times 10^{-4})$
32B	0.0812	2.070	0.907	3.194	24.52
35A	0.5522	1.440	1.426	2.470	5.794
35B	0.5011	1.446	1.390	2.477	5.464

TABLE XXI

HEIGHT OF A TRANSFER UNIT IN AN ENRICHING SECTION
IN THE STATE OF TOTAL REFLUX

Run	Driving Force at the Top of the Column $(Y_U^* - Y_U)_T$ (Sep. x 10^4)	Driving Force at the Bottom of the Column $(Y_U^* - Y_U)_B$ (Sep. x 10^4)	Logarithmic Mean Driving Force $(Y_U^* - Y_U)_{LM}$ (Sep. x 10^4)	Foam Column Separation $(Y_{UT} - Y_{UB})$ (Sep. x 10^4)	Number of Transfer Units N_{ET}	Height of a Transfer Unit H_{ET} (inches)
12B	0.7828	0.2850	0.4926	1.767	3.59	11.8
35A	0.1421	0.08748	0.1125	0.826	7.34	1.70
35B	0.1322	0.08072	0.1057	0.869	8.22	1.12

TABLE XXIII

EXPERIMENTAL DATA FOR A STRIPPING SECTION IN THE STATE OF TOTAL OVERHEAD

Run	Gas Flow Rate	Bottom Product Concentration	Feed Liquid Concentration	Top Product Concentration	Overhead Liquid Flow Rate	Area Averaged Bubble Diameter	Volume Averaged Bubble Diameter
	G^a	C_B	C_F	C_T	L_O	D_A	D_V
	$(cm^3/min.)$	$(\frac{gm\ moles}{cm^3 soln.} \times 10^6)$	$(\frac{gm\ moles}{cm^3 soln.} \times 10^6)$	$(\frac{gm\ moles}{cm^3 soln.} \times 10^6)$	$(cm^3/min.)$	(cm)	(cm)
37A	180.2	2.692	6.436	8.373	1.98	0.0352	0.0356
38A	210.1	1.504	6.125	6.598	6.77	0.0324	0.0330
38B	225.7	1.564	6.491	8.058	2.36	0.0362	0.0374

[a] Gas Pressure of one atmosphere and temperatures from 75.0 to 79.0° F.

TABLE XXIII

NUMBERS NEEDED IN THE CALCULATION OF THE HEIGHT OF A TRANSFER UNIT IN A STRIPPING SECTION IN THE STATE OF TOTAL OVERHEAD

Run	Bottom Product Mole Fraction	Feed Liquid Mole Fraction	Top Product Mole Fraction	Height of Stripping Section
	X_B	X_F	Y_T	Z_S
	$(X_B \times 10^4)$	$(X_F \times 10^4)$	$(Y_T \times 10^4)$	(inches)
37A	0.4746	1.162	1.511	12.5
38A	0.2878	1.106	1.[illegible]	12.5
38B	0.2860	1.172	1.455	12.5

TABLE XXIV

HEIGHT OF A TRANSFER UNIT IN A STRIPPING SECTION IN THE STATE OF TOTAL OVERHEAD

Run	Driving Force at the Top of the Column	Driving Force at the Bottom of the Column	Logarithmic Mean Driving Force	Form Column Separation	Number of Transfer Units	Height of a Transfer Unit
	$(Y_y^* - Y_y)_T$	$(Y_y^* - Y_y)_B$	$(Y_y^* - Y_y)_{LM}$	$(Y_{yT} - Y_{yB})$	N_{ST}	H_{ST}
	(Dr. x 10^4)	(Dr. x 10^4)	(Dr. x 10^4)	(Cap. x 10^4)		(inches)
37A	0.452	0.724	0.577	0.529	0.917	13.0
38A	0.140	0.139	0.140	0.779	5.56	2.25
38B	0.328	0.428	0.376	0.854	2.75	3.56

TABLE XXV

HEIGHTS OF TRANSFER UNITS IN ENRICHING AND STRIPPING SECTIONS

Run	Height of a Transfer Unit	Ratio of Downflow to Upflow	Flow Number
	H (cm)	$\frac{L_D}{L_V}$	$\frac{L_D}{L_V}\sqrt{\frac{L_D}{G + L_D + L_V}}$
24B	17.0	0.649	0.1487
26B	24.0	0.780	0.1306
28B	165.0	0.267	0.03391
29A	46.5	0.475	0.08[illegible]
29B	22.0	0.[illegible]7	0.1272
30B	106.0	0.324	0.05[illegible]
32A	30.0	0.785	0.1309
32B	30.0	1.00	0.1190
35A	4.32	1.00	0.2350
35B	3.[illegible]	1.00	0.2405
37A	34.5	1.00	0.09282
38A	5.72	1.00	0.1740
38B	14.1	1.00	0.[illegible]
38C	11.9	1.657	0.4[illegible]
39A	7.32	1.377	0.3674
40A	10.8	1.682	0.4693
40B	21.3	3.218	0.9590
40C	9.37	2.111	0.5332
41A	3.23	1.465	0.3947
41B	2.54	1.236	0.2905
42C	58.4	4.809	1.822
43A	28.4	2.2[illegible]	0.6705
43B	72.9	2.072	0.6094
43C	42.2	1.660	0.4754

TABLE XXVI

NUMBERS NEEDED FOR A CORRELATION BETWEEN THE AMOUNT OF LIQUID IN THE FOAM AND THE GAS FLOW RATE OF A ONE STAGE SEPARATOR

Run	Bottom Product Concentration	Height of the Column of Foam	Volumetric Fraction of Liquid in the Foam	Gas Flow Rate
	C_B	Z	$\frac{L_0}{G + L_0}$	G
	$(\frac{\text{gm moles}}{\text{cm}^3\text{soln.}} \times 10^6)$	(inches)		$(\text{cm}^3/\text{min.})$
1	6.043	71	0.0450	188.8
2A	[illegible]	71	0.0567	206.3
3	3.505	71	0.0619	219.1
3A	4.134	71	0.0675	219.1
4A	4.183	71	0.0743	196.8
4B	6.306	71	0.0405	147.0
5A	4.958	71	0.0200	139.4
6A	5.686	71	0.0600	108.4
7A	6.003	71	0.0212	133.9
8A	6.701	71	0.0412	133.9
9A	4.979	71	0.0234	135.4
11A	4.173	71	0.0127	113.1
12A	5.679	71	0.0251	144.0
13A	6.251	71	0.0347	144.7
19A	2.762	71	0.0731	199.8
20A	2.679	71	0.0784	232.2
21A	2.720	71	0.0334	133.0
22A	3.446	71	0.0291	159.2
25B	3.492	71	0.0404	161.7
27A	3.418	71	0.0785	214.5
28A	3.130	71	0.0626	157.7
30A	3.434	71	0.0240	147.0
33A	3.313	71	0.0779	208.1

TABLE XXVII

THE CORRELATION FOR THE OVERHEAD LIQUID FLOW RATE

Run	Gas Flow Rate	Top Product Concentration	Fraction of the Overhead Foam Which is Liquid	Foam Density Number
	G	C_T	$\frac{L_O}{G + L_O}$	$\frac{G^3}{C_T}$
	$(cm^3/min.)$	$(\frac{gm\ moles}{cm^3 soln.} \times 10^6)$		$(\frac{cm^{12}}{min.^2 gm\ moles} \times 10^{-12})$
22A	159.2	4.325	0.0291	0.932
23A	160.3	4.698	0.0393	0.877
23B	161.5	5.608	0.0366	0.751
24A	158.4	5.375	0.0439	0.739
24B	159.5	7.238	0.0378	0.521
25A	160.8	4.307	0.0445	0.966
25B	161.7	4.224	0.0404	1.00
25C	160.0	5.294	0.0490	0.744
26A	158.4	4.914	0.0391	0.808
26B	162.0	6.594	0.0370	0.644
27A	214.5	3.640	0.0763	2.71
28A	187.7	3.543	0.0626	1.87
28B	187.3	3.723	0.0578	1.76
29A	188.1	3.866	0.0516	1.72
29B	188.0	4.365	0.0582	1.52
30A	147.0	4.679	0.0240	0.680
30B	149.5	4.984	0.0269	0.670
31A	149.2	5.292	0.0317	0.627
32A	147.4	5.559	0.0400	0.576
33A	208.1	3.514	0.0775	2.56
35A	193.9	7.975	0.0585	0.914
35B	213.0	8.013	0.0614	1.24
37A	180.2	8.373	0.00869	0.699
41A	152.5	6.519	0.0425	0.545
41B	163.7	6.565	0.0473	0.669
44A	183.3	4.301	0.0778	1.43
44B	173.3	4.229	0.0727	1.23
44C	161.9	4.693	0.0542	0.932
45A	158.6	5.415	0.0349	0.711
45B	158.4	6.320	0.0314	0.628
46A	180.7	4.693	0.0723	1.26
46B	180.2	4.679	0.0664	1.27
47A	175.5	6.046	0.0704	0.896

TABLE XXVIII

EXPERIMENTAL DATA FOR THE COMBINED COLUMN

Run	Gas Flow Rate	Bottom Product Concentration	Feed Liquid Concentration	Top Product Concentration	Mole Fraction of Bottom Product	Mole Fraction of Feed Liquid	Mole Fraction of Top Product
	G^b	C_B	C_F	C_T	X_B	X_F	X_T
	(cm³/min.)	$\left(\frac{\text{gm moles}}{\text{cm}^3\text{ soln.}}\right) \times 10^{[illegible]}$	$\left(\frac{\text{gm moles}}{\text{cm}^3\text{ soln.}}\right) \times 10^{[illegible]}$	$\left(\frac{\text{gm moles}}{\text{cm}^3\text{ soln.}}\right) \times 10^{[illegible]}$	$(X_B \times 10^{4})$	$(X_F \times 10^{4})$	$(X_T \times 10^{4})$
44A	1[illegible].5	3.267	[illegible]	4.[illegible]01	[illegible]	[illegible]	[illegible]
44B	17[illegible].5	[illegible]	[illegible]	4.229	[illegible]	[illegible]	[illegible]
44C	10[illegible].9	[illegible]	[illegible]	4.[illegible]	[illegible]	[illegible]	[illegible]
45A	15[illegible].[illegible]	[illegible]	[illegible]	[illegible]	[illegible]	[illegible]	[illegible]
45B	1[illegible].4	[illegible]	[illegible]	[illegible]	[illegible]	[illegible]	[illegible]
46A	1[illegible]0.7	2.9[illegible]	[illegible]	4.[illegible]	[illegible]	[illegible]	[illegible]
46B	1[illegible]0.2	2.[illegible]	4.0[illegible]	4.[illegible]79	[illegible]	[illegible]	[illegible]
47A	17[illegible].5	[illegible]	[illegible]	[illegible]	[illegible]	[illegible]	[illegible]
47B[a]	21[illegible].5	[illegible]	[illegible]	9.[illegible]	[illegible]	[illegible]	[illegible]

[a] This run is outside of the model region and it is not at steady state.

[b] Gas pressure of one atmosphere and temperature from [illegible] to [illegible]°C.

TABLE XXIX

EXPERIMENTAL DATA FOR THE COMBINED COLUMN

Run	Feed Liquid Flow Rate L_F (cm³/min.)	Overhead Liquid Flow Rate L_O (cm³/min.)	Top Product Flow Rate L_T (cm³/min.)	Bottom Product Flow Rate L_F (cm³/min.)	Reflux Liquid Flow Rate L_R (cm³/min.)	Area Averaged Bubble Diameter D_A (cm.)	Volume Averaged Bubble Diameter D_V (cm.)
44A	[illegible]	[illegible]	8.[illegible]	15.24	[illegible]	0.0[illegible]	0.0[illegible]29
44B	[illegible]	1[illegible].59	[illegible]	14.7[illegible]	[illegible]	0.0[illegible]	0.0[illegible]29
44C	22.[illegible]	[illegible].48	[illegible]	1[illegible]	[illegible]	0.0[illegible]	0.0[illegible]29
45A	14.69	[illegible].74	[illegible]	12.01	[illegible]	0.0[illegible]	0.0[illegible]29
45B	14.95	[illegible].14	[illegible]	12.70	[illegible]	0.0[illegible]	0.0[illegible]29
46A	14.[illegible]	[illegible]	[illegible]	[illegible]	[illegible]	0.0[illegible]	0.0[illegible]29
46[illegible]	9.[illegible]	12.82	[illegible]	3.[illegible]	[illegible]	0.02[illegible]	0.0[illegible]
47A	10.02	[illegible]	2.[illegible]	7.26	[illegible]	0.0[illegible]	0.0[illegible]
47[illegible]	[illegible]	[illegible]	0.[illegible]	[illegible]	[illegible]	0.0[illegible]	0.0[illegible]29

Z_F = [illegible]2.2 cm

Z_C = 79.7 cm

Z = 1[illegible]0.[illegible] cm

Column diameter = 4.4[illegible] cm

TABLE XXX

COMPUTER INPUT

Run	X_T	L_T	G	R_{EX}	L_0	Z_E	Z_S	D_A	D_T
44A	.00000[illegible]37	25.41	183.3	0.6947	15.48	82.2	79.7	0.0327	0.0329
44B	.00000[illegible]56	25.24	173.3	0.6064	13.59	82.2	79.7	0.0327	0.0329
44C	.00000[illegible]	22.07	161.9	0.7938	11.48	82.2	79.7	0.0327	0.0329
45A	.00000981	14.65	158.6	1.174	5.74	82.2	79.7	0.0327	0.0329
45B	.00000687	14.58	158.4	1.624	5.14	82.2	79.7	0.0327	0.0329
46A	.00007030	14.55	180.7	0.9358	13.88	[illegible]	[illegible]	[illegible]	0.0329
46B	.00007254	9.96	180.2	0.9845	12.82	82.2	79.7	0.0294	0.0296
47A	.00007010	10.02	175.8	3.822	13.31	82.2	79.7	0.0314	0.0316

TABLE XXXI

COMPUTER RESULTS

Run	$\left(\frac{L_T}{L_B}\right)$	$\left(\frac{L_T}{L_B} + 1\right)X_F$ (GR. x 10^4)	Y_{UE} (Y_{UE} x 10^4)	X_B (X_B x 10^4)	X_T (X_T x 10^4)
44A	0.5361	1.0195	0.7268	0.5221	0.7797
	0.5361	1.0195	0.7122	0.5859	0.7645
	0.5361	1.0195	0.6829	0.5287	0.7342
	0.5361	1.0195	0.6574	0.4841	0.7077
44B	0.5724	1.0466	0.7339	0.5259	0.7717
	0.5724	1.0466	0.7191	0.5899	0.7566
	0.5724	1.0466	0.6896	0.5330	0.7263
	0.5724	1.0466	0.6638	0.4885	0.6998
44C	0.4084	0.9525	0.7527	0.5455	0.8073
	0.4084	0.9525	0.7376	0.6121	0.7916
	0.4084	0.9525	0.7073	0.5606	0.7602
	0.4084	0.9525	0.6808	0.5197	0.7327
45A	0.2198	0.8516	0.8534	0.6529	0.9947
	0.2198	0.8516	0.8365	0.6221	0.9759
	0.2198	0.8516	0.8019	0.5691	0.9385
	0.2198	0.8516	0.7719	0.5265	0.9056

TABLE XXXI - Continued

Run	$(\frac{L_T}{L_B})$	$(\frac{L_T}{L_B} + 1)X_T$ (GR. x 10^4)	Y_{TB} (Y_{TB} x 10^4)	X_B (X_B x 10^4)	X_T (X_T x 10^4)
45B	0.1426	0.7641	0.8388	0.6280	1.067
	0.1426	0.7641	0.8219	0.6012	1.046
	0.1426	0.7641	0.7882	0.5536	1.009
	0.1426	0.7641	0.7587	0.5148	0.9731
46A	0.9716	1.3860	0.7785	0.5918	0.8403
	0.9716	1.3860	0.7746	0.5659	0.8[illegible]
	0.9716	1.3860	0.7590	0.4978	0.8201
	0.9716	1.3860	0.7279	0.3895	0.7876
46B	1.8458	2.0643	0.8254	0.5445	0.9044
	1.8458	2.0643	0.8254	0.4047	0.9023
	1.8458	2.0643	0.8214	0.3540	0.9002
	1.8458	2.0643	0.8173	0.2877	0.8959
47A	0.3802	0.9703	0.7788	0.5938	1.07[illegible]
	0.3802	0.9703	0.7651	0.5237	1.060
	0.3802	0.9703	0.7318	0.4300	1.022
	0.3802	0.9703	0.7044	0.3027	0.9891

TABLE XXXIII

GRAPHICAL RESULTS

Run	Calculated Bottom Product Mole Fraction X_B $(X_B \times 10^4)$	Calculated Top Product Mole Fraction X_T $(X_T \times 10^4)$
44A	0.604	0.772
44B	0.608	0.764
44C	0.627	0.797
45A	0.635	0.9[illegible]
45B	0.615	1.056
46A	0.572	0.537
46B	0.400	0.902
47A	0.562	1.071

NOMENCLATURE

Symbols

a = Empirical constant from the surface excess equation ($1.15 \times 10^{-6} \frac{\text{gm moles}}{\text{cm}^2}$)

a_m = Interfacial area for mass transfer (cm^2/cm^3)

A = Area of the column ($15.52\ \text{cm}^2$)

b = Empirical constant from the surface excess equation ($0.814 \times 10^{-6} \frac{\text{gm moles}}{\text{cm}^2}$)

C = Concentration of sodium lauryl sulfate in water ($\frac{\text{gm moles}}{\text{cm}^3\ \text{soln.}}$)

C_B = Concentration of bottom product stream ($\frac{\text{gm moles}}{\text{cm}^3\ \text{soln.}}$)

C_F = Concentration of feed stream ($\frac{\text{gm moles}}{\text{cm}^3\ \text{soln.}}$)

$C_{Soln.}$ = Gram moles of sodium lauryl sulfate and water per cm^3 of solution ($\frac{\text{gm moles}}{\text{cm}^3\ \text{soln.}}$)

C_T = Concentration of top product stream ($\frac{\text{gm moles}}{\text{cm}^3\ \text{soln.}}$)

D_A = Area averaged bubble diameter (cm)

D_B = Driving force at the bottom of the column

D_{LM} = Logarithmic mean driving force

D_T = Driving force at the top of the column

F_C = Correction factor for scale readings from the Ceno-DuNouy Tensiometer

F_N = Flow number ($\frac{L_D}{L_U}\sqrt{\frac{L_D}{G + L_D + L_U}}$)

G = Gas flow rate ($\text{cm}^3/\text{min.}$)

H = Height of a transfer unit (cm, in.)

H_E = Height of a transfer unit in an enriching section (cm, in.)

H_{ET} = Height of a transfer unit in an enriching section at total reflux (cm, in.)

H_S = Height of a transfer unit in a stripping section (cm, in.)

H_{ST} = Height of a transfer unit in a stripping section at total overhead (cm, in.)

k = Area to volume constant for dodecahedron shaped bubbles (6.59)

k_C = Conductivity cell constant (cm^{-1})

k_m = Over-all mass transfer coefficient (cm/min.)

L = Liquid flow rate (cm^3/min.)

L_B = Bottom product liquid flow rate (cm^3/min.)

L_D = Downflow liquid flow rate (cm^3/min.)

L_F = Feed liquid flow rate (cm^3/min.)

L_O = Overhead liquid flow rate (cm^3/min.)

L_R = Reflux liquid flow rate (cm^3/min.)

L_T = Top product liquid flow rate (cm^3/min.)

L_U = Upflow liquid flow rate (cm^3/min.)

N = Number of transfer units

N_E = Number of transfer units in an enriching section

N_{ET} = Number of transfer units in an enriching section at total reflux

N_M = Mass transfer rate of sodium lauryl sulfate ($\frac{\text{gm moles}}{\text{min.}}$)

N_S = Number of transfer units in a stripping section

N_{ST} = Number of transfer units in a stripping section at total overhead

p = Average number of ions that sodium lauryl sulfate dissociates into

r = Universal gas constant ($8.3144 \times 10^7 \frac{\text{ergs}}{^{o}\text{K gm mole}}$)

R_{EX} = External reflux ratio

S = Scale reading (dynes/cm)

S_C = Specific conductance of sodium lauryl sulfate in water (micromhos/cm)

t = Temperature of the liquid surface (^oK)

T = Surface excess of sodium lauryl sulfate (gm moles/cm^2)

T_B = Surface excess based on X_B (gm moles/cm^2)

T_{DF} = Surface excess based on X_{DF} (gm moles/cm^2)

T_{DFB} = Surface excess based on X_{DFB} (gm moles/cm^2)

T_F = Surface excess based on X_F (gm moles/cm^2)

T_T = Surface excess based on X_T (gm moles/cm^2)

T_{UB} = Surface excess based on X_{UB} (gm moles/cm^2)

X = Mole fraction of sodium lauryl sulfate

X_B = Mole fraction of the bottom product stream

X_D = Mole fraction of the downflow stream

X_{DB} = Mole fraction of downflow stream at the bottom of the column of foam

X_{DF} = Mole fraction of downflow stream just above the feed point

X_{DFB} = Mole fraction of downflow stream just below the feed point

X_F = Mole fraction of feed stream

X_T = X_{DT} = Mole fraction of the top product stream

X_{UB} = Mole fraction of bulk liquid in the upflow stream at the bottom of the column

Y_U = Mole fraction of sodium lauryl sulfate in broken down foam

Y_{UB} = Mole fraction of foam at the bottom of the column

Y_{UF} = Mole fraction of foam at the feed point

Y_{UT} = X_T = Mole fraction of foam at the top of the column

Y_U^* = Equilibrium mole fraction of sodium lauryl sulfate in broken down foam

Y_{UB}^* = Mole fraction of foam in equilibrium with X_{DB}

Y^*_{UF} = Mole fraction of foam in equilibrium with either X_{DFB} or X_{DF}

Y^*_{UT} = Mole fraction of foam in equilibrium with X_T

Z = Height of column of foam (cm, in.)

Z_E = Height of enriching section in the column of foam (cm, in.)

Z_S = Height of stripping section in the column of foam (cm, in.)

Greek Symbol

ϕ = Surface tension (dynes/cm)

Subscripts

B = Plane at the bottom of a foam section

E = Enriching section

I = Input term (material balance)

O = Output term (material balance)

S = Stripping section

T = Plane at the top of a foam section

BIBLIOGRAPHY

BIBLIOGRAPHY

1. Adamson, A. W., "Physical Chemistry of Surfaces," Interscience Publishers, Easton, Penna., 1963.

2. _____, Sanitary Engineering Research Laboratory News Quarterly, University of California, Berkeley, (October, 1964).

3. _____, Chemical Engineering, 68, Part 1, 100 (April 3, 1961).

4. _____, Chemical Engineering, 69, Part 1, 62 (1960).

5. Bikerman, J. J., "Surface Chemistry Theory and Applications," Academic Press Inc., New York, 1958.

6. Bikerman, J. J., Industrial and Engineering Chemistry, 57, No. 1, 90 (1965).

7. Boucher, R. M. G., Chemical Engineering, 68, Part 2, 83 (1961).

8. Brunner, C. A., and Lemlich, R., I & EC Fundamentals, 2, No. 4, 297 (1963).

9. Brunner, C. A., "Foam Fractionation," Ph. D. Dissertation, University of Cincinnati, June 1963.

10. Brunner, C. A., and Stephan, D. G., Industrial and Engineering Chemistry, 57, No. 5, 40 (1965).

11. Eldib, I. A., Journal Water Pollution Federation, 33, No.9, 914 (1961).

12. Eliezer, R., and Everett, R., Industrial and Engineering Chemistry, 55, No. 10, 44 (1963).

13. Farlo, S., and Lemlich, R., A. I. Ch. E. - I. Chem. E. Joint Meeting, London, 63 (June 1965).

14. Farlo, S., "Drainage in a Foam Fractionation Column," Ph. D. Dissertation, University of Cincinnati, 1964.

15. Ferguson, D. E., Chemical Technology Division Annual Progress Report, Oak Ridge National Laboratory, (November 1965).

16. Gaden, E. L., and Kevorkian, V., Chemical Engineering, 63, Part 2, 173 (1956).

17. Gibbs, J. W., "Collected Works," Vol. I., Longmans Geen & Co., New York, N. Y., 1926.

18. Gorman, A. E., Industrial and Engineering Chemistry, 45, No. 12, 2672 (1953).

19. Grieves, R. B., and Bhattacharyya, D., A. I. Ch. E. Journal, 11, No. 2, 274 (1965).

20. Grieves, R. B., Kelman, S., Obermann, W. R., and Wood, R. K., The Canadian Journal of Chemical Engineering, 252 (December 1963).

21. Grieves, R. B., and Wood, R. K., A. I. Ch. E. Journal, 10 , No. 4 456 (1964).

22. Grieves, R. B., and Wood, R. K., Nature, 200, No. 4904, 332 (1963).

23. Haas, P. A., and Johnson, H. F., A. I. Ch. E. Journal, 11, No. 2, 319 (1965).

24. Haas, P. A., "Engineering Development of a Foam Column for Countercurrent Surface-Liquid Extraction of a Surface-Active Solutes," Ph. D. Dissertation, University of Tennessee, June 1965.

25. Harper, D. C., and Lemlich, R., I & EC Process Design and Development, 4, No. 1, 13 (1965).

26. Hastings, K. E.,"A Study of Foam Fractionation in the Sodium Lauryl Sulfate and Water System," Master's Thesis, Michigan State University, East Lansing, June 1964.

27. Karger, B. L., and Rogers, L. B., Analytical Chemistry, 33, No. 9 1165 (1961).

28. Kevorkian, V., and Gaden, E. L., Jr., A. I. Ch. E. Journal, 3, No. 2, 180 (1959).

29. Langmuir, I., J. Am. Chem. Soc., 39, 1848 (1917).

30. Lemlich, R., A. I. Ch. E. Journal, 12, No. 4, 802 (1966).

31. Lemlich, R., and Lavi, E., Science, 134, 191 (July 1961).

32. Leonard, R. A., and Lemlich, R., A. I. Ch. E. Journal, 11, No. 1, 18 (1965).

33. Leonard, R. A., "A Theoretical and Experimental Study of Interstitial Liquid Flow in Foam Fractionation, "Ph. D. Dissertation, University of Cincinnati, 1964.

34. Lewis, G. N., and Randall, M., "Thermodynamics," McGraw-Hill Book Company, Inc., New York, N. Y., 1961.

35. Lewis, W. K., Squires, L., and Broughton, G., "Industrial Chemistry of Colloidal & Amorphous Materials," The Macmillan Company, New York, N. Y., 1943.

36. London, M., Cohen, M., and Hudson, P. B., Journal of the American Chemical Society, 75, Part 2, 1746 (1953).

37. Marshall, J. R., Chemical Engineering, 69, Part 2, 107 (1962).

38. Miles, G. D., and Ross, J., Journal of Physical Chemistry, 48, 280 (1944).

39. Newson, I. H., J. Appl. Chem., 16, No. 2, 43 (1966).

40. Roe, C. P., and Brass, P. C., J. Am. Chem. Soc., 76, 4703 (1954).

41. Rogers, L. B., and Clver, J. W., Science, 135, 430 (1962).

42. Ross, S., and Chen, E. S., Industrial and Engineering Chemistry, 57, No. 7, 40 (1965).

43. Rubin, E., Industrial and Engineering Chemistry, 55, No. 10, 44 (1963).

44. Schnepf, R. W., and Gaden, E. L., Jr., Chemical Engineering Progress, 55, No. 5, 42 (1959).

45. Schoen, H. M., "New Chemical Engineering Separation Techniques," Interscience Publishers, New York, N. Y., 1962.

46. Schoen, H. M., and Mazella, G., Industrial Water and Wastes, 6, 71 (1961).

47. Stephenson, M. E., "Foam Separation of Dilute Aqueous Solutions," Ph. D. Dissertation, University of California, Berkeley, 1964.

48. Treybal, R. E., "Mass Transfer Operations," McGraw-Hill Book Company, Inc. New York, N. Y., 1955.

49. Walling, C., Ruff, E. E., and Thornton, J. L., Jr., Journal of Physical Chemistry, 56, 989 (1952).